Planning and Feedback Control for Mechanical Systems with Nonholonomic Constraints

by

Gregory Charles Walsh

B.S. (University of Maryland at College Park) 1989
M.S. (University of California at Berkeley) 1990
M.A. (University of California at Berkeley) 1994

A dissertation submitted in partial satisfaction of the

requirements for the degree of

Doctor of Philosophy

in

Engineering-Electrical Engineering and Computer Sciences

in the

GRADUATE DIVISION

of the

UNIVERSITY of CALIFORNIA at BERKELEY

Committee in charge:
Professor S. Shankar Sastry, Chair
Professor Jerrold E. Marsden
Professor Roberto Horowitz
Professor John F. Canny

1994

The dissertation of Gregory Charles Walsh is approved:

Chair Date

Date

Date

Date

University of California at Berkeley

1994

Planning and Feedback Control
for Mechanical Systems
with Nonholonomic Constraints

by
Gregory Charles Walsh

Abstract

Planning and Feedback Control
for Mechanical Systems
with Nonholonomic Constraints
by
Gregory Charles Walsh
Doctor of Philosophy in Engineering-Electrical Engineering and Computer Sciences
University of California at Berkeley
Professor S. Shankar Sastry, Chair

S. Shankar Sastry
Chair

The goal of this dissertation is to present a complete strategy for controlling a class of mechanical systems with nonholonomic velocity constraints. Examples considered in this dissertation include a simple wheeled mobile robot, a front wheel drive car, a tiller truck, a satellite mounted with thrusters, and a robot with one unactuated joint called the planar acrobot. Control objectives are limited to achieving some desired configuration. Several new methods are presented to achieve these objectives in efficient ways.

The process of control is broken down into three stages. Given a large initial offset between the configuration and its desired value, first an (optimal) path planner generates an admissible trajectory connecting the initial and desired configurations. Second, an exponentially stabilizing tracking law is applied, insuring that the desired trajectory is followed closely even in the presence of disturbances and modeling errors. Finally, when the configuration variable is near the desired value, we switch to a feedback law which renders the desired configuration asymptotically stable.

The five example mechanical systems, when examined in detail, are shown to have certain structural properties in common. In particular, all except the satellite mounted with

thrusters may be transformed locally into a form called the "Control Canonical Form". The planning, tracking, and regulation problems are solved for this canonical form. The results are then applied to the example systems. The satellite with thrusters, representative of a large class of mechanical systems, requires a different approach.

To my parents.

Contents

List of Figures

Acknowledgements

First and foremost, I would like to express my gratitude and appreciation to my advisor, Shankar Sastry, for his constant guidance, support, and advice. His enthusiasm is infectious, and my years working with him have proven him to be a scientist and a gentleman.

I also wish to express my gratitude to my readers, Professor Roberto Horowitz, Professor John Canny and especially Professor Jerrold Marsden. Jerry's thorough readings has earned him a place as a reader on all three of my graduate degrees. His work has been a great source of inspiration for me.

I would like to thank my recent co-authors, both professors and fellow graduate students. I am thankful for the opportunities I have had to work with people like Professor Richard Montgomery, Professor Richard Murray, Professor Andrew Teel, Professor Jean-Paul Laumond, Linda Bushnell and Dawn Tilbury. I would also like to take this space to thank the hosts of my two summers in France, namely G. Giralt and J.P. Laumond of LAAS, and D. Normond-Cyrot and J.P. Barbot of LSS. I also would like to thank the whole gang at LAAS, who made me welcome and helped me learn French.

I would like to recognize Professor Charles Desoer, who served on my qualifying exam committee, and who provided valuable advice on many occasions. I also wish to thank Professor Ron Fearing, with whom I designed and ran the course EECS192, Mechatronic Design. The Electronic Support Group was also exceeding helpful to this end.

Finally, I would like to acknowledge my debt to the National Science Foundation, who supported my efforts in graduate school first with a three year Graduate Fellowship, and later under grant IRI90-14490. My thanks also goes to the National Aeronautics and Space Administration, who supported me under grant NAG2-243 and the Army Research Office, who supported me under grant DAAL03-91-G0197.

There are many people who deserve my thanks and appreciation. Due to the limited space provided, I regret that I can only mention a handful of those deserving recognition.

Chapter 1

Introduction

The goal of this dissertation is to present a strategy for controlling a class of mechanical systems with nonholonomic velocity constraints. Control objectives are limited to reaching the neighborhood of a goal configuration and remaining in it despite disturbances. Several new methods are presented to achieve these ends in efficient ways.

The process of control is broken down into three stages. The initial configuration space error is, in general, large. First a path planner, optimal or suboptimal as detailed in chapter six, generates a valid trajectory connecting the initial and desired configurations. Second, the exponentially stabilizing tracking law described in chapter five is applied, insuring that this desired trajectory is followed closely even in the presence of disturbances and modeling errors. Finally, when nearby the desired configuration, we use the feedback law of chapter four which renders the desired configuration asymptotically stable.

1.1 Overview of the Dissertation

The dissertation is organized as follows. Chapter two considers methods for building first principle models of a certain class of mechanical systems and Lagrangian mechanics [2, 27] is used as the primary tool. Under certain structural assumptions found in almost every example system considered, the equations of motion are shown to have a canonical form (2.1). This canonical form is the kinematic model (2.3) with integrators attached to the velocity inputs. The inputs of these integrators, the accelerations, are related to the input torques and forces by a memoryless map. The example of the asymmetric satellite fails to fit this form, and is representative of a large class of mechanical systems. We keep

track of the example satellite throughout the dissertation.

Chapter three presents the example mechanical systems used. These systems include Hilare, a wheeled mobile robot, a car, a tiller truck, a satellite mounted with rockets, and a robot with one unactuated joint called the planar acrobot. All of these systems, except for the asymmetric satellite, may be written in a special set of coordinates where the dynamics take the power form (4.2).

Chapter four presents a general theory for explicitly constructing feedback control laws which render goal configurations asymptotically stable. The theory is applied to the car, the fire truck, and finally the satellite. Because the asymmetric satellite does not fit into the power form framework, the theory does not apply and an alternative approach is employed.

These point stabilization laws could be used essentially as large motion planners but are highly inefficient. The remaining two chapters focus on planning and executing large motions. First we address the tracking control problem. Given a desired trajectory, we wish to follow it reliably. The point stabilization laws may be adapted for tracking purposes by handing them a time series on goal configurations spaced along the desired trajectory. With nonlinear systems of this form, this modification tends to be both inadequate and inefficient. Consequently, we construct control laws especially suited to tracking in chapter five.

The final chapter addresses the problem of finding the feasible path. Path planning is inherently a kinematic problem for this class of systems and is studied in that context. Chapter six presents a collection of ad-hoc planners, each exploiting the particular geometry of the examples. A general method for power form systems is also discussed. Chapter six also considers a general method for producing optimal solutions. Optimal methods require the solution of a two-point boundary value problem, and in general are computationally intensive. Because the trajectory is computed before the motion (off line) and not during the motion, there is not a pressing need for computational simplicity.

In summary, we present a complete strategy and results for feedback control of mechanical systems with nonholonomic constraints. Modeling, path planning, tracking and point stabilization issues are addressed for a specific subclass of systems. The original work of the dissertation is concentrated in chapters four, five and six. Needless to say, there is much room for improvement. Point stabilizing control laws would be more robust with respect to disturbances if they had faster convergence rates. Generalizing these laws to larger classes; for example, a class of systems which includes the asymmetric satellite; is a

rich area of great promise. Tracking laws and optimal paths are numerically intensive to compute. By limiting their application to only a small subclass of relevant systems, we may be able to more explicitly solve these problems.

1.2 Notational Conventions

Traditionally the configuration space for a mechanical system is labeled Q with elements q. The configuration space is assumed to be a smooth n-dimensional manifold, with an associated atlas $\{\Phi^j\}$. A chart Φ^j maps elements of Q to $\mathbb{R}^n$, as long as $q \in U^j$, where U^j is an open set in Q. Sometimes the set U^j does not cover all of Q. This presents little difficulty when considering local issues like feedback control. Path planning, however, suffers when several charts must be used. The local view and coordinate chart changes obscure the path planning task.

The fact that all of the configuration spaces for the systems considered in this dissertation may be globally represented as matrix Lie groups gives us an alternative. In summary, for path planning we will use Lie group notation, for feedback control we will use local coordinates. Coordinate vectors in $\mathbb{R}^n$ will typically be written as lower case letters late in the alphabet like x, y, z. Lower case letters in the middle of the alphabet, like i, j, and k, will be indices. Lower case letters early in the alphabet, like a, b, g and h will be used to represent members of Lie groups. The groups themselves are represented by a script capital letter $\mathcal{G}$ and sometimes by $\mathcal{A}$. We often identify $T\mathcal{G}$ with $\mathcal{G} \times \mathfrak{g}$, and $T^*\mathcal{G}$ with $\mathcal{G} \times \mathfrak{g}^*$, where $\mathfrak{g}$ is the Lie algebra of $\mathcal{G}$ and $\mathfrak{g}^*$ its dual. The spaces $\mathfrak{g}, \mathfrak{g}^*$ are finite dimensional vector spaces, hence isomorphic to $\mathbb{R}^n$.

Elements of $\mathfrak{g}$ are denoted $\hat{e}$ or $\hat{\eta}$, with basis elements $\hat{e}_i$. The hat distinguishes the matrix from its corresponding vector representation, denoted E. More explicitly, the vector E is equal to $(E_1, \ldots, E_n)^T$ and given some $E \in \mathbb{R}^n$, the corresponding matrix in $\mathfrak{g}$ is $\hat{e} = \sum_{i=1}^n E_i \hat{e}_i$. Elements of $\mathfrak{g}^*$ are denoted $\hat{p}$, with basis elements $\hat{p}_i$. Thus given $\hat{e} \in \mathfrak{g}$, we have $E_i = \hat{p}_i(\hat{e})$. Again the hat distinguishes the linear operator on matrices, $\hat{p}$, from its corresponding co-vector, denoted P with respect to a basis. We write P as a covector equal to $(P_1, \ldots, P_n)$ where $P_i = \hat{p}(\hat{e}_i)$. Symmetries play an important role in some of the example systems. Symmetries in this dissertation are parameterized by a Lie group $\mathcal{A}$, with elements a and Lie algebra $\mathfrak{a}$. Elements of $\mathfrak{a}$ are labeled $\hat{a}$.

Partial and total derivatives pose notational challenges. We often take partials

of the Lagrangian, L with respect to vector arguments. Consider the Lagrangian written in coordinates $x = \Phi(q)$. The Lagrangian $L(x, \dot{x})$ is a function of two vectors $x = (x_1, \ldots, x_n)^T, \dot{x} = (\dot{x}_1, \ldots, \dot{x}_n)^T$. For the sake of clarity, we use a standard notation for writing the partial derivatives. Given the function $L(x, \dot{x})$, the partial with respect to the vector x is $\frac{\partial L}{\partial x}$. Note that both $\frac{\partial L}{\partial x}$ and $\frac{\partial L}{\partial \dot{x}}$ are row vectors. For example, the row vector $\frac{\partial L}{\partial x}$ is $(\frac{\partial L}{\partial x_1}, \ldots, \frac{\partial L}{\partial x_n})$. For the function $M(x, y, \dot{x}, \dot{y})$, the expression $\frac{\partial M}{\partial \dot{x}}$ is a row vector equal to $(\frac{\partial M}{\partial \dot{x}_1}, \ldots, \frac{\partial M}{\partial \dot{x}_n})$. An example double application would be $\frac{\partial^2 L}{\partial \dot{x} \partial \dot{x}}$, which in this case can be thought of in coordinates as a matrix. The ij^{th} element of this matrix with respect to some basis is equal to $\frac{\partial^2 L}{\partial \dot{x}_i \partial \dot{x}_j}$.

We now write the familiar Euler-Lagrange equations on $\mathbb{R}^n$ in this notation in order to see it in use. Consider the Lagrangian $L(x, \dot{x})$ with $x \in \mathbb{R}^n$.

$$\frac{d}{dt}\frac{\partial L}{\partial \dot{x}} - \frac{\partial L}{\partial x} = 0 \tag{1.1}$$

Note that this is a row (co-)vector equation. Expanding the full time derivative using the chain rule makes the need for the regularity condition clear.

$$\ddot{x}^T \frac{\partial^2 L}{\partial \dot{x} \partial \dot{x}} + \dot{x}^T \frac{\partial^2 L}{\partial x \partial \dot{x}} - \frac{\partial L}{\partial x} = 0 \tag{1.2}$$

To solve for $\ddot{x}$ we need to invert the mass matrix $\frac{\partial^2 L}{\partial \dot{x} \partial \dot{x}}$. A mechanical system always has a positive definite symmetric mass matrix. This condition is referred to as regularity.

A chart summarizes the notational conventions.

Symbol	Description	Elements
Q	Configuration Space	q
$\mathbb{R}^n$	local coordinates of Q	x
$\mathbb{R}^{(n-m)}$	alternate coordinates, "outputs"	y
$\mathbb{R}^m$	alternate coordinates, "zero dynamics"	z
$\mathcal{G}$	Lie Group	g
$\mathfrak{g}$	Lie algebra of $\mathcal{G}$	$\hat{e}, \hat{\eta}$
$\mathbb{R}^n$	Vector representation of $\mathfrak{g}$	E
$\mathfrak{g}^*$	dual of $\mathfrak{g}$	$\hat{p}, \hat{\omega}$
$(\mathbb{R}^n)^*$	co-vector representation of $\mathfrak{g}^*$	P
$\mathcal{A}$	Symmetry group	a
$\mathfrak{a}$	Lie algebra of $\mathcal{A}$	$\hat{a}$

Chapter 2

Mathematical Preliminaries

In this chapter we develop the tools needed for building models of the mechanical systems considered in this dissertation. To this end, we use the notions of Lagrangian mechanics with controls and actuators modeled as force producing mechanisms. A basic understanding of differential geometry, as presented for example in [38], is assumed.

The description of a mechanism $\mathcal{M}$ consists of four parts, $(Q, L, \mathcal{D}, \tau)$. The configuration space Q is an n-dimensional smooth manifold. The Lagrangian L is a real-valued function on TQ. The regular $n-m$ dimensional constraint distribution $\mathcal{D}$ is represented in terms of m linearly independent sections of T^*Q, $\Omega = \{\omega^1, \ldots, \omega^m\}$. Given any vector field $f \in \mathcal{D}$, $\omega^i(f) = 0$ for all i. Actuators and forces are written as p sections of $T^*Q, \{\tau^1, \ldots, \tau^p\}$. The force applied at some given instant is $\tau = \sum_{i=1}^{p} \tau^i \vartheta_i$, where $\vartheta \in \mathbb{R}^p$ is the control input.

The chapter is organized into three sections. The first section considers how to write the Euler-Lagrange equations in the different representations used in the dissertation. The second section studies how velocity constraints arise and how they affect the equations of motion. Finally, the third section presents two special sets of coordinates under which the example mechanical systems have a unified structure. These coordinates are valid if certain rank conditions on the input actuators τ^i are met.

The first special set of coordinates we call control canonical form:

$$\begin{aligned} \dot{x} &= \sum_{i=1}^{(n-m)} f_c^i(x) v_i \\ \dot{v} &= u \ , \end{aligned} \tag{2.1}$$

where the $f_c^i \in \mathcal{D}$ are linearly independent. The configuration variable x is in $\mathbb{R}^n$, and the velocity v is in $\mathbb{R}^{(n-m)}$. The input $u \in \mathbb{R}^{(n-m)}$ are the accelerations, which together with x and v determine the input forces and torques ϑ. The second special set of coordinates we denote control reduced:

$$\begin{aligned} \ddot{y} &= u \\ \dot{z} &= A(y,z)\dot{y} \ . \end{aligned} \tag{2.2}$$

The vector y is in $\mathbb{R}^{(n-m)}$ and the vector z is in $\mathbb{R}^m$. The matrix $A(y,z) \in \mathbb{R}^{(m\times(n-m))}$ is referred to as the connection matrix. As in the previous case, the inputs $u \in \mathbb{R}^{(n-m)}$, along with y and $\dot{y}$ determine the input forces and torques ϑ. That is, there exists a feedback law $\vartheta(y,\dot{y},u)$ under which the equations of motion take this form.

When planning trajectories, we dispense with the acceleration inputs and assume that we have direct control over the velocities v or $\dot{y}$. The reduced model is called kinematic. The equations of motion become

$$\dot{x} = \sum_{i=1}^{(n-m)} f_c^i(x) v_i \tag{2.3}$$

where v is considered the input. The control reduced equations have an analogous form.

There is a hidden assumption of interest. Our model of the actuators assumes we have unlimited control authority, which implies we can arbitrarily chose ϑ. In a real control system, ϑ is limited to a compact set. For our example systems, as long as the commanded acceleration is not too high and as long as the velocity of the vehicle is sufficiently low, we may ignore this constraint. However, outside of this regime, the feedback laws may demand a ϑ which exceeds the abilities of the actuators to deliver. For this reason it is not realistic to think of, for example, a front wheel drive car, in kinematic terms (2.3) if it moves at high speeds.

We assume the example mechanical systems are operated so that the constraints on ϑ are not violated. The dynamics of mechanisms and Lagrangian dynamics in general have long been [2] and currently are subjects of study [3, 27]. Results relevant to our example mechanical systems have been collected in this chapter for the reader's convenience.

2.1 Variational Calculus

It is assumed that the reader is familiar with variational calculus on $\mathbb{R}^n$ [2, 27]. This section is divided into three parts. We first consider diffeomorphisms of the configuration space, and how they affect the computation of the equations of motion. Second we examine which modifications are required when the configuration space is a matrix Lie group and the tangent bundle has been left trivialized. Finally, immersions into higher dimensional spaces are studied. It will be shown that restricting the allowable variations to those which satisfy the induced velocity constraints produces valid solution trajectories.

2.1.1 Diffeomorphisms

In this section we examine the effects of applying a diffeomorphism $x = f(y)$ to the equations of motion. We apply such diffeomorphisms for two reasons. First, the coordinates $x = \Phi(q)$ are in general only valid locally. Coordinate chart changes are required when $q(t)$ leaves the open region were the coordinate chart Φ is valid. Second, we sometimes change coordinates in order to change the equations of motion into, for example, the special forms (2.1), (2.2).

We write the forces, constraints, and Lagrangian in terms of the coordinate vector x and its time derivative $\dot{x}$. Thus for a fixed value of $x, \dot{x}$, and ϑ, $L(x, \dot{x})$ is a real number and τ is row vector. The solution trajectory $x(t)$ satisfies

$$\ddot{x}^T \frac{\partial^2 L}{\partial \dot{x} \partial \dot{x}} + \dot{x}^T \frac{\partial^2 L}{\partial x \partial \dot{x}} - \frac{\partial L}{\partial x} = \tau \tag{2.4}$$

according to the Lagrange-d'Alembert principle. Provided that $\frac{\partial^2 L}{\partial \dot{x} \partial \dot{x}}$ is non-singular, a fixed x, τ and $\dot{x}$ uniquely specifies $\ddot{x}$. The nonsingularity condition is referred to as regularity.

We may write the Lagrangian and forces in terms of the coordinate vector y and its time derivative $\dot{y}$. We now prove that if we apply the Lagrange-d'Alembert principle to the new Lagrangian and the new forces, the solution $y(t)$ produced solves the equation $x(t) = f(y(t))$ for $x(t)$ solving (2.4).

Proposition 1 (Lagrangians under Diffeomorphisms)
Given: $L : T\mathbb{R}^n \to \mathbb{R}$ regular, a set of forces τ and a diffeomorphism $x = f(y)$,
Define: the mapped Lagrangian $\tilde{L}$, $\tilde{L}(y, \dot{y}) = L(f(y), \frac{\partial f}{\partial y}\dot{y})$, and mapped forces $\tilde{\tau} = \tau \frac{\partial f}{\partial y}$,
Then: the trajectories generated by the application of the Euler-Lagrange

operator to $\tilde{L}, \tilde{\tau}$ are the same as those generated by the application of the Euler-Lagrange operator to L, τ.

Proof: We compute the application of the Euler-Lagrange operator to $\tilde{L}$ in terms of the previous Lagrangian L.

$$\begin{aligned} \frac{\partial \tilde{L}}{\partial \dot{y}} &= \frac{\partial L}{\partial \dot{x}} \frac{\partial f}{\partial y} \\ \frac{\partial \tilde{L}}{\partial y} &= \frac{\partial L}{\partial x} \frac{\partial f}{\partial y} + \frac{\partial L}{\partial \dot{x}} \left(\frac{d}{dt} \frac{\partial f}{\partial y} \right) \end{aligned} \tag{2.5}$$

Now compute $\frac{d}{dt} \frac{\partial \tilde{L}}{\partial \dot{y}}$.

$$\frac{d}{dt} \frac{\partial \tilde{L}}{\partial \dot{y}} = \left(\frac{d}{dt} \frac{\partial L}{\partial \dot{x}} \right) \frac{\partial f}{\partial y} + \frac{\partial L}{\partial \dot{x}} \left(\frac{d}{dt} \frac{\partial f}{\partial y} \right) \tag{2.6}$$

The resulting Euler-Lagrange equations, written in terms of L, are then given by:

$$\left(\frac{d}{dt} \frac{\partial \tilde{L}}{\partial \dot{y}} - \frac{\partial \tilde{L}}{\partial y} - \tilde{\tau} \right) = \left(\frac{d}{dt} \frac{\partial L}{\partial \dot{x}} - \frac{\partial L}{\partial x} - \tau(x) \right) \frac{\partial f}{\partial y} \tag{2.7}$$

Since f is a local diffeomorphism, the matrix $\frac{\partial f}{\partial y}$ is nonsingular. This implies that the $\ddot{x}$ which satisfies the equations derived from applying Euler Lagrange to $\tilde{L}$ is the same $\ddot{x}$ which satisfies the equations resulting from the application of Euler-Lagrange to L.

2.1.2 Variational calculus on matrix Lie groups

Viewing the configuration spaces of the mechanical systems considered in this dissertation as matrix Lie groups (see [34, 48] for more details of Lie groups) has two advantages. First, this representation is global in the examples considered, making this formulation attractive for path planning. Second, a matrix Lie group $\mathcal{G}$ has a trivial tangent bundle. This implies we may write second order differential equations which are valid for every configuration.

To clarify, we identify $T\mathcal{G}$ with $\mathcal{G} \times \mathfrak{g}$, where $\mathfrak{g}$, a finite dimensional vector space, is the Lie algebra of $\mathcal{G}$, using the left (body) identification of $T\mathcal{G}$. The velocity of the system is represented by $\hat{e} \in \mathfrak{g}$. The Euler-Lagrange equations imply a formula for the time derivative of $\hat{e}$ given $\hat{e}$ and $g \in \mathcal{G}$. This representation of the implicit differential equation is on a finite dimensional vector space and is valid for every configuration g. In summary,

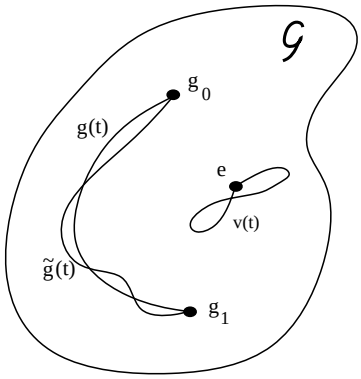

Figure 2.1: A small variation $\tilde{g}(t)$ of some nominal trajectory $g(t)$ is shown. Any variation may be expressed as $v(t)$, and for $v(t)$ close to e, there exists $\eta(t)$ close to zero such that $\mathrm{Exp}(\eta(t)) = v(t)$.

by exploiting the triviality of the tangent bundle, we have found a globally valid coordinate chart in which we may write the differential equations describing the motion. The difficulty with coordinate charts is minimized.

Some definitions are required. Elements g of an n-dimensional matrix Lie group $\mathcal{G}$ will be represented by $(k \times k)$ matrices with matrix multiplication as the group operation. An element $\hat{e} \in \mathfrak{g}$, the Lie algebra of $\mathcal{G}$, is also represented by a $(k \times k)$ matrix. The time derivative of the matrix g is written

$$\dot{g} \;=\; g\hat{e}\;. \tag{2.8}$$

We write the Lagrangian, the constraints, and the forces in terms of $\mathcal{G}$ and $\mathfrak{g}$. The Lagrangian $L(g, \hat{e})$, when evaluated at a particular g and $\hat{e}$, is a real number. The applied force $\hat{\tau}$ as well as partial derivatives of L with respect to its arguments are elements of $\mathfrak{g}^*$, the space of linear operators on $\mathfrak{g}$.

A small variation of a nominal trajectory $g(t)$ is denoted $\tilde{g}(t)$. The variation may be represented by $v(t) = g^{-1}(t)\tilde{g}(t)$. Since the variation is small, the matrix $v(t)$ is close to the identity. Therefore there exists a unique $\hat{\eta}(t)$ close to zero such that $v(t) = \mathrm{Exp}(\hat{\eta}(t))$. The trajectory $\hat{\eta}(t) \in \mathfrak{g}$ will represent the variation of $g(t)$.

We now compute the Euler-Lagrange equations in this special representation. We do so by first considering coordinate charts of $\mathcal{G}$. Note that $\frac{\partial \Phi}{\partial x}$ is a matrix valued linear function. Given some point $x, v \in T\mathbb{R}^n$, written $x = (x_1, \ldots, x_n)^T$ and $v = (v_1, \ldots, v_n)^T$, the

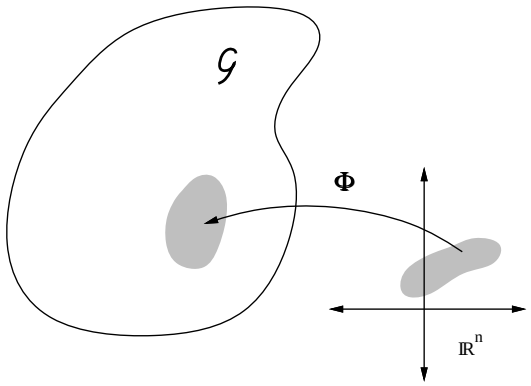

Figure 2.2: A local coordinate chart Φ of $\mathcal{G}$.

derivative of Φ at x in the direction of v is given by the sum of matrices $\sum_{i=1}^{n} \frac{\partial \Phi}{\partial x_i} v_i$. While the discussion below uses a local coordinate chart $g = \Phi(x)$ for $\mathcal{G}$ to compute the equations of motion, it demonstrates how this may be done in terms of the matrices representing the Lie group and the Lie algebra.

Proposition 2 (The Euler-Poincaré Equations [27])

Given: $L : \mathcal{G} \times \mathfrak{g} \to \mathbb{R}$ *regular, applied forces* $\hat{\tau} \in \mathfrak{g}^*$, *implicitly defining a set of Euler-Lagrange equations, and a coordinate chart* $g = \Phi(x)$, *for* $\mathcal{G}$,

Define: *the mapped Lagrangian* $\tilde{L}$, $\tilde{L}(x, \dot{x}) = L(\Phi(x), (\Phi)^{-1} \frac{\partial \Phi}{\partial x} \dot{x})$, *and the mapped applied forces* $\tilde{\tau} = \hat{\tau}((\Phi)^{-1} \frac{\partial \Phi}{\partial x})$,

Then: *the trajectories generated by applying the Euler-Lagrange operator to* $\tilde{L}$ *are the same as implied by (2.9) if we allow* $\hat{\eta}$ *to be arbitrary.*

$$\hat{\tau}(\hat{\eta}) = \left(\frac{d}{dt}\frac{\partial L}{\partial \hat{e}}\right)\hat{\eta} - \left(\frac{\partial L}{\partial g}\right)\hat{\eta} - \left(\frac{\partial L}{\partial \hat{e}}\right)[\hat{e}, \hat{\eta}] \tag{2.9}$$

Proof: We will compute the application of the Euler-Lagrange operator to $\tilde{L}$ in terms of the previous Lagrangian L.

$$\begin{aligned} \frac{\partial \tilde{L}}{\partial \dot{x}} &= \frac{\partial L}{\partial \hat{e}}(\Phi)^{-1}\frac{\partial \Phi}{\partial x} \\ \frac{\partial \tilde{L}}{\partial x} &= \frac{\partial L}{\partial g}(\Phi)^{-1}\frac{\partial \Phi}{\partial x} + \frac{\partial L}{\partial \hat{e}}(\Phi)^{-1}\left(\frac{d}{dt}\frac{\partial \Phi}{\partial x}\right) - \frac{\partial L}{\partial \hat{e}}(\Phi)^{-1}\frac{\partial \Phi}{\partial x}\hat{e} \end{aligned}$$

Now we need to compute $\frac{d}{dt}\frac{\partial \tilde{L}}{\partial \dot{x}} - \frac{\partial \tilde{L}}{\partial x}$. Note that:

$$\frac{d}{dt}\frac{\partial \tilde{L}}{\partial \dot{x}} = \left(\frac{d}{dt}\frac{\partial L}{\partial \hat{e}}\right)(\Phi)^{-1}\frac{\partial \Phi}{\partial x} - \frac{\partial L}{\partial \hat{e}}\hat{e}(\Phi)^{-1}\frac{\partial \Phi}{\partial x} + \frac{\partial L}{\partial \hat{e}}(\Phi)^{-1}\left(\frac{d}{dt}\frac{\partial \Phi}{\partial x}\right) . \tag{2.10}$$

Notice that two terms will cancel each other, another two will form the Lie bracket. The Euler-Lagrange equations are therefore

$$\begin{aligned}\left(\frac{d}{dt}\frac{\partial \tilde{L}}{\partial \dot{x}} - \frac{\partial \tilde{L}}{\partial x} - \tilde{\tau}\right) &= \left(\frac{d}{dt}\frac{\partial L}{\partial \hat{e}}\right)(\Phi)^{-1}\partial\Phi - \frac{\partial L}{\partial \hat{e}}\left[\hat{e}, (\Phi)^{-1}\partial\Phi\right] \\ &\quad -\frac{\partial L}{\partial g}(\Phi)^{-1}\partial\Phi - \hat{\tau}\left((\Phi)^{-1}\frac{\partial \Phi}{\partial x}\right)\end{aligned} \tag{2.11}$$

which is equivalent to (2.9). Given any arbitrarily chosen $\hat{\eta}$ there exists a unique $v \in \mathbb{R}^n$ with $v = (v_1, \ldots, v_n)^T$ such that $\hat{\eta} = (\Phi)^{-1}\left(\sum_{i=1}^n v_i \frac{\partial \Phi}{\partial x_i}\right)$.

Example (The Rigid Body): The configuration space for the rigid body is its orientation, which we represent by a three by three rotation matrix g. The space of all such rotation matrices is the Lie group $SO(3)$ with Lie algebra $so(3)$. Traditionally, the velocity of a rigid body is left (body) identified. The coordinate vector in $\mathbb{R}^3$ of the left identified Lie algebra element is referred to as the body angular velocity.

The body angular velocity is traditionally written ω and is regarded as a vector in $\mathbb{R}^3$. We write the corresponding Lie algebra element as $\hat{\omega}$. The map relating the two is

$$\hat{\omega} = \begin{bmatrix} 0 & -\omega_3 & \omega_2 \\ \omega_3 & 0 & -\omega_1 \\ -\omega_2 & \omega_1 & 0 \end{bmatrix} .$$

Since $\hat{\omega}$ is the left identified element, the time derivative of the matrix g is given by

$$\dot{g} = g\hat{\omega} . \tag{2.12}$$

The Lagrangian has a particularly simple form,

$$L(g, \omega) = \omega^T J \omega \tag{2.13}$$

where J is a positive definite symmetric matrix. Because it is symmetric, there exists an orthonormal basis in which it is diagonal. We assume ω is represented in terms of one of this basis (the principal axes). We label the diagonal elements of J by J_i.

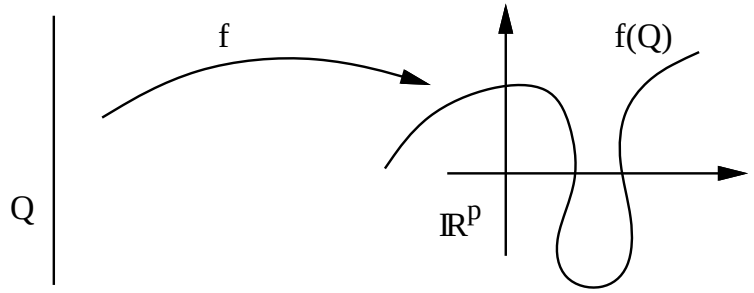

Figure 2.3: An immersion of the configuration space Q, seen in local coordinates.

First we need to calculate some terms,

$$\begin{aligned} \frac{\partial L}{\partial g}(g,\hat{\omega}) &= 0 \\ \frac{\partial L}{\partial \hat{e}}(g,\hat{\omega}) &= \widehat{J\omega} \ . \end{aligned}$$

We now apply the Euler-Lagrange operator to this Lagrangian.

$$\hat{\tau}(\hat{\eta}) = \left(\frac{d}{dt}\frac{\partial L}{\partial \hat{e}}(\hat{\eta}) - \frac{\partial L}{\partial g}(\hat{\eta}) - \frac{\partial L}{\partial \hat{e}}([\hat{\omega},\hat{\eta}]\right)$$

We now map the Lie algebra $so(3)$ to $\mathbb{R}^3$, and compute the equations of motion by chosing $\eta_i = e_i$, the standard basis elements in $\mathbb{R}^3$. We write,

$$\tau_i = J_i\dot{\omega}_i - (J\omega)^T(\omega \times e_i) \ ,$$

which is, using vector identities,

$$J\dot{\omega} = J\omega \times \omega + \tau \ . \tag{2.14}$$

These are the Euler equations for the rigid body.

2.1.3 Immersions of Q

Suppose we have an immersion of Q into a higher dimensional manifold M. In coordinates, it is given by a map $f : \mathbb{R}^n \to \mathbb{R}^p$, where $p > n$, written $y = f(x)$. Given a $y(t)$ in the image of Q under f, there exists locally a unique $x(t)$ such that $y(t) = f(x(t))$ for all time t. The time derivative of $x(t)$ is equal to $\frac{\partial f^{-1}}{\partial y}\dot{y}(t) = \left(\frac{\partial f}{\partial x}^T\frac{\partial f}{\partial x}\right)^{-1}\frac{\partial f}{\partial x}^T\dot{y}(t)$. Because f is an immersion the matrix $\frac{\partial f}{\partial x}$ is full rank, the matrix inverse is well defined. Using these observations, we define a mapped Lagrangian $\tilde{L}(y,\dot{y})$, using the lift of f^{-1}, and mapped forces $\tilde{\tau} = \tau\frac{\partial f^{-1}}{\partial y}$.

The equations of motion in higher dimensional space are found by taking variations only in directions which obey the implicit velocity constraints. What follows is a restatement of the covariance of the Euler-Lagrange equations, as noted by Lagrange.

Proposition 3 (Immersions of Q)

Given: $L : T\mathbb{R}^n \to \mathbb{R}$ *regular, implicitly defining a set of Euler-Lagrange equations, and a local immersion* $y = f(x)$, *where* $y \in \mathbb{R}^p$ *with* $p > n$,

Define: the mapped Lagrangian $\tilde{L}$, $\tilde{L}(y, \dot{y}) = L(f^{-1}(y), \frac{\partial f^{-1}}{\partial y}\dot{y})$, *and the mapped applied forces* $\tilde{\tau} = \tau \frac{\partial f^{-1}}{\partial y}$,

Then: the trajectories generated by a restricted application of the Euler-Lagrange operator to $\tilde{L}$ *are the same as the trajectories generated by the free application of the Euler-Lagrange operator to* L.

Proof: Again we compute the application of Euler Lagrange to $\tilde{L}$ in terms of the previous Lagrangian L. The formula is identical to the coordinate change case. The resulting Euler Lagrange equations, written in terms of L, are then given by:

$$\left(\frac{d}{dt}\frac{\partial \tilde{L}}{\partial \dot{y}} - \frac{\partial \tilde{L}}{\partial y} - \tilde{\tau}\right) = \left(\frac{d}{dt}\frac{\partial L}{\partial \dot{x}} - \frac{\partial L}{\partial x} - \tau\right)\frac{\partial f^{-1}}{\partial y} \tag{2.15}$$

So the only variations δy which restrict the above expression are those which are not contained in the null space of the matrix $\frac{\partial f^{-1}}{\partial y}$. Because of the holonomic constraint, the only allowable variations are given by $\delta y = \frac{\partial f}{\partial x}\delta x$. The product $\frac{\partial f^{-1}}{\partial y}\frac{\partial f}{\partial x}$ is the identity map. We conclude that the restricted application Euler-Lagrange to $\tilde{L}$ is equivalent to the free application of Euler Lagrange to L.

In conclusion, when computing the equations of motion in the space of the y's, we compute the Euler Lagrange equations as before and restrict only for the variations in the range of $\frac{\partial f}{\partial x}$, or if you wish, all directions satisfying (horizontal) the holonomic constraints implied by the immersion. The remaining degrees of freedom must be solved for using the constraint equations. This method of restricting the allowable variations is also referred to as the Lagrange-d'Alembert principle [3].

2.2 Symmetries and Constraints

Two more issues need addressing before writing the final system equations. First, the systems considered often have externally imposed velocity constraints which are not

holonomic. Second, the Lagrangian may have symmetries which, in turn, imply velocity constraints in the form of conservation laws. Understanding how these constraints change the equations of motion is the focus of this section.

2.2.1 Symmetries

Since we use both a Lie group setting and coordinates, we develop Noether's theorem [2, 27] for each. First we define what a symmetry is in coordinates. As before, a symmetry will be a mapping $h : \mathbb{R}^m \times \mathbb{R}^n \to \mathbb{R}^n$ where $\mathbb{R}^n$ is the configuration space in local coordinates and $\mathbb{R}^m$ is the symmetry group in local coordinates.

A mapping h is a symmetry of L if

$$L(h(y,x), \frac{\partial h}{\partial x}\dot{x}) \quad = \quad L(x,\dot{x}) \ . \tag{2.16}$$

The infinitesimal generator of the symmetry is written $d_1 h$, which is equal to $(\frac{\partial h}{\partial y})^T$.

There are both left and right infinitesimal generators in the general matrix Lie group setting. As before, we denote the Lagrangian $L(g,\hat{e})$, where $g \in \mathcal{G}$ and $\hat{e} \in \mathfrak{g}$. Also as before, we use the left (body) identification of the velocities, therefore $\dot{g} = g\hat{e}$.

A symmetry h is an action of a matrix Lie group $\mathcal{A}$ on $\mathcal{G}$. This map may be lifted onto $T\mathcal{G}$. For example, the map $\frac{\partial h}{\partial g}(a,g) : \mathfrak{g} \to T_{h(a,g)}\mathcal{G}$. In our context, we need the map from $\mathfrak{g} \to \mathfrak{g}$. The lift of $h(a,g)$ to $\mathcal{G} \times \mathfrak{g}$ follows.

$$\begin{aligned} h_\ell : \mathcal{A}, \mathcal{G}, \mathfrak{g} \quad &\to \quad \mathcal{G}, \mathfrak{g} \\ a, g, \hat{e} \quad &\to \quad h(a,g), (h(a,g))^{-1} \frac{\partial h}{\partial g}(a,g)\hat{e} \end{aligned} \tag{2.17}$$

Now we are ready to define a symmetry. A mapping $h : \mathcal{A} \times \mathcal{G} \to \mathcal{G}$ is a symmetry of L if

$$L(h(a,g), (h(a,g))^{-1} \frac{\partial h}{\partial g}(a,g)\hat{e}) \quad = \quad L(g,\hat{e}) \tag{2.18}$$

for all $a \in \mathcal{A}, g \in \mathcal{G}$, and $\hat{e} \in \mathfrak{g}$.

There are two instances of symmetries deserving attention. Often the map $h(a,g)$ may be separated, that is, may be written as $h(a)g$ (a right symmetry) or $gh(a)$ (a left symmetry). For the right (material) symmetry

$$g, \hat{e} \quad \to \quad h(a)g, \hat{e} \tag{2.19}$$

and for the left (space) symmetry,

$$g, \hat{e} \quad \to \quad gh(a), h^{-1}(a)\hat{e}h(a). \tag{2.20}$$

2.2.2 Conservation Laws

First we present Noether's theorem in coordinates [2], then we generalize it to the matrix Lie group setting [27]. Proofs are included for the reader's convenience.

Proposition 4 (Noether's Theorem in Coordinates [2, 27])
Given: $L : T\mathbb{R}^n \to \mathbb{R}$ *regular, implicitly defining a set of Euler-Lagrange equations, actuators* $\tau \in T^*\mathbb{R}^n$, *and symmetry* $h : \mathbb{R}^m \times \mathbb{R}^n \to \mathbb{R}^n$,
Then: *the scalar* $\frac{\partial L}{\partial \dot{x}}(d_1 h(e_i))$ *is a constant of the motion for every vector* e_i *in* $\mathbb{R}^m$, *for which* $\tau(d_1 h(e_i)) = 0$.

Proof: Consider first the meaning of symmetry.

$$\begin{aligned} 0 &= \frac{d}{d\epsilon}\left(L(h(y+\epsilon e_i, x), \frac{\partial h}{\partial x}(y+\epsilon e_i, x)\dot{x})\right)|_{\epsilon=0} \\ &= \frac{\partial L}{\partial x}(d_1 h(e_i)) + \frac{\partial L}{\partial \dot{x}}\left(e_i^T \frac{\partial^2 h}{\partial y \partial x}\dot{x}\right) \\ &= \frac{\partial L}{\partial x}(d_1 h(e_i)) + \frac{\partial L}{\partial \dot{x}}\left(\frac{d}{dt} d_1 h(e_i)\right) \end{aligned} \tag{2.21}$$

Using the Euler-Lagrange equations; namely, $\frac{\partial L}{\partial x}(\cdot) + \tau(\cdot) = \frac{d}{dt}\frac{\partial L}{\partial \dot{x}}(\cdot)$, in (2.21) we see

$$\begin{aligned} \tau(d_1 h(e_i)) &= \left(\frac{d}{dt}\frac{\partial L}{\partial \dot{x}}\right)(d_1 h(e_i)) + \frac{\partial L}{\partial \dot{x}}\left(\frac{d}{dt} d_1 h(e_i)\right) \\ &= \frac{d}{dt}\left(\frac{\partial L}{\partial \dot{x}}(d_1 h(e_i))\right) , \end{aligned} \tag{2.22}$$

which completes the proof.

For the Lie group setting, we first have to express the notion that derivatives of the Lagrangian with respect to the symmetry group $\mathcal{A}$ are zero. To do so, we introduce the infinitesimal generator of the symmetry. We can generate small left variations of a as follows:

$$\tilde{a}(\epsilon) = a \ \mathrm{Exp}(\epsilon \hat{a}). \tag{2.23}$$

where $\hat{a} \in \mathfrak{a}$, the Lie algebra of $\mathcal{A}$. Right variations can be generated in a similar manner. Define the left infinitesimal generator of the symmetry h by

$$\hat{\eta}_{\mathcal{A}}(\hat{a}) = h^{-1}(a, g)\frac{d}{d\epsilon}\left(h(a \ \mathrm{Exp}(\epsilon \hat{a}), g)\right)|_{\epsilon=0} \ . \tag{2.24}$$

To first order, we have $h\left(a\ \mathrm{Exp}(\hat{a}), g\right) \approx g\ \mathrm{Exp}(\hat{\eta}_{\mathcal{A}}(\hat{a}))$. Note that $\hat{\eta}_{\mathcal{A}}$ is a function of g, a and $\hat{a}$. Right infinitesimal generators may be defined in the same manner, with the first order approximation of h being $\mathrm{Exp}(\hat{\eta}_{\mathcal{A}}(\hat{a}))g$.

Proposition 5 (Noether's Theorem on the Left [27])

Given: $L : \mathcal{G} \times \mathfrak{g} \to \mathbb{R}$ *regular, implicitly defining a set of Euler-Lagrange equations, actuators* $\hat{\tau} \in \mathfrak{g}^*$*, and symmetry* $h : \mathcal{A} \times \mathcal{G} \to \mathcal{G}$*, with left infinitesimal generator* $\hat{\eta}_{\mathcal{A}}(\cdot)$*, mapping* $\mathcal{G} \times \mathcal{A} \times \mathfrak{a} \to \mathfrak{g}$*,*

Then: the scalar $\frac{\partial L}{\partial \hat{e}}(\hat{\eta}_{\mathcal{A}}(\hat{a}))$ *is a constant of the motion for every* $\hat{a} \in \mathfrak{a}$*, provided that* $\hat{\tau}(\hat{\eta}_{\mathcal{A}}(\hat{a})) = 0$.

Proof: The derivative of the Lagrangian with respect to a is zero. This and the Euler-Lagrange equations are all that are needed.

$$\begin{aligned} 0 &= \frac{d}{d\epsilon} L\left(h(\tilde{a}, g), (h(\tilde{a}, g))^{-1} \frac{\partial h}{\partial g}(\tilde{a}, g)\hat{e}\right)|_{\epsilon=0} \\ &= \frac{\partial L}{\partial g}(\hat{\eta}_{\mathcal{A}}) + \frac{\partial L}{\partial \hat{e}}\left(-\hat{\eta}_{\mathcal{A}} h^{-1} \frac{\partial h}{\partial g}\hat{e} + h^{-1}\frac{\partial^2 h}{\partial a \partial g}\hat{e}\right) \end{aligned} \tag{2.25}$$

Due to the Euler-Lagrange equations, we have along trajectories of the system

$$\frac{dL}{\partial g}(\cdot) + \hat{\tau}(\cdot) = \left(\frac{d}{dt}\frac{\partial L}{\partial \hat{e}}\right)(\cdot) - \frac{\partial L}{\partial \hat{e}}([h^{-1}\frac{\partial h}{\partial g}\hat{e}, \cdot]) \tag{2.26}$$

So we may write

$$\begin{aligned} \hat{\tau}(\hat{\eta}_{\mathcal{A}}) &= \left(\frac{d}{dt}\frac{\partial L}{\partial \hat{e}}\right)(\hat{\eta}_{\mathcal{A}}) - \frac{\partial L}{\partial \hat{e}}\left(h^{-1}\frac{\partial h}{\partial g}\hat{e}\hat{\eta}_{\mathcal{A}} - \hat{\eta}_{\mathcal{A}} h^{-1}\frac{\partial h}{\partial g}\hat{e}\right) + \frac{\partial L}{\partial \hat{e}}(-\hat{\eta}_{\mathcal{A}} h^{-1}\frac{\partial h}{\partial g}\hat{e} + h^{-1}\frac{\partial^2 h}{\partial a \partial g}\hat{e}) \\ &= \left(\frac{d}{dt}\frac{\partial L}{\partial \hat{e}}\right)(\hat{\eta}_{\mathcal{A}}) + \frac{\partial L}{\partial \hat{e}}\left(\frac{d}{dt}(\hat{\eta}_{\mathcal{A}})\right) \\ &= \frac{d}{dt}\left(\frac{\partial L}{\partial \hat{e}}(\hat{\eta}_{\mathcal{A}})\right) \end{aligned} \tag{2.27}$$

The proof is then complete.

Remark (Noether's Theorem on the Right): Suppose we have defined a right infinitesimal generator $\hat{\eta}_{\mathcal{A}}$. Using the relation that the left infinitesimal generator of the right action is equal to $h^{-1}\hat{\eta}_{\mathcal{A}} h$, we see that $\frac{\partial L}{\partial \hat{e}}(h^{-1}\hat{\eta}_{\mathcal{A}} h)$ are constants of the motion for all $\hat{a} \in \mathfrak{a}$.

Example (The Rigid Body): The rigid body has a right (material) symmetry with symmetry group $SO(3)$. For some $a \in SO(3)$, the map $h(a, g)$ is given by

$$h(a, g) = ag \ . \tag{2.28}$$

The lift of h does not change the left (body) angular velocity, and since the Lagrangian $L(g, \omega)$ is not dependent on g, it is preserved by the lift of h. We assume that $\hat{\tau} = 0$.

To find the conserved quantities, we need to compute the infinitesimal generator of the action h. The right infinitesimal generators for the right symmetry can be represent by the basis elements $\hat{e}_i$ of $so(3)$. As noted before, the left generator in terms of the right generator is $g^{-1}\hat{e}_i g$. Thus we have $\frac{\partial L}{\partial \hat{e}}(g^{-1}\hat{e}_i g)$ is conserved for each basis element $\hat{e}_i$. Expressed in vector form we have

$$\begin{aligned} \frac{\partial L}{\partial \hat{e}}(g^{-1}\hat{e}_i g) &= (J\omega)^T g^T e_i \\ &= e_i^T (gJ\omega) \ . \end{aligned} \tag{2.29}$$

The vector $gJ\omega$ is the spatial angular momentum of the rigid body. For this reason, the map generated by Noether's theorem is sometimes referred to as the momentum map [27].

Remark (Internal Forces): The rate of change with respect to time of the conserved quantities in the presence of applied forces is equal to $\tau(\hat{\eta}_{\mathcal{A}}(\cdot))$, where $\tau \in \mathfrak{g}^*$ is the applied force. Forces for which $\tau(\hat{\eta}_{\mathcal{A}}(\cdot)) = 0$ for all $\hat{a} \in \mathfrak{a}$ are called internal. They do not affect the conserved quantities.

Remark (Affine Velocity Constraints): Noether's theorem normally is viewed as generating a momentum map, J, mapping $T\mathcal{G}$ to $\mathfrak{a}^*$ [27], where the value of J is a constant of the motion. However, for a fixed momentum in $\mathfrak{a}^*$, it can also be seen as generating an affine constraint on the allowable configuration space velocities.

2.2.3 Kinematic Constraints

Not all velocity constraints arise from conservation laws. Some of the systems studied in this dissertation have nonholonomic kinematic constraints. Such constraints are generated typically by requirements that a contact not slide. For example, consider

a rolling wheel: the frictionally induced requirement that it not slide sideways imposes a nonholonomic kinematic constraint.

In coordinates we may write the constraints as a collection of m row vectors $\omega_i = (\omega_i^1(x), \ldots, \omega_i^n(x))$, linearly independent at each x. A nominal trajectory $x(t)$ is said to satisfy these constraints if $\omega_i \dot{x}(t) = 0$ for all i. In the Lie group context, such constraints may be written as sections of $\mathfrak{g}^*$, that is, a collection of m functions $\omega_i : \mathcal{G} \to \mathfrak{g}^*$. A trajectory $g(t)$ is said to satisfy the velocity constraints if $\omega_i \left(g^{-1}(t)\dot{g}(t)\right) = 0$ for all i and t.

We apply the Lagrange-d'Alembert principle to model the dynamics of the system [3]. A nominal solution $x(t)$ is considered valid if it satisfies the velocity constraints ω_i and if it extremizes the Lagrangian with respect to variations which also satisfy the ω_i. The variational argument only produces $2n - m$ equations, so the constraints must be added to make a complete description of the system. We will consider computing the equations of motion in coordinates.

Consider a local diffeomorphism $x = \Phi(y, z)$, with $z \in \mathbb{R}^m$ and $y \in \mathbb{R}^{(n-m)}$. The chart is chosen so that we map the constraints ω to $\omega = dz - A(y, z)dy$. The matrix $A(y, z)$ is as defined in (2.2). The Lagrangian in these set of coordinates is $L(y, z, \dot{y}, \dot{z})$, and the forces divide into τ_1, which operates on $\dot{y}$, and τ_2 which operates on $\dot{z}$. We can always construct locally this kind of chart by considering any locally valid set of coordinates x, reordering the coordinate functions in a non-unique way, and dividing by a nonsingular coefficients matrix.

Allowable variations are parameterized by δy, and are given by $(\delta y, A\delta y)$. Thus the restricted Euler Lagrange equations are

$$\tau_1 + \tau_2 A = \left(\frac{d}{dt}\frac{\partial L}{\partial \dot{y}} - \frac{\partial L}{\partial y}\right) + \left(\frac{d}{dt}\frac{\partial L}{\partial \dot{z}} - \frac{\partial L}{\partial z}\right) A \; . \tag{2.30}$$

We now expand (2.30) in order to solve for $\ddot{y}$ in terms of $y, z, \dot{y}$. Once we have $\ddot{y}$, we may evolve the system of equations using the connection form. That is to say,

$$\dot{z} = A(y, z)\dot{y} \; . \tag{2.31}$$

Expanding the equations above we see

$$\begin{aligned} \tau_1 + \tau_2 A = \; & \dot{y}^T \frac{\partial^2 L}{\partial y \partial \dot{y}} + \dot{z}^T \frac{\partial^2 L}{\partial z \partial \dot{y}} + \ddot{y}^T \frac{\partial^2 L}{\partial \dot{y} \partial \dot{y}} + \ddot{z}^T \frac{\partial^2 L}{\partial \dot{z} \partial \dot{y}} \\ & + \dot{y}^T \frac{\partial^2 L}{\partial y \partial \dot{z}} A + \dot{z}^T \frac{\partial^2 L}{\partial z \partial \dot{z}} A + \ddot{y}^T \frac{\partial^2 L}{\partial \dot{y} \partial \dot{z}} A + \ddot{z}^T \frac{\partial^2 L}{\partial \dot{z} \partial \dot{z}} A \\ & - \left(\frac{dL}{\partial y} + \frac{\partial L}{\partial z} A\right) \; . \end{aligned} \tag{2.32}$$

Differentiate (2.31) to obtain an expression for $\ddot{z}$ in terms of $y, z, \dot{y}$. We find that $\ddot{z} = (\frac{d}{dt}A)\,\dot{y} + A\ddot{y}$. Thus we may write that

$$\ddot{y}^T M(y,z,\dot{y}) + N(y,z,\dot{y}) \;=\; \tilde{\tau} \tag{2.33}$$

where

$$\begin{aligned}
M(y,z,\dot{y}) &= \left(\frac{\partial^2 L}{\partial\dot{y}\partial\dot{y}} + A^T\frac{\partial^2 L}{\partial\dot{z}\partial\dot{y}} + \frac{\partial^2 L}{\partial\dot{y}\partial\dot{z}}A + A^T\frac{\partial^2 L}{\partial\dot{z}\partial\dot{z}}A\right)\\
N(y,z,\dot{y}) &= \dot{y}^T\left(\frac{\partial^2 L}{\partial y\partial\dot{y}} + A^T\frac{\partial^2 L}{\partial z\partial\dot{y}} + \frac{\partial^2 L}{\partial y\partial\dot{z}}A + A^T\frac{\partial^2 L}{\partial z\partial\dot{z}}A\right)\\
&\quad +\dot{y}^T\left(\frac{d}{dt}A\right)^T\left(\frac{\partial^2 L}{\partial\dot{z}\partial\dot{y}} + \frac{\partial^2 L}{\partial\dot{z}\partial\dot{z}}A\right)\\
&\quad -\left(\frac{\partial L}{\partial y} + \frac{\partial L}{\partial z}A\right)\\
\tilde{\tau} &= \tau_1 + \tau_2 A
\end{aligned} \tag{2.34}$$

The regularity condition is now explicitly obvious. We require that $M(y,z,\dot{y})$ be an invertible matrix in order to solve for $\ddot{y}$.

2.3 Reduction

In this section we exploit the structure that velocity constraints impose upon a mechanical system. We find coordinate charts and an actuator feedback which reduces the dimensionality of the system. The procedure of reduction is well known [20, 27, 28].

First, if the velocity constraints are holonomic, there exists special sets of coordinates, (y,z) in which $z = f(y)$ for a function f. The equations of motion are found by applying the Euler-Lagrange operator to the Routhian [28], a real-valued function of y and $\dot{y}$. In this case the Routhian happens to be the Lagrangian. To reconstruct the trajectory from $y(t)$, we apply the formula $z = f(y)$.

In the final section we handle the general case which includes possibly nonholonomic velocity constraints. Provided some conditions on the input actuators are met, there exists special coordinates in which we may solve for $y(t)$ independently of $z(t)$. Such reduction, however, requires feedback control. To reconstruct the trajectory from $y(t)$ we integrate the connection. In general, the connection is dependent on y, $\dot{y}$, and z. If there is no dependence on z, well call the reduction principal.

2.3.1 Holonomic Reduction

Suppose the constraints Ω are holonomic. Then there exists coordinates $x = \Phi(y, z)$ for $\mathbb{R}^n$ where in the position in z space, known as the fiber, is a function of the position y space, known as the base. Thus we write

$$z = f(y) \tag{2.35}$$

and further the velocity constraint maps to

$$\dot{z} = \frac{\partial f}{\partial y}\dot{y}. \tag{2.36}$$

We will substitute these formulas directly into the Lagrangian, forming a reduced Lagrangian $\tilde{L}$. The implicitly defined differential equation resulting from the application of the Euler-Lagrange equations to the reduced Lagrangian will be shown to be identical to the equations implied by the restricted variational principle of the last section.

Proposition 6 (Holonomic Reduction)
Given: $L : T\mathbb{R}^n \to \mathbb{R}$ *regular, applied forces* τ, *and a set of holonomic velocity constraints* ω_i
Then: there exists a diffeomorphism $x = \Phi(y, z)$, *a reduced Lagrangian* $\tilde{L}(y, \dot{y})$, *and mapped applied forces* $\tilde{\tau} = \tau_1 + \tau_2 \frac{\partial f}{\partial y}$, *such that the trajectories generated by applying freely the Euler-Lagrange operator to* $\tilde{L}$ *are the same as those generated by the restricted application of the Euler-Lagrange operator on* L.

Proof: We have already selected a diffeomorphism $x = \Phi(y, z)$ and shown that we may lift the map Φ and make an equivalent Lagrangian $L(y, z, \dot{y}, \dot{z})$. In these coordinates, the restricted variational principle states:

$$\tau_1 + \tau_2 \frac{\partial f}{\partial y} = \left(\frac{d}{dt}\frac{\partial L}{\partial \dot{y}} - \frac{\partial L}{\partial y}\right) + \left(\frac{d}{dt}\frac{\partial L}{\partial \dot{z}} - \frac{\partial L}{\partial z}\right)\frac{\partial f}{\partial y}\ . \tag{2.37}$$

Some detail remains to be sorted, of course, because the terms involving $\ddot{z}$ have not been removed. This attention will be proven unneeded.

We now write the reduced Lagrangian $\tilde{L}(y, \dot{y})$ by substituting in the formulas for z and for $\dot{z}$.

$$\tilde{L}(y, \dot{y}) = L(y, f(y), \dot{y}, \frac{\partial f}{\partial y}\dot{y}) \tag{2.38}$$

The Euler-Lagrange equations, in local coordinates, state that $\frac{d}{dt}\frac{\partial \tilde{L}}{\partial \dot{y}} - \frac{\partial \tilde{L}}{\partial y} = \tau_1 + \tau_2 \frac{\partial f}{\partial y}$. For comparison, we need to compute this in terms of the unreduced Lagrangian L. First, the individual terms.

$$\begin{aligned} \frac{\partial \tilde{L}}{\partial \dot{y}} &= \frac{\partial L}{\partial \dot{y}} + \frac{\partial L}{\partial \dot{z}}\frac{\partial f}{\partial y} \\ \frac{\partial \tilde{L}}{\partial y} &= \frac{\partial L}{\partial y} + \frac{\partial L}{\partial z}\frac{\partial f}{\partial y} + \frac{\partial L}{\partial \dot{z}}\left(\frac{d}{dt}\frac{\partial f}{\partial y}\right) \end{aligned} \tag{2.39}$$

Thus we have,

$$\begin{aligned} \tau_1 + \tau_2 \frac{\partial f}{\partial y} &= \frac{d}{dt}\left(\frac{\partial L}{\partial \dot{y}} + \frac{\partial L}{\partial \dot{z}}\frac{\partial f}{\partial y}\right) - \frac{\partial L}{\partial y} - \frac{\partial L}{\partial z}\frac{\partial f}{\partial y} - \frac{\partial L}{\partial \dot{z}}\left(\frac{d}{dt}\frac{\partial f}{\partial y}\right) \\ &= \left(\frac{d}{dt}\frac{\partial L}{\partial \dot{y}} - \frac{\partial L}{\partial y}\right) + \left(\frac{d}{dt}\frac{\partial L}{\partial \dot{z}} - \frac{\partial L}{\partial z}\right)\frac{\partial f}{\partial y} + \left(\frac{\partial L}{\partial \dot{z}} - \frac{\partial L}{\partial \dot{z}}\right)\left(\frac{d}{dt}\frac{\partial f}{\partial y}\right) \end{aligned} \tag{2.40}$$

The term involving $\left(\frac{d}{dt}\frac{\partial f}{\partial y}\right)$ is cancelled, making the resulting equations identical to the constrained variation equations.

Given a set of holonomic constraints, we may simply insert them into the Lagrangian and compute the Euler Lagrange equations on the reduced space. If we did not notice the constraints were holonomic and applied the Euler Lagrange equations with restricted variations, our solution trajectories would not change. The trajectory $x(t)$ may be computed from $y(t)$, that is $x(t) = \Phi(y(t), f(y(t)))$.

2.3.2 Maximally Actuated Systems

No matter where the velocity constraints derive from, we will write the equations of motion for the actuated system in a special form (2.1). Under a set of mild conditions on the actuators τ^k, there exists a feedback law $\vartheta(x, \dot{x}, u)$ such that the equations of motion take the form

$$\begin{aligned} \dot{x} &= \sum_{i=1}^{(n-m)} f_c^i(x) v_i \\ \dot{v} &= u \end{aligned} \tag{2.41}$$

where the linearly independent vector fields $f_c^i(x)$ null the row vectors $\omega_i(x)$ for all x, the vector $v(t) \in \mathbb{R}^{(n-m)}$ are the velocities, input vector $u(t) \in \mathbb{R}^{(n-m)}$ are the accelerations. We may also express this differential equation in matrix Lie group notation. Given some chart $g = \Phi(x)$, we pick $(n-m)$ $\mathfrak{g}$-valued functions of $\mathcal{G}$ so that $f_c^i(x) = (\partial\Phi)^{-1}\Phi\hat{e}_c^i(\Phi)v_i$.

The dynamics in the Lie group setting then take the form

$$\begin{aligned} \dot{g} &= g(\sum_{i=1}^{(n-m)} \hat{e}_c^i(g)v_i) \\ \dot{v} &= u \ . \end{aligned} \tag{2.42}$$

where v, u are the velocities and inputs of equation (2.41). We state the result in the form of a proposition, in coordinates.

Proposition 7 (Maximally Actuated Systems)

Given: $L : T\mathbb{R}^n \to \mathbb{R}$ *regular,* m *1-form constraint equations* $\omega_k = 0$,
and a collection of actuators τ^j,

Choose:a basis of $(n-m)$ *linearly independent vector fields*
functions f_c^i *satisfying the constraints* ω_i,

Then: if the matrix $B_{ij} = \tau_j(f_c^i)$, *where* $B(x) \in \mathbb{R}^{p\times(n-m)}$ *is full rank for all* $x \in \mathbb{R}^n$, *there exists a smooth control* $\vartheta(x, \dot{x}, u)$ *such that the system evolves as described in (2.41).*

Systems with a full rank B are called maximally actuated.

Proof: The vector $v \in \mathbb{R}^{n-m}$ parameterizes the allowable variations. We have simply defined an isomorphism of the velocities. We need to compute $\dot{v}$, and pick τ so that the theorem is satisfied. First we build a special set of coordinates.

In any particular set of coordinates x, write the form constraints with respect to this basis. Label the j^{th} coordinate function of ω_i by $\omega_{ij}(x)$. The matrix $\Omega(x)$ describes all of the form constraints.

$$\Omega(x) = \begin{bmatrix} \omega_{11}(x) & \cdots & \omega_{1n}(x) \\ \vdots & & \vdots \\ \omega_{m1}(x) & \cdots & \omega_{mn}(x) \end{bmatrix}. \tag{2.43}$$

By regularity we have that $\Omega(x)$ is of full rank. By a non-unique reordering of the basis, we may assume that $\Omega(x) = [\Omega^1(x)\Omega^2(x)]$ where $\Omega^2(x)$ is a $m \times m$ matrix nonsingular for some neighborhood $U \in \mathbb{R}^n$. Now we are ready to define our local diffeomorphism. Set $y = (x_1, \cdots, x_{n-m})^T$ and $z = (x_{n-m+1}, \cdots, x_n)^T$. This clearly defines a diffeomorphisms.

The form constraints can then be written

$$\dot{z} = A(y, z)\dot{y} \tag{2.44}$$

where $A(y,z) = -\left(\Omega^2\right)^{-1}\Omega^1$ and is also known as the connection matrix. Certainly there exists a locally non-singular matrix $C(y,z)$ so that $\dot{y} = C(y,z)v$. Thus we have that $\ddot{y} = C(y,z)\dot{v} + \left(\frac{d}{dt}C(y,z)\right)v$. Substituting this into (2.33), we know that

$$\dot{v}^T C^T(y,z) M(y,z,v) - \tilde{N}(y,z,v) \;=\; \tilde{\tau}\ . \tag{2.45}$$

where $\tilde{N} = N + v^T\left(\frac{d}{dt}C(y,z)M(y,z,v)\right)^T$. The force applied, $\tilde{\tau}$, is a row vector with components

$$\tilde{\tau}^k \;=\; \sum_{i=1}^{p} \vartheta_i \tilde{\tau}^i(f_c^k) \tag{2.46}$$

which may be written as $\tilde{\tau} = \vartheta B(y,z,v)$. If the matrix $B(y,z,v) \in \mathbb{R}^{p\times(n-m)}$ is full rank, set

$$\vartheta(y,z,v,u) \;=\; \left(u^T C(y,z)M(y,z,v) - \tilde{N}(y,z,v)\right) B^{\dagger}(y,z,v)\ . \tag{2.47}$$

Under this set of inputs, we see that $\dot{v} = u$. The system evolves according to (2.41), whether written in Lie group form or in coordinates. The rank condition on B can usually be checked by inspection.

Remark (Controlled Reduction): The set of coordinates (y,z) are special. We could have chosen ϑ so that $\ddot{y} = u$. A system under this set of coordinates with this feedback law is called control reduced,

$$\begin{aligned} \ddot{y} &= u \\ \dot{z} &= A(y,z)\dot{y}\ . \end{aligned} \tag{2.48}$$

We may evolve the equations for y without regards to the variables z. The variables z may be reconstructed at a later time by integrating the connection matrix.

Remark (Principal Systems): If the connection matrix A is not a function of z, then such a system is called principal. All systems in chained form are principal, as are all examples used in this thesis except for the asymmetric satellite, which presents a new challenges.

Remark (Input-Output Linearization): The procedure just outlined is of course input-output linearization with a very careful choice of output functions, y. All outputs are relative degree two, which might be expected in a mechanical system. The dynamics z correspond to the zero dynamics, and are always stable because of the nature of the connection.

Chapter 3

Example Systems

We now introduce a collection of example mechanical systems. Hilare, a mobile robot developed at LAAS in Toulouse, France, provides us with a simple model of a nonholonomic mechanical system with a three state configuration space and two control torques. A front wheel drive car is slightly more complicated, having four dimensional configuration space and two input actuators. A fire truck is also considered, with a six dimensional configuration space and three input actuators. Other applications besides mobile robots have nonholonomic constraints. We will consider a satellite mounted with rocket thrusters, providing two input torques, and a three linked robot with a free joint called the planar acrobot.

Thanks to the work of chapter two, there are no obtuse conditions to check in order to write the equations of motion. All we need to do is check if the system is maximally actuated, which is usually done by inspection. We may then write the equations of motion in control canonical form (2.1) with state x, unless coordinates charts are a problem as is the case with the satellite. All of the models are second order. However, since controlling a velocity through an integrator is a well understood problem, the kinematic analysis (2.3) found in the literature is justified for the systems that can be written in control canonical form, as long as the mechanism is operated in a regime where the feedback laws demand attainable ϑ.

We then choose relative degree 2 outputs labeled y, and input-output linearize the system with respect to them. The zero (remaining) dynamics (labeled with z) are then computed. Careful choice of outputs y will ensure the examples are control reduced. For all cases except the asymmetric satellite, this will also be principal. The equations of motion

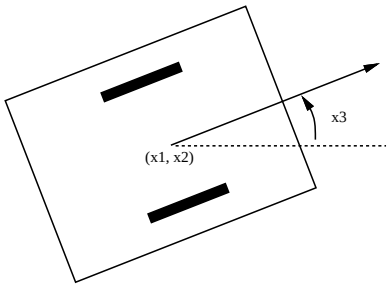

Figure 3.1: Model of the mobile robot Hilare.

will locally reduce to:

$$\begin{aligned} \ddot{y} &= u \\ \dot{z}_j^k &= \frac{1}{k!}\left(y_0\right)^k \dot{y}_j \quad 1 \leq k \leq \ell_j,\ 1 \leq j \leq p\ . \end{aligned} \tag{3.1}$$

3.1 Hilare

Hilare is a wheeled mobile robot created at LAAS, Laboratoire d'Automatique et d'Analyse des Systèmes, located in Toulouse, France [23]. This robot has two parallel wheels which can be controlled independently. By commanding the same velocity to both wheels, the robot moves in a straight line. By commanding velocities with the same magnitude but opposite directions, the robot pivots about its axis. Although the actual input is the acceleration, we first perform the kinematic analysis and check for maximal actuation. See Figure 3.1 for a diagram of Hilare. The control canonical form of Hilare's dynamics is as follows. The vector v is the velocity vector of the system.

$$\begin{aligned} \begin{bmatrix} \dot{x}_1 \\ \dot{x}_2 \\ \dot{x}_3 \end{bmatrix} &= \begin{bmatrix} \cos(x_3) \\ \sin(x_3) \\ 0 \end{bmatrix} v_1 + \begin{bmatrix} 0 \\ 0 \\ 1 \end{bmatrix} v_2 \\ \dot{v} &= u \end{aligned} \tag{3.2}$$

Note from Figure 3.1 that the coordinates (x_1, x_2) represent the position of the robot in the plane, and $x_3 \in S^1$ is its orientation. Consequently, the configuration space Q is $\mathbb{R}^2 \times S^1$. The configuration space may also be viewed as the Lie group $SE(2)$. This fact is explained in more detail in chapter 6. The wheels provide our two input torques, and the system

is clearly maximally actuated. We can thus find a smooth control law so that $\dot{v} = u$, the inputs.

3.1.1 Input-Output Linearization

We now consider a choice of output functions y.

$$\begin{aligned} y_0 &= \cos(x_3)x_1 + \sin(x_3)x_2 \\ y_1 &= x_3 \end{aligned} \tag{3.3}$$

The dynamics of y can be computed by differentiation.

$$\begin{aligned} \dot{y} &= \begin{bmatrix} 1 & -\sin(x_3)x_1 + \cos(x_3)x_2 \\ 0 & 1 \end{bmatrix} v \\ &= D(x)v \\ \ddot{y} &= f_0(x, \dot{x}) + D(x)u \end{aligned} \tag{3.4}$$

The matrix $D(x)$ is the decoupling matrix for this choice of outputs. Its determinant is 1. Under the choice of inputs $u = D^{-1}(x)\left(\tilde{u} - f_0(x, \dot{x})\right)$, the output dynamics decouple.

$$\ddot{y} = \tilde{u} \tag{3.5}$$

This is a four state linear system. The remaining state is a zero dynamic under this feedback, meaning it is not observed through the outputs.

3.1.2 Zero Dynamics

There is only one state left. We will chose the z coordinate as to make $x = \Phi(y, z)$ a global diffeomorphism.

$$z = \sin(x_3)x_1 - \cos(x_3)x_2 \tag{3.6}$$

The dynamics can be computed by differentiation.

$$\begin{aligned} \dot{z} &= \left(\cos(x_3)x_1 + \sin(x_3)\right) v_2 \\ &= y_0 \dot{y}_1 \end{aligned} \tag{3.7}$$

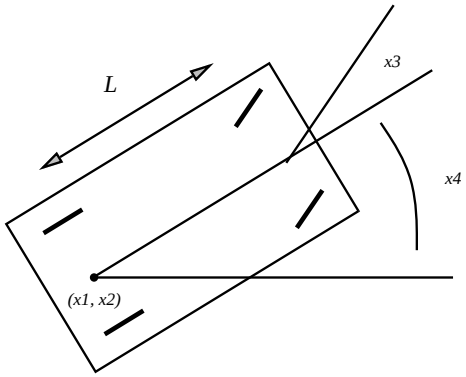

Figure 3.2: The front wheel drive car.

The system is then principal under this choice of feedback. It is in fact a power form, dynamics given by,

$$\begin{aligned} \ddot{y} &= \tilde{u} \\ \dot{z} &= y_0 \dot{y}_1 \ . \end{aligned} \tag{3.8}$$

3.2 The Front Wheel Drive Car

We consider now a front-wheel drive car. This system is also controllable [31], although two levels of Lie brackets must be taken to show this. We first consider the kinematic model. A sketch of the car is found in Figure 3.2.

The dynamics, in control canonical form, of the front wheel drive car are

$$\begin{aligned} \begin{bmatrix} \dot{x}_1 \\ \dot{x}_2 \\ \dot{x}_3 \\ \dot{x}_4 \end{bmatrix} &= \begin{bmatrix} \cos(x_4) \\ \sin(x_4) \\ 0 \\ \frac{1}{L}\tan(x_3) \end{bmatrix} v_1 + \begin{bmatrix} 0 \\ 0 \\ 1 \\ 0 \end{bmatrix} v_2 \\ \dot{v} &= u \end{aligned} \tag{3.9}$$

where $(x_1, x_2) \in \mathbb{R}^2$ is the position of the car in the plane, $x_3 \in S^1$ is the angle of the front wheels with respect to the car (or the steering wheel angle), $x_4 \in S^1$ is the orientation of the car with respect to some reference frame, and the constant L is the length of the wheel base. The configuration space Q of the car is then $\mathbb{R}^2 \times T^2$. The configuration space may

be viewed as the product of Lie groups $SE(2)$ and S^1. The system is clearly maximally actuated.

3.2.1 Input-Output Linearization

Assume without loss of generality that L = 1. Consider the choice of outputs given below.

$$\begin{aligned} y_0 &= x_1 \\ y_1 &= \sec^3(x_4)\tan(x_3) \end{aligned}$$

As before, simple differentiation yields the dynamics.

$$\begin{aligned} \dot{y} &= \begin{bmatrix} \cos(x_4) & 0 \\ -3\sec^3(x_4)\tan(x_4)\tan^2(x_3) & \sec^3(x_4)\sec^2(x_3) \end{bmatrix} v \\ &= D(x)v \\ \ddot{y} &= f_0(x) + D(x)u \end{aligned} \tag{3.10}$$

The decoupling matrix has determinant $\sec^2(x_3)\sec^2(x_4)$. The determinant is zero when the front wheels are oriented perpendicular to the body, or when the car is oriented perpendicular to the world frame. Away from this subset of configurations, the matrix is invertible. In particular, it is invertible near $x = 0$. Choose inputs $u = D^{-1}(\tilde{u} - f_0(x))$. Under this choice of controls, the outputs decouple.

$$\ddot{y} = \tilde{u} \tag{3.11}$$

This captures four of the six states of the system. The zero dynamics are therefore two dimensional.

3.2.2 Zero Dynamics

We now will compute the remaining dynamics, parameterized by z. Again, we choose z to make the chart $x = \Phi(y, z)$ a local diffeomorphism.

$$\begin{aligned} z_1 &= x_1\sec^3(x_4)\tan(x_3) - \tan(x_4) \\ z_2 &= x_2 + \frac{1}{2}x_1^2\sec^3(x_4)\tan(x_3) - x_1\tan(x_4) \end{aligned} \tag{3.12}$$

It may be verified through differentiation that the dynamics of z are given by

$$\begin{aligned} \dot{z}_1 &= y_0 \dot{y}_1 \\ \dot{z}_2 &= \frac{1}{2} (y_0)^2 \dot{y}_1 \ . \end{aligned} \tag{3.13}$$

The system, in these coordinates and under this choice of feedback, is principal. The dynamics are in fact power form, given as follows.

$$\begin{aligned} \ddot{y} &= u \\ \dot{z}_1 &= y_0 \dot{y}_1 \\ \dot{z}_2 &= \frac{1}{2} (y_0)^2 \dot{y}_1 \end{aligned} \tag{3.14}$$

This transformation only holds locally.

3.3 The Fire Truck System

The fire truck is the next example system we consider. This system is of interest because it has more than two inputs. It is shown to be controllable in [6]. A fire truck is sometimes called a tiller truck, and has a rear set of wheels which may by steered. The dynamics of the fire truck in control canonical form are

$$\begin{bmatrix} \dot{x}_1 \\ \dot{x}_2 \\ \dot{x}_3 \\ \dot{x}_4 \\ \dot{x}_5 \\ \dot{x}_6 \end{bmatrix} = \begin{bmatrix} 1 \\ \tan x_4 \\ 0 \\ \frac{\tan x_3}{L_0 \cos x_4} \\ 0 \\ \frac{-\sin(x_5 - x_4 + x_6)}{L_1 \cos x_5 \cos x_4} \end{bmatrix} v_1 + \begin{bmatrix} 0 \\ 0 \\ 1 \\ 0 \\ 0 \\ 0 \end{bmatrix} v_2 + \begin{bmatrix} 0 \\ 0 \\ 0 \\ 0 \\ 1 \\ 0 \end{bmatrix} v_3$$
$$\dot{v} = u \tag{3.15}$$

The configuration space is six dimensional. The Cartesian location of the center of the rear axle of the cab is given $(x_1, x_2) \in \mathbb{R}^2$; the steering angle of the front wheels relative to the cab's orientation is $x_3 \in S^1$; the absolute cab orientation with respect to the horizontal axis of the inertial frame is $x_4 \in S^1$; the steering angle of the rear wheels with respect to the trailer body is $x_5 \in S^1$; and the absolute trailer orientation is $x_6 \in S^1$. The configuration space Q is therefore $SE(2) \times T^3$. The constants L_0 and L_1 correspond to physical parameters

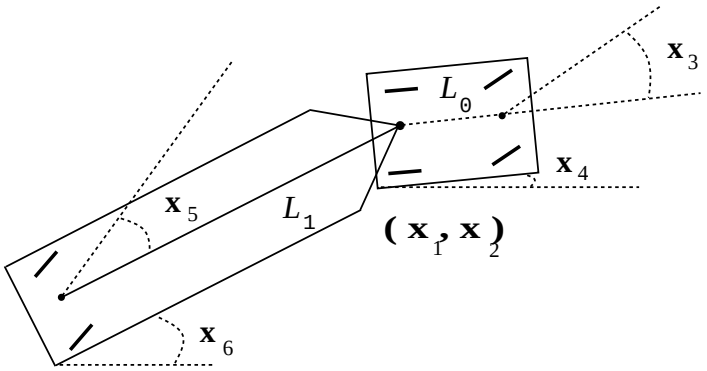

Figure 3.3: The fire truck or tiller truck.

of the system. The three scalars v_1, v_2 and v_3 correspond to the driving velocity, the cab's steering velocity and the trailer's steering velocity, respectively. The system is clearly maximally actuated. Thus we can find a control law smoothly dependent on u so that $\dot{v} = u$.

3.3.1 Input-Output Linearization

We now choose three output functions y.

$$\begin{aligned} y_0 &= x_1 \\ y_1 &= \frac{\tan x_3}{L_0 \cos^3 x_4} \\ y_1 &= \frac{-\sin(x_5 - x_4 + x_6)}{L_1 \cos x_5 \cos x_4} \end{aligned}$$

As before, we will differentiate the outputs y and input-output linearize them. They are relative degree two.

$$\begin{aligned} \dot{y} &= \begin{bmatrix} 1 & 0 & 0 \\ * & \frac{1}{L_0} \sec^2 x_3 \sec^3 x_4 & 0 \\ * & 0 & \frac{\cos(x_5 - x_4 + x_6)}{L_1 \cos x_4 \cos x_5} + \frac{\sin(x_5 - x_4 + x_6) \sin x_5}{\cos x_4 \cos^2 x_5} \end{bmatrix} v \\ &= D(x)v \\ \ddot{y} &= f_0(x, v) + D(x)u \end{aligned} \tag{3.16}$$

Clearly near $x = 0$ the matrix $D(x)$ is invertible. Choosing $u = D^{-1}(x)\left(\tilde{u} - f_0(x, v)\right)$, the dynamics decouple.

$$\ddot{y} = \tilde{u} \tag{3.17}$$

This captures six of nine states of the system. The zero dynamics are computed in the next subsection.

3.3.2 Zero Dynamics

Again, we pick z to make $x = \Phi(y, z)$ a local diffeomorphism. This choice will transform the system into power form, a principal system.

$$\begin{aligned} z_2^1 &= -\tan x_4 + x_1 \frac{\tan x_3}{L_0 \cos^3 x_4} \\ z_3^1 &= x_6 - x_1 \frac{\tan x_3}{L_0 \cos^3 x_4} + \frac{1}{2} x_1^2 \frac{\tan x_3}{L_0 \cos^3 x_4} \\ z_2^2 &= -x_2 - x_1 \frac{\sin(x_5 - x_4 + x_6)}{L_1 \cos x_5 \cos x_4} \end{aligned} \tag{3.18}$$

The indices on z_j^k denote the state's relation to the input variables. Their dynamics may be verified to be

$$\begin{aligned} \dot{z}_2^1 &= y_0 \dot{y}_1 \\ \dot{z}_3^1 &= y_0 \dot{y}_2 \\ \dot{z}_2^2 &= \frac{1}{2} (y_0)^2 \dot{y}_1 \ . \end{aligned} \tag{3.19}$$

Thus the total system dynamics are given locally as a power form system. We will write them as

$$\begin{aligned} \ddot{y} &= u \\ \dot{z}_2^1 &= y_0 \dot{y}_1 \\ \dot{z}_3^1 &= y_0 \dot{y}_2 \\ \dot{z}_2^2 &= \frac{1}{2} (y_0)^2 \dot{y}_1 \ . \end{aligned} \tag{3.20}$$

3.4 The Planar Acrobot

Consider a planar three linked robot with revolute joints. The two joints between the links have motors, the joint connecting the machine to earth is unactuated. We assume there is no friction in this middle joint.

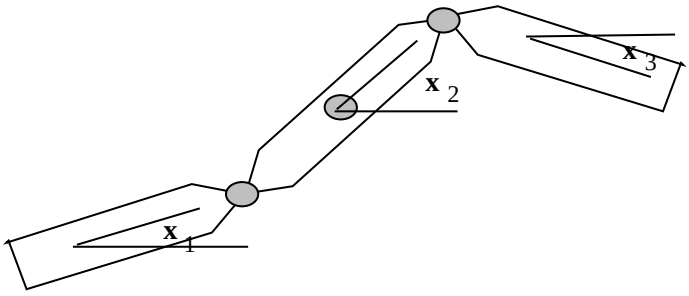

Figure 3.4: The planar robot can be considered as a planar restriction of a space based robot.

The configuration Q of the machine is given by the total orientation of each joint, and is consequently T^3. The variable x_i measures the angle of link i with respect to the inertial frame. The first step in analyzing this system is to write the Lagrangian. From there we may compute the velocity constraint on the system and hence write the equations of motion in controlled canonical form. A global diffeomorphism will make this system principal. The Lagrangian is

$$L(x,\dot{x}) \quad = \quad \frac{1}{2}\sum_{i=1}^{3}\dot{x}_i^2 a_i(x) \tag{3.21}$$

where the functions $a_i(x)$ are

$$\begin{aligned} a_1(x) &= k_{11} + k_{12}\cos(x_1 - x_2) + k_{13}\cos(x_1 - x_3) \\ a_2(x) &= k_{21}\cos(x_1 - x_2) + k_{22} + k_{23}\cos(x_2 - x_3) \\ a_3(x) &= k_{31}\cos(x_1 - x_3) + k_{32}\cos(x_3 - x_2) + k_{33} \ . \end{aligned}$$

There is a symmetry h acting on the system which corresponds to rotating the system about the free joint. The symmetry group is S^1. It is expressed as

$$h(\theta,x) \quad = \quad x + \theta I \ . \tag{3.22}$$

Now we apply Noether's theorem. In this case, we see

$$\left[\begin{array}{ccc} a_1(x) & a_2(x) & a_3(x) \end{array}\right]\dot{x} \tag{3.23}$$

is conserved. We will not bother writing the equations of motion in terms of x. We immediately proceed to the input-output linearization since we only have internal actuators and since this constraint is symmetry induced.

3.4.1 Controlled Principal Reduction

Chose the internal variables as outputs. That is, pick

$$\begin{aligned} y_1 &= x_1 - x_2 \\ y_2 &= x_3 - x_2 \ . \end{aligned} \tag{3.24}$$

The system is clearly maximally actuated with respect to these outputs, so there exists a feedback law smooth with respect to u such that $\ddot{y} = u$. This four state linear system characterizes all but one of the states of the system. As before, we chose the coordinate z in order to complete the diffeomorphism $x = \Phi(y, z)$. We choose z to be the symmetry group coordinate, represented by x_2, total world orientation of the robot. We may use the velocity constraint to solve for the connection. The equations of motion are

$$\begin{aligned} \ddot{y} &= u \\ \dot{z} &= b_1(y)\dot{y}_1 + b_2(y)\dot{y}_2 \end{aligned} \tag{3.25}$$

with the following definitions

$$\begin{aligned} v(y) &= \left(a_1(y) + a_2(y) + a_3(y)\right)^{-1} \\ b_1(y) &= -v(y)a_1(y) \\ b_2(y) &= -v(y)a_3(y) \ . \end{aligned} \tag{3.26}$$

3.4.2 Singular Configurations

A kinematic model of the planar acrobot would consider the internal joint velocities as inputs to the system. We write

$$\begin{bmatrix} \dot{y}_1 \\ \dot{y}_2 \\ \dot{z} \end{bmatrix} = \begin{bmatrix} 1 \\ 0 \\ b_1(y) \end{bmatrix} v_1 + \begin{bmatrix} 0 \\ 1 \\ b_2(y) \end{bmatrix} v_2 \ . \tag{3.27}$$

Which defines two vector fields fields $f_c^1(y)$, $f_c^2(y)$. For our system, their Lie bracket is given by

$$[f_c^1, f_c^2] = \begin{bmatrix} 0 \\ 0 \\ \xi(y) \end{bmatrix} \tag{3.28}$$

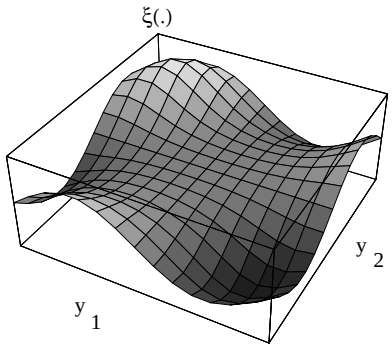

Figure 3.5: A plot of $\xi(\cdot)$ as a function of y. Note the periodic nature. There is a one dimensional submanifold of singular configurations.

with the function $\xi(y)$ as

$$2\left(v(y)\right)^2 \quad \left(a_1 k_{23}\sin(y_2) - a_3 k_{12}\sin(y_1) + a_2 k_{13}\sin(y_1 - y_2)\right) \ . \tag{3.29}$$

It may be verified also that $\xi(y) = \det(f_c^1, f_c^2, [f_c^1, f_c^2])$. Thus $f_c^1, f_c^2, [f_c^1, f_c^1]$ are linearly dependent on the set where $\xi(y)$ is zero. At these points, we must take Lie brackets twice to demonstrate controllability [11]. We will refer to the configurations where $\xi(y)$ is zero as singular configurations.

3.5 Satellite Mounted with Thrusters

We finish the examples chapter with a mechanical system that does not fit nicely into the principal bundle framework presented above, the satellite mounted with thrusters. We model the satellite as a rigid body mounted with thrusters which provide input torques about the first two principal axes. The Lagrangian exhibits symmetries, but these actuators do not provide internal forces, thus the conservation laws are not satisfied. Ignoring the conservation laws, the system is not maximally actuated. A maximally actuated satellite would have a six state input-output linearization, and consequently would capture the entire dynamics of the system.

Recall that the configuration space for the rigid body is its orientation, which we represent by a three by three rotation matrix g. The space of all such rotation matrices is the Lie group $SO(3)$ with Lie algebra $so(3)$. Traditionally, the velocity of a rigid body is

left (body) identified. The coordinate vector in $\mathbb{R}^3$ of the left identified Lie algebra element is referred to as the body angular velocity. The application of the Euler-Lagrange operator to this system yields

$$J\dot{\omega} = \tau - w \times Jw \ . \tag{3.30}$$

where J is a diagonal matrix with diagonal entries J_i. These are the Euler equations for the rigid body (2.14). The input torque τ_i denote the input torque about principal axis i. The control system[1] for the satellite is:

$$\begin{aligned} \begin{bmatrix} \dot{\omega}_1 \\ \dot{\omega}_2 \\ \dot{\omega}_3 \end{bmatrix} &= \begin{bmatrix} \frac{J_2 - J_3}{J_1}\omega_2\omega_3 \\ \frac{J_3 - J_1}{J_2}\omega_3\omega_1 \\ \frac{J_1 - J_2}{J_3}\omega_1\omega_2 \end{bmatrix} + \begin{bmatrix} \frac{\tau_1}{J_1} \\ \frac{\tau_2}{J_2} \\ 0 \end{bmatrix} \\ \dot{g} &= g\hat{\omega} \end{aligned}$$

The dynamics simplify after the following input transformation,

$$\begin{aligned} \tau_1 &= J_1\left(u_1 + \frac{J_3 - J_2}{J_1}\omega_2\omega_3\right) \\ \tau_2 &= J_2\left(u_2 + \frac{J_1 - J_3}{J_2}\omega_3\omega_1\right) \ . \end{aligned}$$

Under these inputs, the equations of motion become:

$$\begin{aligned} \begin{bmatrix} \dot{\omega}_1 \\ \dot{\omega}_2 \\ \dot{\omega}_3 \end{bmatrix} &= \begin{bmatrix} u_1 \\ u_2 \\ \alpha\omega_1\omega_2 \end{bmatrix} \ . \\ \dot{g} &= g\hat{\omega} \end{aligned} \tag{3.31}$$

The constant $\alpha := \frac{J_1 - J_2}{J_3}$. At first glance, one can see the standard theory fails because there is a drift term given by $\alpha\omega_1\omega_2$. If α is zero, we may write the equations of motion in locally in power form and apply all of the theory in the following chapters. Such a system is called symmetric. In general, however, a satellite will not be symmetric. We keep track of both cases in the sequel to this chapter, noting the modifications that the asymmetric satellite requires.

[1] This is nothing more than Meyer's model[7, 13, 29] of the satellite except we have found it more convenient to evolve the inverse of the orientation matrix they use.

3.5.1 Input-Output Linearization

In this section we input-output linearize [19] the system (3.31) for both the symmetric and asymmetric cases. The most natural choice of output is the pointing direction given by $g(t)e_3 : SO(3) \to S^2$ because it is output controllable and because the control dynamics involving ω_3 and rotations about e_3 do not appear in these output functions and their derivatives. We show the outputs are of relative degree two, consequently, the outputs can capture only a 4 dimensional subset of the full state. Even accepting this limitation there are further problems, since coordinate charts which cover S^2 are bound to have singularities. For example, the popular Euler angle parameterizations of $SO(3)$, when projected to S^2, give us familiar longitude and latitude measurements which have two singularities.

Projective plane coordinates of S^2 have only one point of singularity whose position we may choose. The north pole corresponds to the identity configuration and as this is our goal orientation, we choose the singular point to be maximally far away, the south pole. The south pole is mapped to infinity; adding it to the projective plane is the classic one-point compactification of $\mathbb{R}^2$.

We can find the output functions by a similar triangles argument. The outputs are given by:

$$\begin{aligned} y_1 = h_1(g,\omega) &= \frac{e_1^T g e_3}{1 + e_3^T g e_3} \\ y_2 = h_2(g,\omega) &= \frac{e_2^T g e_3}{1 + e_3^T g e_3}. \end{aligned} \tag{3.32}$$

We have scaled the outputs by $\frac{1}{2}$. Note that for all $g \in SO(3)$ of the form $g = \mathrm{Exp}(\psi \hat{e}_3)$, y_1 and y_2 are zero.

Proposition 8 (Outputs for the Satellite)
Given: a control system on $TSO(3)$ whose evolution is described by equation (3.31),
Then: the output y of equation (3.32) is of relative degree two for all $\|y\| < \infty$.

Proof: Apply standard exact linearization techniques [19].

$$\dot{y}_i = \frac{e_i^T g \hat{\omega} e_3}{1 + e_3^T g e_3} - \frac{e_i^T g e_3 e_3^T g \hat{\omega} e_3}{(1 + e_3^T g e_3)^2}$$

The derivative of the outputs then becomes

$$\begin{bmatrix} \dot{y}_1 \\ \dot{y}_2 \end{bmatrix} = A(g) \begin{bmatrix} \omega_1 \\ \omega_2 \end{bmatrix}. \tag{3.33}$$

If we denote $g_{ij} = e_i^T g e_j$, the ij^{th} element of the matrix g, the matrix $A(g)$ is

$$A(g) = \frac{-1}{(1+g_{33})^2} \begin{bmatrix} (1+g_{33})g_{12} - g_{13}g_{32} & -(1+g_{33})g_{11} + g_{13}g_{31} \\ (1+g_{33})g_{22} - g_{23}g_{32} & -(1+g_{33})g_{21} + g_{23}g_{31} \end{bmatrix}.$$

Because $\omega \times e_3 = e_1\omega_2 - e_2\omega_1$, ω_3 does not appear in the decoupling matrix, $A(g)$.

In computing the determinant, is useful to recall that $g_{33} = (g_{11}g_{22} - g_{12}g_{21})$ which follows directly from $g^{-1} = g^T$ plus the standard formula for the inverse of a matrix in terms of cofactors. The determinant is then:

$$\det(A(g)) = \frac{1}{(1+g_{33})^2}$$

The determinant is bounded for every y_1, y_2 bounded because having $g_{33} = -1$ corresponds to being at the south pole of S^2. In terms of the outputs y_1, y_2, the determinant[2] of the decoupling matrix is $\frac{1}{4}(1+y_1^2+y_2^2)^2$.

The chosen outputs are then relative degree two. The second differential is

$$\begin{bmatrix} \ddot{y}_1 \\ \ddot{y}_2 \end{bmatrix} = f_0(g,\omega) + A(g) \begin{bmatrix} u_1 \\ u_2 \end{bmatrix}.$$

Therefore with the choice of inputs $u = A^{-1}(g)(v - f_0(g,\omega))$ it may be verified that the output dynamics become:

$$\begin{aligned} \ddot{y}_1 &= v_1 \\ \ddot{y}_2 &= v_2. \end{aligned} \tag{3.34}$$

This linear system is trivially controllable.

If the outputs were zero, then $y_1 = \dot{y}_1 = y_2 = \dot{y}_2 = 0$. By equation (3.33), $\omega_1 = \omega_2 = 0$, thus from equation (3.31) we see that $\dot{\omega}_3 = 0$. The system will be rotating at the constant rate ω_3 about the e_3 axis. Thus, the zero dynamics manifold is TS^1. Further, the trajectories are bounded.

[2] In the standard Euler angle parameterization, the determinant is given by the formula $\frac{1}{(1+\cos(\theta)\cos(\phi))^2}$.

3.5.2 Zero Dynamics

To solve for the zero dynamics, we require a coordinate chart for $SO(3)$ which will keep track of this rotation ψ about e_3 as measured in the body frame.

Euler angles, although a favorite of the literature [7, 13], are not advisable for this system. The xyz Euler angle chart, when projected down to S^2, is not symmetric. Any Euler angle chart which is symmetric, for example the zyz chart, is singular at the north pole. Of course, singularities are unavoidable [38]. Recall that by chosing a coordinate chart, we have implicitly chosen in the tangent space of S^2 a direction which is, for example, the e_1 axis under $\psi = 0$. If this could be done smoothly, then we will have constructed a non-vanishing smooth section on TS^2.

An optimal choice of coordinate chart would, therefore, be symmetric and have a singularity at one point; say, conveniently, the south pole. Such a chart exists but is not standard. Listing, a psychologist studying the movement of the eye, noted that the eye moves in a way which minimally twists the optic nerve. Listing's law [15, 25] describes this subset of $SO(3)$ which is actually $\mathbb{R}P^2$. The same subset of $SO(3)$ describes the configuration space of a cat which does not twist its spinal cord [30]. It can be thought of as the image under the exponential map of a two dimensional subspace of $so(3)$. We will use polar coordinates of $\mathbb{R}^2$ in order to parameterize the subspace. Thus $g_\ell(\theta, \phi) = \mathrm{Exp}(\phi(\cos(\theta)\widehat{e_1 + \sin}(\theta)e_2))$ for any $\theta, \phi \in T^2$. The formula for $g_\ell(\theta, \phi)$ is given by

$$\begin{bmatrix} \cos^2(\theta)(1-\cos(\phi)) + \cos(\phi) & \cos(\theta)\sin(\theta)(1-\cos(\phi)) & \sin(\phi)\sin(\theta) \\ \cos(\theta)\sin(\theta)(1-\cos(\phi)) & \sin^2(\theta)(1-\cos(\phi)) + \cos(\phi) & -\sin(\phi)\cos(\theta) \\ -\sin(\phi)\sin(\theta) & \sin(\phi)\cos(\theta) & \cos(\phi) \end{bmatrix}.$$

The complete chart is $g(\theta, \phi, \psi) = g_\ell(\theta, \phi)\ \mathrm{Exp}(\psi \hat{e}_3)$. It may be verified that the equation for the decoupling matrix has the following pleasing form in these coordinates:

$$A(g) = \frac{(1 + y_1^2 + y_2^2)}{2} \begin{bmatrix} -\sin(\psi) & -\cos(\psi) \\ \cos(\psi) & -\sin(\psi) \end{bmatrix}$$

In keeping with the previous notation, we identify $z_1 = \psi$ and $z_2 = \omega_3$.

Proposition 9 (Zero Dynamics for the Satellite)

Given a control system on $TSO(3)$ whose evolution is described by equation (3.31) and has been input-output linearized as in Proposition 8,

Then the remaining dynamics, parametrized by $z_1 = \psi$ and $z_2 = \omega_3$ are given by:

$$\dot{z}_1 = \frac{2}{(1+y_1^2+y_2^2)}(y_2\dot{y}_1 - y_1\dot{y}_2) + z_2$$
$$\dot{z}_2 = \frac{-2\alpha}{(1+y_1^2+y_2^2)^2}\left(\sin(2z_1)(\dot{y}_2^2 - \dot{y}_1^2) + 2\cos(2z_1)\dot{y}_1\dot{y}_2\right)$$

where z_1 is measured as in the Listing parameterization.

Proof: The derivative of z_2 may be computed directly using equation (3.33). To compute the derivative of z_1, differentiate the Listing coordinate chart $g(\theta, \phi, \psi)$, identifying ψ with z_1.

$$\begin{aligned}\dot{g} = g\hat{\omega} &= g_\ell \hat{\omega}^\ell \operatorname{Exp}(z_1\hat{e}_3) + \dot{z}_1 g\hat{e}_3 \\ &= g(\widehat{\operatorname{Exp}(-z_1\hat{e}_3)\hat{\omega}^\ell}) + \dot{z_1} g\hat{e}_3\end{aligned}$$

This implies that:

$$z_2 = \omega_3^\ell + \dot{z}_1$$

The quantity ω_3^ℓ may be computed directly from the derivative of the matrix $g_\ell(\phi, \theta)$. The equation for $\dot{z}_1$ is therefore given by:

$$\dot{z}_1 = z_2 - (1 - \cos(\phi))\dot{\theta}$$

The angles ϕ, θ and their derivatives depend only on y and $\dot{y}$. It may be verified that the dynamics are then:

$$\begin{aligned}\dot{z}_1 &= \frac{2}{(1+y_1^2+y_2^2)}(y_2\dot{y}_1 - y_1\dot{y}_2) + z_2 \\ \dot{z}_2 &= \frac{-2\alpha}{(1+y_1^2+y_2^2)^2}\left(\sin(2z_1)(\dot{y}_2^2 - \dot{y}_1^2) + 2\cos(2z_1)\dot{y}_1\dot{y}_2\right)\end{aligned} \tag{3.35}$$

We consider the symmetric and asymmetric cases separately. Note that the four states $y_1, y_2, \dot{y}_1$ and $\dot{y}_2$ constitute a controllable linear system and are therefore easy to stabilize to a point. The challenge then rests with the remaining dynamics, z.

Remark (Chained Form Coordinates): Seeing the "area form" appearance of the ψ dynamics, one might be tempted to try to find chained form coordinates. This is indeed

possible. Consider the following transformation.

$$\begin{aligned} x_1 &= \frac{y_1}{\sqrt{1+y_1^2+y_2^2}} \\ x_2 &= \frac{y_2}{\sqrt{1+y_1^2+y_2^2}} \\ x_3 &= \psi \end{aligned}$$

It may be verified through direct computation that the derivative of x_3, in terms of these new variables, is given by the following.

$$\dot{x}_3 = x_2\dot{x}_1 - x_1\dot{x}_2$$

We have found, therefore, chained form coordinates for the two thruster satellite problem. We include this for interest, since it is not used in what follows.

Remark (Quaternions): By using 4 real numbers to parameterize $SO(3)$, quaternions avoid the singularities associated with other coordinate charts. The natural split of the configuration space of the satellite with 2 torque inputs into a point in S^2 and a rotation about e_3, when mapped to quaternions, produces the Hopf fibration of S^3 .

To see this, notice that $q_\ell = \cos(\frac{\phi}{2}) + i\sin(\frac{\phi}{2})\cos(\theta) + j\sin(\frac{\phi}{2})\sin(\theta)$. The total rotation is given by $q_\ell \cdot \left(\cos(\frac{\psi}{2}) + k\sin(\frac{\psi}{2})\right)$, which is

$$q_\ell q_z = \cos(\frac{\phi}{2})\cos(\frac{\psi}{2}) + i\sin(\frac{\phi}{2})\cos(\theta - \frac{\psi}{2}) + j\sin(\frac{\phi}{2})\sin(\theta - \frac{\psi}{2}) + k\cos(\frac{\phi}{2})\sin(\frac{\psi}{2}).$$

The Hopf fibration coordinates are typically given by $\left(\cos(\frac{\phi}{2})\exp(i\psi), \sin(\frac{\phi}{2})\exp(i\psi+\theta)\right)$, which if mapped to quaternions properly are nearly the same as the Listing parameterization.

It is also of interest to consider the form as written in terms of these quaternions. The article [49] uses them to some degree in studying fully–actuated satellite systems. The form, in these coordinates, is:

$$\begin{aligned} \frac{1}{4}\omega_3 = &\left(q_0q_1q_2 - q_0^2q_3 - \frac{1}{2}q_3\right)\dot{q}_0 + \left(-q_0q_1q_3 + q_1^2q_2 + \frac{1}{2}q_2\right)\dot{q}_1 + \\ &\left(-q_0q_2q_3 + q_2^2q_1 - \frac{1}{2}q_1\right)\dot{q}_2 + \left(q_1q_2q_3 - q_3^2q_0 + \frac{1}{2}q_0\right)\dot{q}_3 \ . \end{aligned}$$

This is none other than the mechanical connection on TS^3 [27].

Chapter 4

Point Stabilization

We are interested in stabilizing control laws for control systems of the form

$$\begin{aligned} \dot{x} &= \sum_{i=0}^{p} f_c^i(x) v_i \\ \dot{v} &= u \end{aligned} \tag{4.1}$$

where x in $\mathbb{R}^n$, a local set of coordinates for Q, along with $v \in \mathbb{R}^{p+1}$ are the state of the system, $u \in \mathbb{R}^{p+1}$ are the inputs and $f_c^i(x)$ are smooth vector fields in $\mathbb{R}^n$, linearly independent for all x. The problem then is, given a nonlinear control system of the form in equation (4.1), find a control law $u(x, v, t)$ which makes the origin globally asymptotically stable.

Mechanical systems with nonholonomic velocity constraints cannot be stabilized to a point in their configuration space with smooth static state feedback [5]. Consequently, the traditional techniques of linearization, gain scheduling, and exact linearization fail. It was shown in [12] that there do exist time periodic smooth feedback laws which render points asymptotically stable, though their convergence rate was shown to be limited in [32]. Explicit control laws were soon developed in the author's work [40, 42], on which this chapter is based.

We focus on a special class of systems, those which can be transformed locally into power form. While this condition seems restrictive, all mechanical systems considered in the dissertation meet this requirement except for the asymmetric satellite. All systems in chained form, for example, may be transformed into power form. Single generator, multiple

input power form systems have dynamics

$$\begin{aligned} \ddot{y}_j &= u_j, \quad 0 \leq j \leq p \\ \dot{z}^k_{j0} &= \frac{1}{k!}\left(y_0\right)^k \dot{y}_j, \quad 1 \leq k \leq \ell_j, \ 1 \leq j \leq p \end{aligned} \tag{4.2}$$

where $y \in \mathbb{R}^{p+1}$ are the base coordinates, and $z \in \mathbb{R}^{(n-p-1)}$ are the fiber coordinates.

This particular form of equations is well suited to strategy we employ to explicitly construct stabilizing control laws. The space is clearly divided into a linear control space, covered by $y, \dot{y}$, and a nonlinear section z whose dynamics are governed entirely by the movement in the y space. We will perturb a linearly stable control law on the y space. The perturbation, which will stabilize the zero dynamics, will be higher-order in z. As the z goes to zero, the perturbation of y goes to zero.

First we present a stabilizing control law for a (p+1)-input, p-chain, single-generator control systems in power form. We draw heavily on the author's previous work [42], although the proof and the law are new. Then we apply the theory to several of the example systems. First we feedback stabilize the car with six states, then the fire truck with nine. Because these systems are locally in power form, applying the theory will be straightforward. We consider the satellite last, with two input torques and a two dimensional fiber. While the symmetric case is standard, the asymmetric case requires some new theory, as seen in [44].

4.1 A Stabilizing Control Law

The control law will be defined as follows. We will pick a new set of outputs $e(t)$ for the system (4.2) and exponentially stabilize them. The outputs $e(t)$ will be a perturbed version of $y(t)$, where the perturbation $p(z,t)$ is chosen to render the zero dynamics stable. We define the perturbed outputs as,

$$e(t) = y(t) - p(z,t) \tag{4.3}$$

which are relative degree two, since they depend only on the configuration and time. Differentiate them.

$$\begin{aligned} \dot{e} &= \dot{y} - \frac{\partial p}{\partial z} A(y)\dot{y} - \frac{\partial p}{\partial t} \\ &= \left(I - \frac{\partial p}{\partial z} A\right)\dot{y} - \frac{\partial p}{\partial t} \end{aligned} \tag{4.4}$$

To see the inputs u, we must differentiate again.

$$\ddot{e} \;=\; \left(I - \frac{\partial p}{\partial z}A\right) u + f_0(y, \dot{y}, z, t) \tag{4.5}$$

Notice for small y and small z, the matrix $(I - \frac{\partial p}{\partial z}A)$ is invertible. We are ready to define the control law.

Proposition 10 (An Locally Asymptotically Stabilizing Control Law)
Given: *a $p+1$-input, p-chain, single-generator control system whose evolution in time is given by:*

$$\begin{aligned} \ddot{y}_j &= u_j \text{ for } 0 \le j \le p \\ \dot{z}_j^k &= \frac{1}{k!}(y_0)^k \dot{y}_j \text{ for } 1 \le k \le \ell_j \text{ and for } 1 \le j \le p, \end{aligned} \tag{4.6}$$

Define: *the perturbation vector $p(z,t)$ to be*

$$\begin{aligned} p_0(z,t) &= p_0(z)\cos(t) \\ p_j(z,t) &= \sum_{h=1}^{\ell_j} p_{jh}(z)\sin(ht) \text{ for } 1 \le j \le p \end{aligned} \tag{4.7}$$

where $p_0(z) = \sum_{j=1}^{p}\sum_{k=1}^{\ell_j}\left(z_j^k\right)^2$ and $p_{jh}(z) = c_j^h z_j^h$ with each $c_h^j < 0$.
and define the error outputs $e(t)$ to be

$$e(t) \;=\; y(t) - p(z(t), t)\ . \tag{4.8}$$

Then: *the control*

$$u \;=\; -\left(I - \frac{\partial p}{\partial z}A\right)^{-1}(f_0 + k_1 e + k_2 \dot{e})\ , \tag{4.9}$$

where $k_1, k_2 > 0$, renders the origin $(y, \dot{y}, z) = 0$ locally asymptotically stable.

Proof: The outline of the proof is as follows: first we change coordinates to the $(e, \dot{e}, z)$ system. In these coordinates the system divides into a linearly stable part parameterized by

the $e, \dot{e}$ coordinates, and a higher order time-varying part parameterized by the z variables. We then apply center manifold theory. The center manifold corresponds to $e(t) = \dot{e}(t) = 0$. The dynamics on the center manifold are exactly $\dot{z} = A(p)\dot{p}$. We then show that p had been chosen so these dynamics are asymptotically stable. Given that $p(0,t) = 0$, we have that y and $\dot{y}$ goes to zero as z goes to zero, completing the proof.

The coordinate change, $(y, z) \to (e, z)$ is valid globally for the configuration space variables due to its triangular nature. However, the matrix $(I - \frac{\partial p}{\partial z}A)$ must be nonsingular in order to solve for $\dot{y}$ in terms of $\dot{e}$. We assume e and p are small enough so that this may be done. Under the control law defined, the system closed loop dynamics are given by

$$\begin{aligned} \ddot{e} &= -(k_1 e + k_2 \dot{e}) \\ \dot{z} &= \left(I - A(e+p)\frac{\partial p}{\partial z}\right)^{-1} \left(A(e+p)\dot{e} + A(e+p)\frac{\partial p}{\partial t}\right) \end{aligned} \tag{4.10}$$

Note that the $\dot{z}$ equation is at least of order 2 in $z, e, \dot{e}$, and that the dynamics of e are linearly stable. We may apply a slightly modified version of center manifold theory.

We now introduce the generalization of the center manifold theorem which appears in [40]. The following statement uses the notation of [9].

Lemma 11 ("Time–varying" Center Manifold)
Given: the system

$$\begin{aligned} \ddot{e} &= B_1 e + B_2 \dot{e} + g(e, \dot{e}, z, w) \\ \dot{z} &= Az + f(e, \dot{e}, z, w) \\ \dot{w} &= Sw \ . \end{aligned} \tag{4.11}$$

with $e \in \mathbb{R}^{p+1}$, $z \in \mathbb{R}^{n-p-1}$, *and* $w \in \mathbb{R}^k$, *and* k *sufficiently large.*

Assume: *the eigenvalues of* A *and* S *have zero real part, and further,*
the functions f, g *and* h *are* C^2. *In addition assume*
$f(0,0,0,w) = 0$, $\partial_i f(0,0,0,w) = 0$, *for* $i = 1,2,3$,
$g(0,0,0,w) = 0$ *and* $\partial_i g(0,0,0,w) = 0$ *for* $i = 1,2,3$.

Then: *given* $M > 0$, *there exists a center manifold for (4.11),*
$e = h_1(z,w), \dot{e} = h_2(z,w)$ *for* $\|w\| < M$, $\|z\| < \delta(M)$,

for some $\delta > 0$ and dependent on M, where
$h(z, w)$ is C^2 and $h(0, w) = 0$.

To apply this result to our system, create the vector w, with $w_1^j = \cos(jt)$ and $w_2^j = \sin(jt)$. Note that the dimension of w, given by k, is then twice the maximum ℓ_j of the chains in (4.2) for $1 \leq j \leq p$. The differential equation describing the evolution of this vector may be written as $\dot{w} = Sw$, with the eigenvalues of S having zero real part. We can then substitute an element of the vector w for each of the time–varying terms in the equations. In this form, we may apply the "Time-varying" Center Manifold theorem [9].

Consequently there exists locally a center manifold given by $e = \dot{e} = 0$. The dynamics on this center manifold determine the asymptotic dynamics of the total system. We now examine closely the dynamics of z on the center manifold. Recall that

$$\dot{z}_j^k = \frac{1}{k!} (y_0)^k \dot{y}_j \tag{4.12}$$

where on the center manifold, we have that

$$\begin{aligned} y_0(z,t) &= p_0(z)\cos(t) \\ y_j(z,t) &= \sum_{k=1}^{\ell_j} p_{jk}(z)\sin(kt) \ . \end{aligned} \tag{4.13}$$

Clearly we need to solve for $\dot{y}_j$.

$$\dot{y}_j = \sum_{h=1}^{\ell_j} \left(h\cos(ht)p_{jh}(z) + \sin(ht)\frac{\partial p_{jh}}{\partial z}\dot{z} \right) \tag{4.14}$$

Using this formula, we may solve for the dynamics of chain j.

$$\begin{aligned} \dot{z}_j^k &= \frac{1}{k!} (y_0)^k \dot{y}_j \\ &= \frac{1}{k!} (p_0(z)\cos(t))^k \left(\sum_{h=1}^{\ell_j} \left(h p_{jh}(z)\cos(ht) + \frac{\partial p_{jh}}{\partial z}\sin(ht)\dot{z}_j \right) \right) \end{aligned} \tag{4.15}$$

We now expand some of the powers. Note that $\cos^k(t) = \sum_{i=1}^k \alpha_{ki}\cos(it)$ where $\alpha_{ki} \geq 0$, and $\alpha_{kk} > 0$. The first term then divides into two parts, a time average zero section and a steady state section.

$$\dot{z}_j^k = \frac{1}{k!} p_0^k(z) \sum_{i=1}^{k} \sum_{h=1}^{\ell_j} \alpha_{ki} \left(\cos(ht)\cos(it)p_{jh}(z) + \sin(ht)\cos(it)\frac{\partial p_{jh}}{\partial z}\dot{z}_j \right) \tag{4.16}$$

Using the identities,

$$\begin{aligned}\cos(ht)\cos(it) &= \frac{1}{2}\left(\cos((h-i)t)+\cos((h+i)t)\right)\\ \sin(ht)\cos(it) &= \frac{1}{2}\left(\sin((h+i)t)+\sin((h-i)t)\right)\end{aligned}$$

we see that equations (4.16) for $\dot{z}_j^k$ divides into 3 parts, an average part $\bar{f}(z)$, a time average zero part $\tilde{f}(z,t)$ with cosine time variations, and finally a term $\dot{z}$ dependent, time average zero, with only sine time variations. We label this last term $v_j^k(z,t)\dot{z}$. The average piece is as follows,

$$\bar{f}_j^k(z) = \sum_{h=1}^{k} \beta_{jh}^k p_0^k(z) p_{jh}(z) \ . \tag{4.17}$$

with $\beta_{jk}^k > 0$, and all other $\beta_{jh}^k \geq 0$. We now examine the dynamics of $\dot{z}_j$ on the whole.

$$\left(I - V_j(z,t)\right)\dot{z}_j = \bar{f}_j(z) + \tilde{f}(z,t) \tag{4.18}$$

We wish to solve for the dynamics of z_j, and this requires a matrix inverse. We know that $\|V_j(z,t)\| < 1$, thus we may approximate the inverse in power series form. Recall that the i^th row of V_j is of order $2i$. The i^{th} row of $O_j(z,t)$, the sum of the tail of the power series, is of order at least $2i+2$.

$$\dot{z}_j = \left(I + V_j(z,t) + O_j(z,t)\right)\left(\bar{f}(z) + \tilde{f}(z,t)\right) \tag{4.19}$$

Note that $V_j(z,t)\bar{f}_j(z)$ is of time average zero, $V_j(z,t)\tilde{f}_j(z,t)$ involves terms of $\sin(ht)\cos(it)$ thus will be of time average zero as well. In conclusion, we have

$$\dot{z}_j = \bar{f}_j(z) + \tilde{f}_j(z,t) + o_j(z,t) \tag{4.20}$$

where $\bar{f}_j^i(z)$ and $\tilde{f}_j^i(z,t)$ is of order $(2i+1)$, and $o_j^i(z,t)$ is of order $(2i+2)$ in z.

Our proof is nearly complete. We need to apply averaging theory in order to move the time average zero terms up to higher order. This requires a non-standard version of averaging theory, because we need to preserve the order of each component of $\bar{f}_j, \tilde{f}_j$.

Lemma 12 ("Averaging" Transformation)

Consider: the time–varying nonlinear system

$$\dot{x} = f(x,t) \tag{4.21}$$

where f is of period T , C^r, and where the i^{th} entry of
the vector f satisfies $f_i = O(x)^{2k+1}$, with $k \geq 1$.

Then: *there exists a C^r local change of coordinates $x = y + \Psi(y,t)$ under which (4.21) becomes*

$$\dot{y} = \bar{f}(y) + \hat{f}(y,t)$$

where $\bar{f}$ is the time average of f and $\hat{f}_i(y,t) = O(y)^{2k+2}$ and of period T.

Proof: The proof closely resembles a result described in [18]. We will divide $f(x,t)$ into its time average, given by $\bar{f}(x)$, and the remainder $\tilde{f}(x,t)$. We make the coordinate change:

$$x = y + \Psi(y,t)$$

with $\Psi(y,t)$ specified later. We now solve for the dynamics of y.

$$(I + D_y\Psi)\,\dot{y} + \frac{\partial \Psi}{\partial t} = \dot{x} = \bar{f}(y+\Psi) + \tilde{f}(y+\Psi,t)$$
$$\dot{y} = (I + D_y\Psi)^{-1}\left(\bar{f}(y+\Psi) + \tilde{f}(y+\Psi,t) - \frac{\partial \Psi}{\partial t}\right)$$

Set $\frac{\partial \Psi}{\partial t} = \tilde{f}(y,t)$. As $\tilde{f}(y,t)$ has zero mean, Ψ is a bounded function of time. Furthermore, this implies that Ψ is of higher order, thus the coordinate change is valid locally. Expanding the terms, we see:

$$\dot{y} = (I + D_y\Psi)^{-1}\left(\bar{f}(y) + f(y+\Psi,t) - f(y,t)\right)$$
$$= \left(I - D_y\Psi + O(\|D_y\Psi\|^2)\right)\left(\bar{f} + D_y f\Psi + O(\|\Psi\|^2)\right)$$
$$= \bar{f}(y) + \hat{f}(y,t)$$

Now we will check the order of $\hat{f}_i$.

$$\hat{f} = D_y f\Psi - D_y\Psi\left(\bar{f}(y) + f_i(y+\Psi,t) - f_i(y,t)\right) \tag{4.22}$$

As the order of the element f_i is $2k+1$, the elements of the corresponding row of $D_y f$ are of order $2k$. The lowest order in Ψ, as it is the time integral of $\tilde{f}$, is 3 from the case $k = 1$. We conclude that the first term is of order $2k+3$. The same argument holds for the second term, as the element Ψ_i is of order $2k+1$, the elements of the corresponding row of $D_y\Psi$ is of order $2k$. The product is then at least of order $2k+3$.

We can apply this averaging theory in order to find a time varying coordinate chart $\tilde{z}$ such that

$$\dot{\tilde{z}} \;=\; \bar{f}_j(\tilde{z}) + \tilde{o}_j(z,t) \tag{4.23}$$

where $\tilde{o}_j^i(z,t)$ is of order $(2i+2)$ and $f_j^i(z)$ is of order $(2i+1)$. We are almost done. All we need to do is apply a special case Lyapunov result found in [40, 42].

Lemma 13 (Case Specific Lyapunov Result) *Given: the time–varying nonlinear system*

$$\dot{y} \;=\; \bar{f}(y) + \tilde{f}(y,t) \tag{4.24}$$

where $y \in \mathbb{R}^n$. *If*

$$\|\tilde{f}(y,t)\| \le \gamma_i \|y\|^{2(1+i)}$$

for all y *in some open neighborhood of the origin and*

$$\bar{f}_j^k(z) \;=\; \sum_{h=1}^{k} \gamma_j^{hk} \|z\|^{2k} z_h \;, \tag{4.25}$$

with $\gamma_j^{kk} < 0$,

Then: *the origin of (4.24) is locally asymptotically stable.*

In our application, $\gamma_j^{hk} = c_j^h \beta_h^k$. The proof is finished. Each chain has locally asymptotically stable dynamics, thus the total system is stabilized.

Remark (Chained-form systems): Chained form systems are locally much like power form systems. In fact, given a $p+1$ input, $p(p+1)$ chained form system described by

$$\begin{aligned}
\ddot{x}_j^0 &= u_j \quad 0 \le j \le p \\
\dot{x}_{ji}^1 &= x_j^0 v_i \quad j > i \;\; and \;\; x_{ij}^1 := x_i^0 x_j^0 - x_{ji}^1 \\
\dot{x}_{ji}^k &= x_{ji}^{k-1} v_i \quad 1 \le k \le \ell_j,\; 0 \le j, i \le p;\;\; j \ne i \;,
\end{aligned}$$

there exists a global transformation to power form given by

$$\begin{aligned}
y_j &= x_j^0 \; 0 \le j \le p \\
z_{ji}^k &= (-1)^k x_{ji}^k + \sum_{n=0}^{k-1} (-1)^n \frac{1}{(k-n)!} \left(x_i^0\right)^{k-n} x_{ji}^n \; 1 \le k \le \ell_j,\; 1 \le j \le p,\; 0 \le i \le p \;.
\end{aligned} \tag{4.26}$$

Corallary 2.1 [40] may be easily extended to the multiple input case. We may therefore conclude that the controls (4.9) will locally asymptotically stabilize the chained form system as well the power form.

Remark (Globally Stabilizing Laws): Although of little practical interest due to the local nature of the coordinate charts and due to the poor large motion behavior of feedback laws, these laws may be made global with little effort. Essentially, the effect of the perturbation has to be limited for large z. This may be done by using saturation functions. That is, function which for small values of z are identity maps, as to preserve the local stability properties, but for larger values of z reach at never exceed some limit ϵ. The only additional difficultly is the matrix inverse of $(I - \frac{\partial p}{\partial z}A)$, which might not be well defined for large values of y or e. In regions of the state space where y is large, implying that e is large since $p(z,t)$ is bounded by saturation functions, we may employ the law $\ddot{y} = k_1 y + k_2 \dot{y}$, making y dynamics linearly stably. At some point, y will be sufficiently small so that the matrix will be invertible. There we may smoothly transit to the local (in terms of y and e) law.

4.2 Applications

The control laws developed in the previous section are directly applicable to every example system except for the satellite and the planar acrobot. The acrobot requires little modification and locally is much like Hilare, so we will skip this example. The car and the fire truck, however, are more sophisticated.

4.2.1 Power form systems

First consider the front wheel drive car. Figure 4.1 shows the results of applying the stabilizing control law to the four dimensional power system. The constants c_i were chosen to be 1 and the initial condition is given by $x = (0, 0, 0, 1)$. This corresponds to a parallel parking maneuver in the original set of coordinates. The first two plots in Figure 4.1 show the evolution of the state variables as a function of time. Note that the convergence rate of x_4 dominates the convergence of the other variables. The plot in the upper right shows trace of the back wheel of the automobile and the plot in the lower right shows the wheel and steering velocities. The effect of saturation functions is illustrated in Figure 4.2.

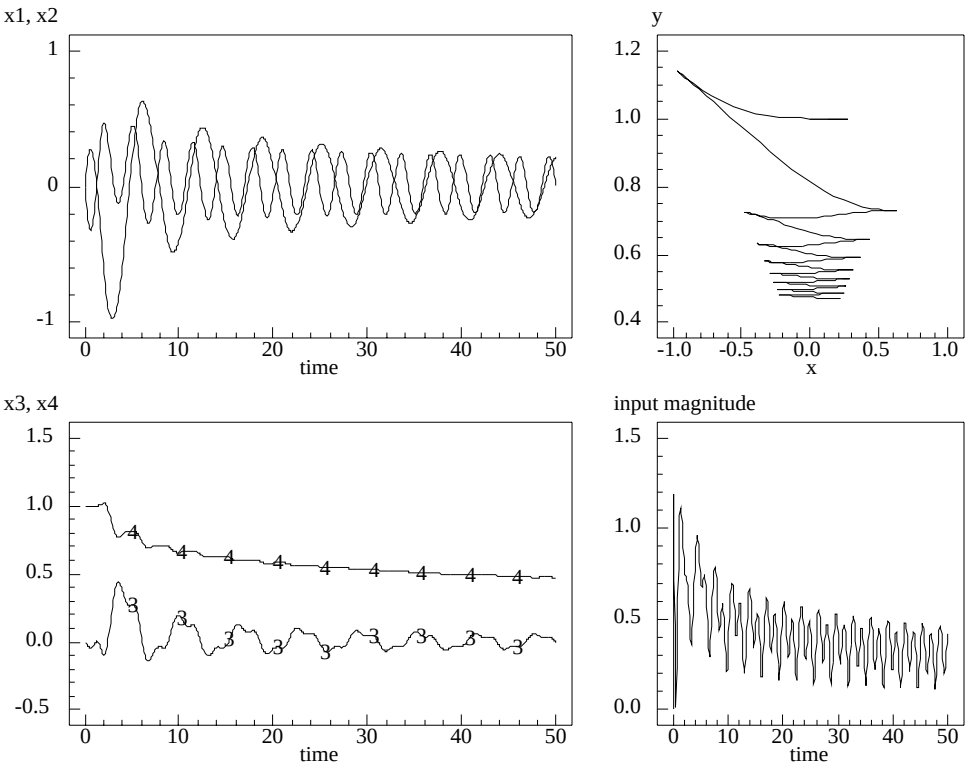

Figure 4.1: Stabilization of a four dimensional, two input power system

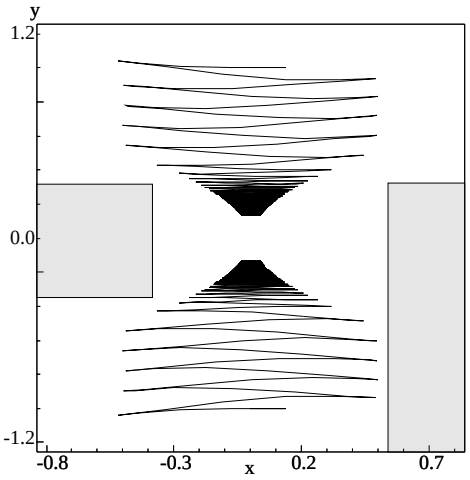

Figure 4.2: Phase plane plot, x versus y, of two simulations. Note the effects of the saturation function on the limits of travel in the x direction.

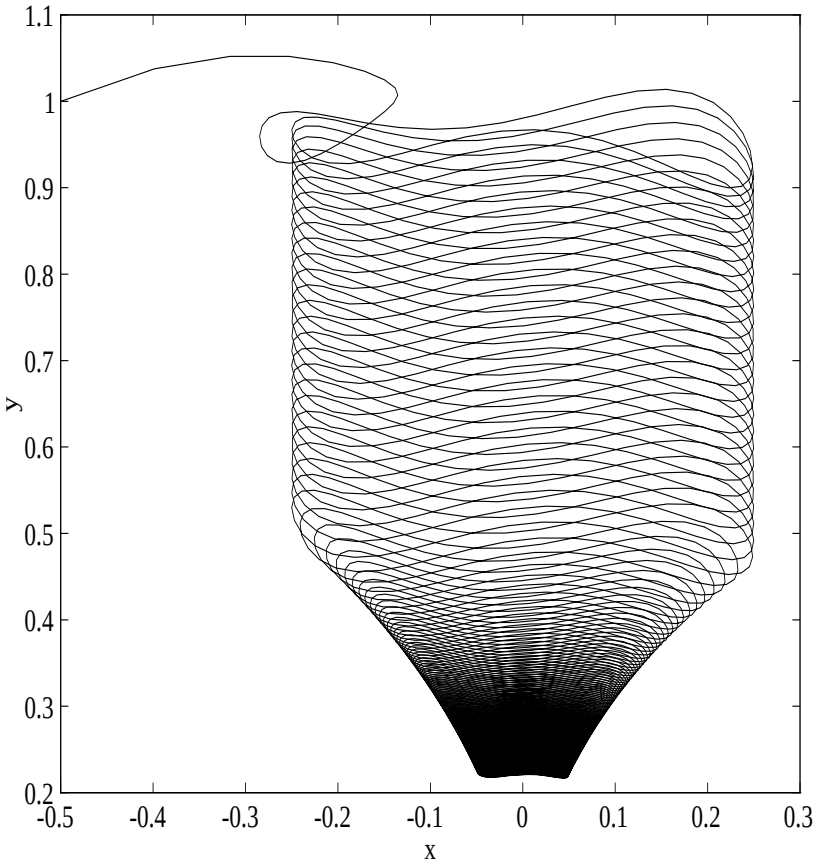

Figure 4.3: X–Y Trajectory of the Parallel Parking Maneuver

The Fire Truck

We now present the simulation of the fire truck system. The simulation was performed on the system in power form with the states being stabilized to the origin from a given initial point. The c_1, c_2, c_3 are chosen to be 1, and saturation functions were employed to insure global convergence. The coordinates in power form were then transformed back into the original coordinates for analysis and a movie animation. Figure 4.3 shows the x-y plot for a parallel parking maneuver, starting from an arbitrary initial point that illustrates the control law. The plot contains Lissajous figures.

Figure 4.4 shows the slow convergence of the y position of the center of the rear axle of the cab for the same parallel parking maneuver.

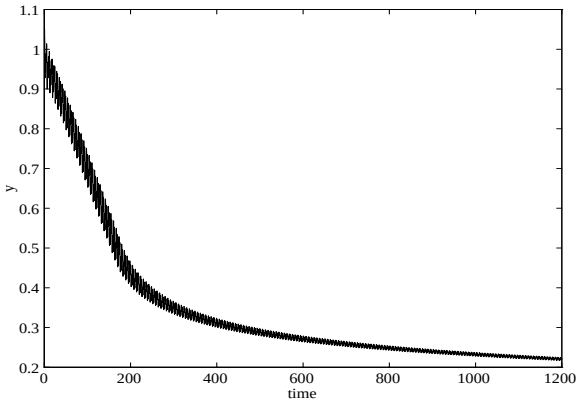

Figure 4.4: Y–Trajectory of the Parallel Parking Maneuver

4.2.2 The Satellite

The symmetric satellite has one uncontrollable state, z_2. Under the assumption that z_2 is zero, the system has essentially 5 states and looks like a power form system of the most basic type. The asymmetric satellite does not fit into this simplified picture, so some new theory is made to fit this special case.

The Symmetric Satellite

First we simulate the symmetric satellite. If z_2 is zero, the angle z_1 may be stabilized. Control of the phase of z_1 when ω_3 is not zero is an identical problem. There is no need to subdivide this problem into two cases.

As before we will employ saturation functions. Simulations of the control law have been run. Figure 4.5 shows the trajectory of the systems in the projective plane space. Figure 4.6 shows the effect of this trajectory on the coordinate ψ.

An Asymmetric Stabilizer

We present, in this final subsection, the regulator for the asymmetric satellite. A look at the system in the coordinates presented here gives some idea as to how a regulator may be constructed.

To present the law, first we define some outputs involving a periodic forcing function, $\cos(t)$. The control law stabilizes the outputs exponentially, and in doing so the

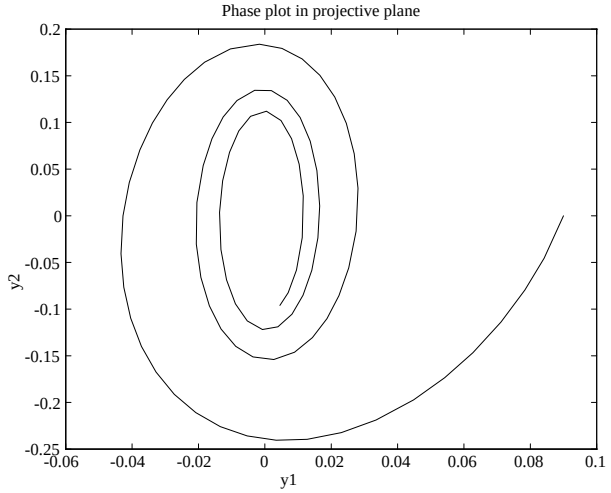

Figure 4.5: The is a phase plot of y_1, y_2 for the symmetric satellite. Notice how the resulting figure is essentially spiral in the y_1, y_2 space, steadily decreasing in size as the error along the fiber z_1 is reduced.

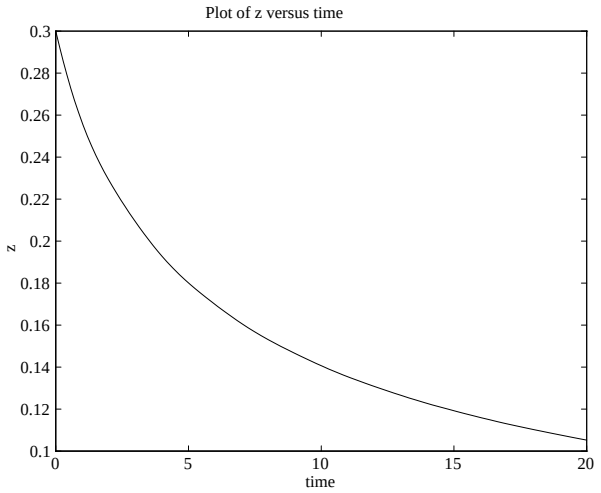

Figure 4.6: This is a plot of z_1 vs. time for the symmetric satellite. The error reduces steadily, albeit slowly.

asymmetric satellite follows albeit somewhat more slowly.

Now we define the relative degree one outputs. The output e is defined to be

$$e = \begin{bmatrix} \omega_1 \\ \omega_2 \end{bmatrix} + \begin{bmatrix} (z_1 + z_2)\cos(t) \\ -\alpha(z_1 + z_2)^2 \cos(t) \end{bmatrix} + \begin{bmatrix} -\sin(z_1) & \cos(z_1) \\ -\cos(z_1) & -\sin(z_1) \end{bmatrix} \begin{bmatrix} y_1 \\ y_2 \end{bmatrix} \tag{4.27}$$

Differentiate the output and notice that:

$$\dot{e} = \begin{bmatrix} u_1 \\ u_2 \end{bmatrix} + f_1(h, y, z, t)$$

Proposition 14 (The Asymmetric Stabilizer)

Given a control system on $TSO(3)$ whose evolution
is described by equation (3.31)
with $\alpha \neq 0$,
Then all smooth control laws $u(R, \omega, t)$ of the form
$u = -(e + f_1(e, y, z, t))$
with $k_i > 0$ as in the definition of y and
render the point $R = I, \omega = 0$
locally asymptotically stable.

Proof: The outline of the proof is as follows. First, we solve for the dynamics of the systems under these inputs. Second, we perform a transformation of y_2 to remove a time-varying first order dependence. Then, we examine the linearization of the system about 0.

The linearization is time-invariant. Thus, we may apply center manifold theory [40, 42]. We then solve the dynamics on the center manifold and consider their average. The average system is shown to be stable.

Let's first examine the dynamics of ω under these controls.

$$\begin{aligned} \omega_1 &= -\frac{2}{\alpha}(z_1 + z_2)\cos(t) + \sin(z_1)y_1 - \cos(z_1)y_2 \\ \omega_2 &= \frac{2}{\alpha}(z_1 + z_2)^2 \cos(t) + \cos(z_1)y_1 + \sin(z_1)y_2 \end{aligned}$$

We know that $\dot{y} = A(y, z_1)\omega$, thus we have:

$$\begin{aligned}\dot{y}_1 &= \frac{1 + y_1^2 + y_2^2}{2}\left(-\sin(z_1)\omega_1 - \cos(z_1)\omega_2\right) \\ \dot{y}_2 &= \frac{1 + y_1^2 + y_2^2}{2}\left(\cos(z_1)\omega_1 - \sin(z_1)\omega_2\right)\end{aligned}$$

Which is to say, to a certain order,

$$\begin{aligned}\dot{y}_1 &= -y_1 + \frac{-1}{\alpha}\left(z_2(z_1 + z_2)\right)\cos(t) + O(3, t) \\ \dot{y}_2 &= -y_2 - \frac{1}{\alpha}\left(z_1 + z_2\right)\cos(t) + O(2, t)\end{aligned}$$

We wish to compute the third order terms of $\dot{z}_1$ and $\dot{\omega}$ explicitly. To this end, we need to find expressions for y on the center manifold to a certain order. Start with y_2. Define $\tilde{y}_2$ as follows:

$$\tilde{y}_2 = y_2 + Az_1\sin(t) + Bz_2\sin(t) + Cz_1\cos(t) + Dz_2\cos(t)$$

Thus we can say:

$$\begin{aligned}\dot{\tilde{y}}_2 &= -\left(y_2 + Az_1\sin(t) + Bz_2\sin(t) + Cz_1\cos(t) + Dz_2\cos(t)\right) \\ &\quad + \left(A - C\right)z_1\sin(t) \\ &\quad + \left(B + A - D\right)z_2\sin(t) \\ &\quad + \left(C + A - \frac{1}{\alpha}\right)z_1\cos(t) \\ &\quad + \left(D + B + C - \frac{1}{\alpha}\right)z_2\cos(t) \\ &\quad + O(2, t)\end{aligned}$$

We wish all but the first term to be zero. Thus we have $A = C = \frac{1}{2\alpha}$. Adding the 3^{rd} and 5^{th} lines gives us $2B = 0$, which implies that $D = \frac{1}{2\alpha}$.

Finally we have,

$$y_2 = \frac{-1}{2\alpha}\left(z_1\sin(t) + (z_1 + z_2)\cos(t)\right) + O(2, t)$$

Now solve for y_1 in a similar manner. Define:

$$\tilde{y}_1 = y_1 + (Az_1^2 + Bz_1z_2 + Cz_2^2)\cos(t) + (Dz_1^2 + Ez_1z_2 + Fz_2^2)\sin(t)$$

The dynamics follow.

$$\begin{aligned}
\dot{\tilde{y}}_1 &= -\left(y_1 + (Az_1^2 + Bz_1z_2 + Cz_2^2)\cos(t) + (Dz_1^2 + Ez_1z_2 + Fz_2^2)\sin(t)\right) \\
&\quad + z_1^2\cos(t)\,(A+D) \\
&\quad + z_1z_2\cos(t)\left(B + 2A + E - \frac{1}{\alpha}\right) \\
&\quad + z_2^2\cos(t)\left(C + B + F - \frac{1}{\alpha}\right) \\
&\quad + z_1^2\sin(t)\,(D-A) \\
&\quad + z_1z_2\sin(t)\,(E - B + 2D) \\
&\quad + z_2^2\sin(t)\,(F - C + E) \\
&\quad + O(3,t)
\end{aligned}$$

This implies that $D = A = -A = 0$. Then we have that $E = B = \frac{1}{2\alpha}$. This means $F = 0$, and $C = \frac{1}{2\alpha}$. In summary,

$$\begin{aligned}
y_1 &= \frac{-1}{2\alpha}\left((z_2(z_1+z_2))\cos(t) + (z_1z_2)\sin(t)\right) + O(3,t) \\
y_2 &= \frac{-1}{2\alpha}\left(z_1\sin(t) + (z_1+z_2)\cos(t)\right) + O(2,t)
\end{aligned}$$

Recall, to some order,

$$\begin{aligned}
\omega_1 &= \frac{1}{\alpha}(z_1+z_2)\cos(t) + z_1y_1 - y_2 \\
\omega_2 &= \frac{-1}{\alpha}(z_1+z_2)^2\cos(t) + y_1 + z_1y_2
\end{aligned}$$

This implies,

$$\begin{aligned}
\omega_1 &= \frac{3}{2\alpha}(z_1+z_2)\cos(t) + \frac{1}{2\alpha}z_1\sin(t) + O(2,t) \\
\omega_2 &= \frac{-3}{2\alpha}(z_1+z_2)^2\cos(t) - \frac{1}{2\alpha}z_1(z_1+z_2)\sin(t) + O(3,t)
\end{aligned} \tag{4.28}$$

We are ready to solve for the dynamics of z_2.

$$\begin{aligned}
\dot{z}_2 &= \alpha\omega_1\omega_2 \\
&= \frac{-1}{4\alpha}\left(9(z_1+z_2)^3\cos^2(t) + z_1^2(z_1+z_2)\sin^2(t)\right) \\
&\quad + \frac{1}{4\alpha}\left(z_1(z_1+z_2)^2\sin(2t)\right) + O(4,t)
\end{aligned}$$

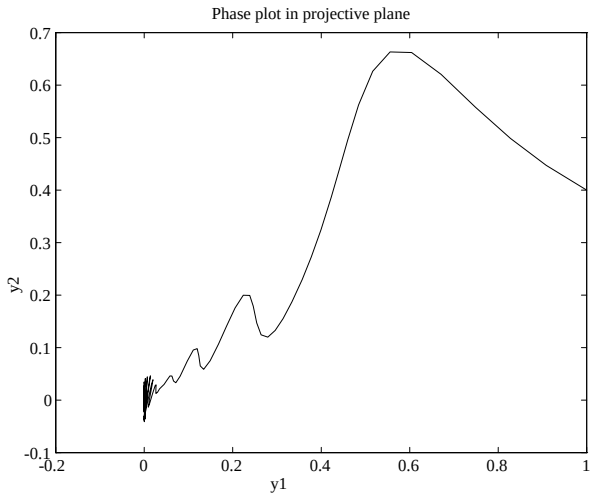

Figure 4.7: This phase plot shows the history of the satellite in (y_1, y_2) space for the asymmetric satellite. After the initial transient wherein the large error in (y_1, y_2) is corrected, the satellite wobbles back and forth about the origin.

Now solve for the dynamics of z_1.

$$\dot{z}_1 = z_2 + \frac{2}{1 + y_1^2 + y_2^2}(y_2\dot{y}_1 - y_1\dot{y}_2) = z_2 + O(4, t)$$

There are no third order terms in the dynamics of z_1 because of the area form cancellation.

After an application of averaging, we see that

$$\begin{aligned} \dot{\tilde{z}}_1 &= z_2 + O(3, t) + O(4) \\ \dot{\tilde{z}}_2 &= -\frac{1}{8\alpha}(z_1 + z_2)(2z_1 + 3z_2)(4z_1 + 3z_2) + O(4) \end{aligned} \tag{4.29}$$

where $o(3, t)$ is order 3 and time average zero, and where the terms $o(4)$ represent terms order 4 or higher.

To prove asymptotic stability, consider the family of quadrilaterals parameterized by δ with corners given by $(a, b, c, d) = ((\delta, \frac{-1}{4}\delta^3)(\delta - \delta^3, \delta^3), (-\frac{3}{4}\delta^3, -\delta^3), (-\delta + 2\delta^3, -\delta^3),)$. For small δ, the origin is enclosed by this quadrilateral. A gradient calculation also shows that for sufficiently small δ, the vector field points everywhere inward.

Simulations were run of the law. Figure (4.7) shows the path in the projective plane space. Figure (4.8) shows z_1 and z_2 converging to zero.

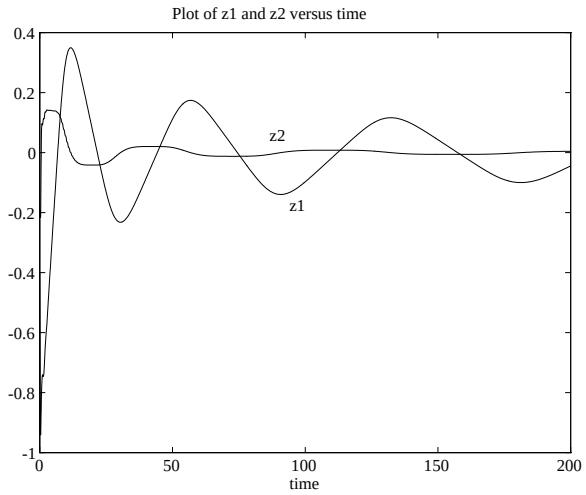

Figure 4.8: This plot shows the time history of z_1 and z_2 for the asymmetric satellite. Note they converge at a slower than linear rate. The damping can be improved with different choice of gains k_1 and k_2.

4.3 Conclusion

We have solved the point stabilization problem for our class of mechanical systems. Such solutions are basic results. They may be extended to achieve several other standard control objectives, for example, path planning and trajectory tracking. The performance with regards to these other tasks is lacking. The trajectories it produces are far from optimal. For example, see figure (4.3) for the fire truck. The slow convergence rate of the regulators when they are adapted for the purpose of tracking.

Consequently, these feedback laws are useful for regulation, that is, maintaining some configuration in the presence of disturbances. For large motions, entirely new strategies are required. The rest of this dissertation is devoted to solving the problems associated with large motions.

Chapter 5

Trajectory Tracking

In this chapter, we develop a set of control laws which stabilize about *trajectories* instead of points, using the results found in [47]. For reasons we will explain shortly, the tracking laws are not generalized from the point stabilization results of chapter 4. Instead, given a feasible trajectory $g(\cdot)$ (or $x(\cdot)$) parameterized by time, with velocities $v(\cdot)$, and nominal inputs $u(\cdot)$ generated by an open-loop path planner, we compute the linearization of the system about this nominal trajectory. If the linear time-varying system thus obtained is uniformly completely controllable in a certain sense (to be made explicit), we write a linear time-varying feedback law which will locally exponentially stabilize the system about the nominal trajectory.

We start with a short comparative study of methods for achieving large motions for our class of mechanical systems. First, do we need to study path planning at all given the regulators we have developed in chapter 4? This may be answered by looking at the kinds of paths produced by the smooth feedback stabilizers (see figure 4.3). Our experience is that the regulators make local decisions, moving the robot in the way which will immediately improve the error on the short term. Path planning, one the other hand, produces more efficient larger-scale paths.

Second, if we do solve the path planning problem, why do we need to study the tracking problem? In a real world situation there are many types of disturbances which would lead to great error. For example, the initial configuration of the system might be slightly in error. Figure 5.1 shows the result of such initial error.

We may adapt regulators for tracking by adding a feed-forward term. Figure 5.2 shows the application of such a strategy to the robot Hilare. The law is applied with twenty

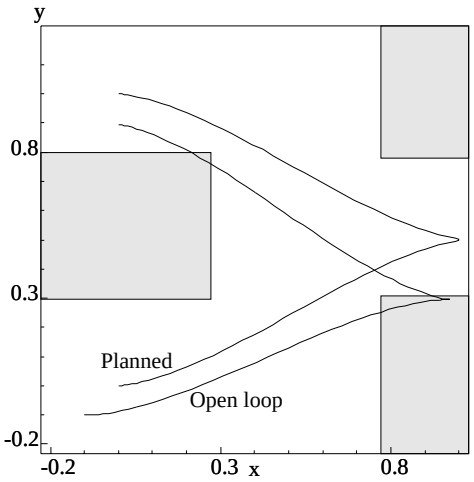

Figure 5.1: The figure shows the path of the robot Hilare with zero initial error, and the path with some small initial error.

seven different initial condition errors, all near the correct starting point.

Better performance is achieved by the laws developed in this chapter. For the purpose of comparison, we simulate the robot Hilare with one of the tracking controllers developed here. The gains are chosen as to make the control efforts of the two laws roughly equal. All twenty seven initial condition errors are chosen to be the same as in the earlier runs.

The problem solved in this chapter is: given a nonholonomic system, a feasible desired trajectory to follow, a known clearance between obstacles, and a measure of accuracy of the sensors, find a control law which will stabilize the system to this path, avoiding the obstacles robustly in the face of disturbances.

In the examples, we focus on mobile robots with an objective of creating a composite controller that will: first, have off-line computation of a trajectory which avoids the obstacles [24]; second, apply the control law given here to stabilize the system to the open loop collision-free trajectory; third, while executing, use sensors to detect possible collisions due to poor *a priori* information. In this case, new information can be used to update the model of the environment and restart the process. Such a controller would be able to reject many types of disturbances including noise in the sensors, initial condition errors, and errors introduced along the trajectory.

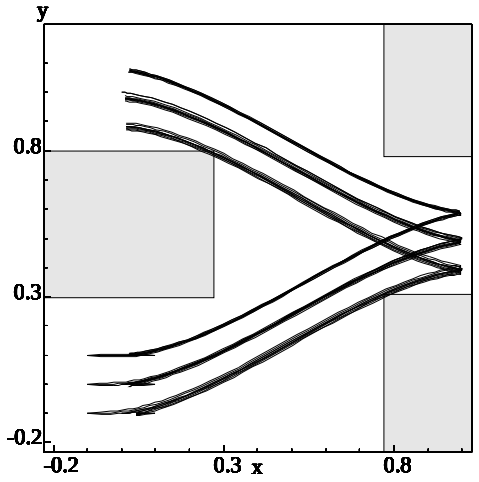

Figure 5.2: Simulation of the regulator law adapted for tracking, shown as a $x_1 - x_2$ phase plot. Note that while the law corrects well for error in the x_1 and x_3 directions, it performs poorly in correcting along the x_2 direction.

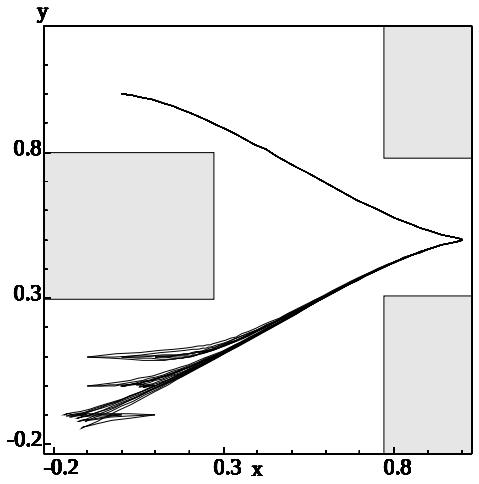

Figure 5.3: Simulation of the tracking control law, shown as a $x_1 - x_2$ phase plot. No matter the direction of the perturbation, the controller tracks the desired trajectory exponentially fast.

5.1 Linearizations

Nominally, we are given a desired trajectory as $g^0(\cdot)$ with $g^0(t) \in \mathcal{G}, v^0(\cdot)$ with $v^0(t) \in \mathbb{R}^p$, and $u^0(\cdot)$ with $u^0(t) \in \mathbb{R}^p$ in the matrix Lie group setting (see equation (2.42)). Since linear control theory is written for systems in coordinates, we first need to find a valid coordinate chart Φ for $\mathcal{G}$. The desired trajectory is then, expressed in coordinates, $x^0(t) \in \mathbb{R}^n$, $v^0(t) \in \mathbb{R}^p$, and $u^0(t) \in \mathbb{R}^p$ at each time t with dynamics given by (2.1). We then compute the linearization of the mechanism about the trajectory and apply linear control theory to the result.

There is one difficulty to this approach. The nominal trajectory may or may not reside completely inside the region of validity of the coordinate chart Φ. The feedback control laws computed in this chapter depend on the choice of coordinate chart, and if we change regions and charts we change control laws. The effects of switching is outside the scope of this dissertation.

If a coordinate chart covering the area of interest can be found, then the procedure outlined in the next subsection is used. A general procedure for constructing a coordinate chart valid in an open region about any C^2 trajectory is given in the following subsection.

5.1.1 Locally Valid Linearizations

Suppose we have a coordinate chart Φ for $\mathcal{G}$ which is valid for the entire trajectory. The state of the system at time t is given by $(\Phi(g(t)), v(t))$. In general the dynamics are written

$$\begin{aligned} \dot{x} &= f(x, v) \\ \dot{v} &= u \end{aligned} \tag{5.1}$$

where $x \in \mathbb{R}^n$ are the coordinates, $v \in \mathbb{R}^p$ are the velocities, $u \in \mathbb{R}^p$ are the inputs, $x^0(\cdot)$ is the desired trajectory, $v^0(\cdot)$ is the desired velocity, and $u^0(\cdot)$ are the nominal inputs. The vector field $f(x, v)$ is at least C^2 with respect to x and v. The linearization may proceed in the standard way, with the linear time varying system matrixes $A(t), B(t)$ given by:

$$\begin{aligned} A(t) &:= \begin{bmatrix} \frac{\partial f}{\partial x}(x^0(t), v^0(t)) & \frac{\partial f}{\partial v}(x^0(t), v^0(t)) \\ 0 & 0 \end{bmatrix} \\ B(t) &:= \begin{bmatrix} 0 \\ I \end{bmatrix} \end{aligned}$$

5.1.2 Linearizations Valid for Entire Trajectories

A coordinate chart valid for a neighborhood about the trajectory may always be found, provided that the desired trajectory $g^0(\cdot)$ is C^2. What follows is a constructive procedure for building such a chart provided one does not already exist.

Recall that the exponential map $\mathrm{Exp} : \mathfrak{g} \to \mathcal{G}$ is a local diffeomorphism. Thus we may write $g(t) = g^0(t)\ \mathrm{Exp}(\hat{\eta}(t))$, assuming that $g(t)$ is close to $g^0(t)$. Using a basis for $\mathfrak{g}$ and $\mathfrak{g}^*$, define $N_i(t) = \hat{p}_i(\hat{\eta}(t))$. Given $t \in \mathbb{R}$ and $N(t) \in \mathbb{R}^n$ we may find $g(t)$. Provided that $g(t)$ is close to $g^0(t)$, we may find $N(t)$.

Now we wish to solve for the dynamics of N to first order. Consider the dynamics of g.

$$\dot{g}(t) \quad = \quad g(t) \left((\ \mathrm{Exp}(\hat{\eta}(t)))^{-1}\, \hat{e}_c^0\ \mathrm{Exp}(\hat{\eta}(t)) + \dot{\hat{\eta}} \right) \tag{5.2}$$

We need a series expansion of the first term, with respect to $\hat{\eta}$.

$$(\ \mathrm{Exp}(\hat{\eta}(t)))^{-1}\, \hat{e}_c^0\ \mathrm{Exp}(\hat{\eta}(t)) \quad = \quad \hat{e}_c^0 + [\hat{e}_c^0, \hat{\eta}] + h.o.t \tag{5.3}$$

We can also consider the system equation variation.

$$\dot{g}(t) \quad = \quad g(t) \left(\hat{e}_c^0 + \frac{d\hat{e}_c^0}{\partial g}(\hat{\eta}(t)) + \frac{\partial \hat{e}_c^0}{\partial v}(v - v^0) + h.o.t \right) \tag{5.4}$$

By setting the two observations equal to each other, we solve for $\dot{N}_i = \hat{p}_i(\dot{\hat{\eta}}(t))$.

$$\dot{\hat{\eta}}(t) = \frac{\partial \hat{e}_c^0}{\partial g}(\hat{\eta}(t)) - [\hat{e}_c^0, \hat{\eta}] + \frac{\partial \hat{e}_c^0}{\partial v}(v - v^0) + h.o.t \tag{5.5}$$

As before, we may identify $x = N$, and the linearization matrices $A(t), B(t)$.

$$\begin{aligned} A(t) \quad &:= \quad \begin{bmatrix} A_{11}(t) & A_{12} \\ 0 & 0 \end{bmatrix} \\ B(t) \quad &:= \quad \begin{bmatrix} 0 \\ I \end{bmatrix} \end{aligned} \tag{5.6}$$

where $(A_{11})_{ij} = \hat{p}_i \left(\frac{\partial \hat{e}_c^0}{\partial g}(\hat{e}_j) - [\hat{e}_c^0, \hat{e}_j] \right)$ and $(A_{12})_{ij} = \hat{p}_i \left(\frac{\partial \hat{e}_c^0}{\partial v_j} \right)$.

5.2 An Exponentially Stabilizing Control Law

No matter what type of chart is chosen, the equations of motion become

$$\begin{aligned} \dot{x} &= f(x,v) \\ \dot{v} &= u \\ x &\in \mathbb{R}^n \text{ coordinates} \\ v &\in \mathbb{R}^p \text{ velocities} \\ u &\in \mathbb{R}^p \text{ inputs} \\ x^0(\cdot) &\quad \text{desired trajectory} \\ v^0(\cdot) &\quad \text{desired velocity} \\ u^0(\cdot) &\quad \text{nominal inputs} \end{aligned} \tag{5.7}$$

with $f(x,v)$ C^2 with respect to x and u.

Inspired by the result on linear systems found in [10], we have picked the following control law.

Proposition 15 (A Tracking Control Law)

Given: a system of the form (5.7), a desired trajectory $x^0(\cdot)$, velocities $v^0(\cdot)$, and a nominal input $u^0(\cdot)$, each bounded for all t, define the following:

$$A(t) := \begin{bmatrix} \frac{\partial f}{\partial x}(x^0(t), v^0(t)) & \frac{\partial f}{\partial v}(x^0(t), v^0(t)) \\ 0 & 0 \end{bmatrix}$$

$$B(t) := \begin{bmatrix} 0 \\ I \end{bmatrix}$$

Define: $\Phi(t, t_0) \in \mathbb{R}^{(n+p)\times(n+p)}$, *to be the solution to the differential equation* $\dot{\Phi}(t,t_0) = A(t)\Phi(t,t_0)$ *with* $\Phi(t_0,t_0) = I$. *Further, define for some* $\alpha > 0$

$$H_c(t_0,t) = \int_{t_0}^{t} e^{6\alpha(t_0-\tau)}\Phi(t_0,\tau)B(\tau)B(\tau)^T\Phi(t_0,\tau)^T d\tau$$

If there exists a δ *such that* $H_c(t, t+\delta)$ *is bounded away from singularity for all* t, *then define* $P_c(t)$ *as follows,*

$$P_c(t) \;:=\; H_c^{-1}(t, t+\delta)\ .$$

If: *there exist two numbers p_c^m, p_c^M such that*

$$0 \;<\; p_c^m I < P_c(t) < p_c^M I \quad \forall t \in \mathbb{R}_+\ ,$$

Then: *for any function $\gamma : \mathbb{R}_+ \to [\frac{1}{2}, \infty)$, continuous and bounded, the linear time-varying feedback law:*

$$u \;=\; u^0 - \gamma(t) B(t)^T P_c(t) \begin{bmatrix} x - x^0 \\ v - v^0 \end{bmatrix}$$

locally, uniformly, exponentially stabilizes the system (5.7) to the desired trajectory $x^0(t)$ and the desired velocities $v^0(t)$ at a rate greater than $2\alpha p_c^m (p_c^M)^{-1} > 0$.

Remark: If the linear time-varying system is uniformly completely controllable over intervals of length $\delta > 0$ then $H_c(t, t+\delta)$ is uniformly invertible.

Proof: First, define the error signal e and error input w as

$$\begin{aligned} e &= \begin{bmatrix} x - x^0 \\ v - v^0 \end{bmatrix} \in \mathbb{R}^{(n+p)} \\ w &= u - u^0 \in \mathbb{R}^p\ . \end{aligned}$$

We solve for the dynamics of these error signals using the Taylor series expansions

$$\begin{aligned} \dot{e} &= \begin{bmatrix} f(x^0 + e^1, v^0 + e^2) - f(x^0, v^0) \\ w \end{bmatrix} \\ &= A(t)e + B(t)w + \text{h.o.t.}\ . \end{aligned}$$

All terms with dependencies on x^0, v^0, u^0 will be rewritten as functions of time. In addition to $A(t), B(t)$, define $o(e, v, t)$ to be the higher order terms

$$o(e, v, t) \;=\; \begin{bmatrix} f(x^0 + e^1, v^0 + e^2) - f(x^0, v^0) \\ w \end{bmatrix} - A(t)e - B(t)w\ .$$

Note that since $w = -\gamma(t) B^T(t) P_c(t) e$, we may rewrite $o(e, v, t)$ so it depends only on e, t; call this $\hat{o}(e, t)$. As $x^0(t), v^0(t), u^0(t)$ are bounded for all t, $B(t)$ is bounded for all t which

implies that $\|\gamma(t)B^T(t)P_c(t)e\| \leq K\|e\|$ for some $K < \infty$ as $\gamma(t), P_c(t)$ are also bounded for all t. Given this we may show

$$\lim_{\|e\|\to 0} \sup_{t\geq 0} \frac{\|\hat{o}(e,t)\|}{\|e\|} = 0 \ . \tag{5.8}$$

Thus we have

$$\begin{aligned} \dot{e} &= A(t)e + B(t)w + o(e,v,t) \\ \dot{e} &= \tilde{A}(t)e + \hat{o}(e,t) \end{aligned} \tag{5.9}$$

with

$$\tilde{A} = A(t) - \gamma(t)B(t)B(t)^T P_c(t) \ .$$

Inspired by [10], we pick a Lyapunov function

$$V(e,t) = e^T P_c(t) e \ . \tag{5.10}$$

and calculate its time derivative along trajectories of the system (5.9). One may verify that

$$\begin{aligned} \dot{P}_c(t) &= -6\alpha P_c(t) - P_c(t)A(t) - A^T(t)P_c(t) \\ &\quad + P_c(t)[B(t)B^T(t) - e^{-4\alpha\delta}\Phi(t,t+\delta)B(t+\delta)B^T(t+\delta)\Phi^T(t,t+\delta)]P_c(t) \ . \end{aligned}$$

Thus the time derivative of the Lyapunov function is

$$\begin{aligned} \dot{V}(e,t) &= -e^T[6\alpha P_c(t) + (2\gamma(t)-1)P_c(t)B(t)B^T(t)P_c(t)]e \\ &\quad - e^T e^{-4\alpha\delta} P_c(t)\Phi(t,t+\delta)B(t+\delta)B^T(t+\delta)\Phi^T(t,t+\delta)P_c(t)e \\ &\quad + 2e^T P_c(t)\hat{o}(e,t) \ . \end{aligned} \tag{5.11}$$

Note that if $\gamma(t) \geq \frac{1}{2}, \forall t$, then the first two terms in (5.11) are less than or equal to $-6\alpha p_c^m \|e\|^2$. Secondly, because of (5.8), there exists a number $\epsilon > 0$ such that

$$\|\hat{o}(e,t)\| \leq \alpha p_c^m (p_c^M)^{-1}\|e\|, \forall e \text{ such that } \|e\| \leq \epsilon \ ,$$

which implies

$$|2e^T P_c(t)\hat{o}(e,t)| \leq 2\alpha p_c^m \|e\|^2, \forall \|e\| \leq \epsilon \ .$$

Thus, as in [10], we may say

$$\dot{V}(e,t) \leq -4\alpha p_c^m \|e\|^2 . \tag{5.12}$$

Further we may state

$$\dot{V}(e,t) \leq -4\alpha p_c^m (p_c^M)^{-1} V(e,t) . \tag{5.13}$$

Finally we conclude

$$\begin{aligned} V(e,t) &\leq V(e_0,t_0) e^{-4\alpha p_c^m (p_c^M)^{-1}(t-t_0)} \\ \|e(t)\| &\leq \|e(t_0)\| \sqrt{\frac{p_c^M}{p_c^m}} e^{-2\alpha p_c^m (p_c^M)^{-1}(t-t_0)} , \end{aligned} \tag{5.14}$$

which gives us the specified convergence rate for the error signals.

5.2.1 Convergence Rate Estimation

This convergence rate may be shown to be independent of p_c^m and p_c^M. To demonstrate this, define z, y:

$$\begin{aligned} z &= ey \\ y &\in \mathbb{R} \quad \text{with} \\ \dot{y} &= \alpha y \end{aligned}$$

Now we wish to solve for the dynamics of z.

$$\dot{z} = (\tilde{A} + \alpha I) z + \hat{o}(e,t) y$$

We will pick the same Lyapunov equation and calculate its derivative, using the same arguments as before,

$$\begin{aligned} V(z,t) &= z^T P_c(t) z \\ \dot{V}(z,t) &\leq -4\alpha p_c^m \|z\|^2 + 2 z^t P_c(t) \hat{o}(e,t) y . \end{aligned}$$

Given the exponential convergence of e when it starts sufficiently close to the origin, we may say that after some time T the last factor may be bounded as follows,

$$|2 z P_c(t) \hat{o}(e,t) y| \leq 2\alpha p_c^m \|z\|^2 .$$

Thus we may write, as before,

$$\dot{V}(z,t) \leq -2\alpha p_c^m \|z\|^2 .$$

And following equations (8) and (9) we will obtain the same convergence rate, $(p_c^M)^{-1}$. However, we may note

$$\|z\| = e^{\alpha(t-t_0)}|y_0|\|e\| .$$

Thus, if z is exponentially convergent at a rate $(p_c^M)^{-1}$ after some time T, then e is exponentially convergent at a rate $(p_c^M)^{-1} + \alpha > \alpha$ after some time T, thus for a sufficiently large k we may state

$$\|z\| \leq ke^{-\alpha(t-t_0)}\|z_0\| .$$

5.2.2 Causal Control Laws

For some regulator applications, it is desirable for the controller to be "causal", that is to not need information on the future desired trajectory of the system. To deal with this concern, define $P_r(t)$, similar to $P_c(t)$, again assuming the inverse in the formula exists,

$$P_r(t) = (H_c(t, t-\delta))^{-1} .$$

Notice that this matrix is dependent on past values of the trajectory and not on future values. As before, if there exists two numbers p_r^m and p_r^M such that

$$0 < p_r^m I < P_r(t) < p_r^M I \quad \forall t \in \mathbb{R}_+ ,$$

then for any $\gamma : \mathbb{R}_+ \to [\frac{1}{2}, \infty)$, continuous and bounded, the linear time varying feedback law

$$u = u^0 - \gamma(t)B(t)^T P_r(t)(x - x^0)$$

locally uniformly exponentially stabilizes the system (1) at a rate greater then α.

The proof is similar to the last control law and so will be left to the interested reader. It is useful to note

$$\begin{aligned}\dot{P}_r(t) = & -6\alpha P_r(t) - P_r(t)A(t) - A^T(t)P_r(t) \\ & + P_r(t)[B(t)B^T(t) - e^{4\alpha\delta}\Phi(t, t-\delta)B(t-\delta)B^T(t-\delta)\Phi^T(t, t-\delta)]P_r(t) .\end{aligned}$$

Finally, it should be noted that it is equivalent to design a velocity feedback law for all of these systems.

5.3 Applications

We apply this control law to three example systems. The first is a kinematic system with a simple structure, allowing for the explicit computation of the control laws. The second is the Hilare-like mobile robot and the third example is a front wheel drive car.

5.3.1 The Heisenberg Control Algebra

Here we consider one of the simplest nonholonomic systems: the kinematic system whose control Lie algebra is the Heisenberg algebra with two generators [4]. Starting with a simple example will help with what follows. The differential equations are as follows,

$$\begin{aligned} \dot{x_1} &= u_1 \\ \dot{x_2} &= u_2 \\ \dot{x_3} &= x_2 u_1 \ . \end{aligned} \tag{5.15}$$

This system's straightforward structure allows us to compute the control laws in closed form. We will investigate two trajectories for this system, a "trivial" trajectory which is just a point, and a straight line.

Much of the control law can be found without reference to the specific form of the desired trajectory. The first step is to find the matrices $A(t), B(t)$.

$$\begin{aligned} A(t) &= \frac{\partial f}{\partial x}(x^0, u^0) \\ &= \begin{bmatrix} 0 & 0 & 0 \\ 0 & 0 & 0 \\ 0 & u_1^0 & 0 \end{bmatrix} \\ B(t) &= \begin{bmatrix} 1 & 0 \\ 0 & 1 \\ x_2^0(t) & 0 \end{bmatrix} \end{aligned} \tag{5.16}$$

With these, the state transition matrix associated with this particular $A(t)$ can be found. Using the fact that $\Phi(t_0, t_0) = I$ and that $\Phi(t, t_0)$ satisfies the differential equation $\dot{\Phi}(t, t_0) = A(t)\Phi(t, t_0)$, it can be shown that

$$\Phi(t, t_0) = \begin{bmatrix} 1 & 0 & 0 \\ 0 & 1 & 0 \\ 0 & x_1^0(t) - x_1^0(t_0) & 1 \end{bmatrix} .$$

Now that we have the state transition matrix, we solve for the derivative of $H_c(t_0,t)$ as follows,

$$\begin{aligned}\dot{H}_c(t_0,t) &= e^{4\alpha(t_0-t)}\Phi(t_0,t)B(t)B(t)^T\Phi^T(t_0,t) \\ &= e^{4\alpha(t_0-t)}\begin{bmatrix} 1 & 0 & x_2^0(t) \\ 0 & 1 & x_1^0(t_0)-x_1^0(t) \\ x_2^0(t) & x_1^0(t_0)-x_1^0(t) & \left(x_2^0(t)\right)^2+\left(x_1^0(t_0)-x_1^0(t)\right)^2 \end{bmatrix}\end{aligned}$$

The first nominal trajectory that we choose is the trivial one, where the system stays fixed at a given point for all time. Note that stabilizing to this trajectory is equivalent to finding a point stabilization feedback law. The trajectory is highly degenerate in the sense that both nominal inputs are zero. We choose our desired point $x^0(t)$ to be the origin, $(0,0,0)$.

It may be shown that in this case, $H_c(t_0,t)$ has the following form (for $\alpha = 1$)

$$H_c(t_0,t) = \begin{bmatrix} 1-e^{t_0-t} & 0 & 0 \\ 0 & 1-e^{t_0-t} & 0 \\ 0 & 0 & 0 \end{bmatrix}.$$

Thus the matrix $H_c(t,t+\delta)$ is not invertible for any choice of δ, we cannot find the matrix $P_c(t) = H_c^{-1}(t,t+\delta)$ which is used in the definition of the control law, and therefore the method presented in this paper cannot be used to stabilize the system (5.15) to a point.

The second sample trajectory will be less trivial. We have chosen the straight line in state space described by $x^0(t) = (0,t,0)$, with nominal input $u^0(t) = (0,1)$. This trajectory is somewhat degenerate in the sense that one of the nominal inputs is zero. However, since the matrix H_c is invertible, our strategy will work for this trajectory. In fact, the determinant of H_c is independent of time, as can be seen by the following formula (where $\alpha = 1$):

$$\det\left(H_c(t,t+\delta)\right) = 1-e^{3\delta}+(3+\delta^2)(e^{-2\delta}-e^{-\delta})$$

We can choose any value of δ for which the previous expression is non-zero. In our simulation, $\delta = 1$ was chosen. (Note: nearly identical simulation results are obtained for the trajectory given by $u^0(t) = (1,0)$).

The initial error for this simulation was $(0.2,-0.3,0.2)$. The simulation was run for 8 seconds, and the results are given in Figures 5.4 - 5.6. Since the graphs of the state variables were in general difficult to interpret, we have instead shown the error coordinates $e(t)$ and the error inputs $w(t)$ versus time.

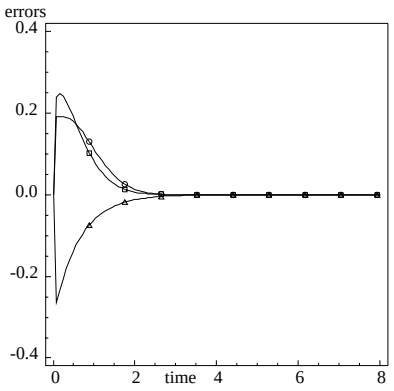

Figure 5.4: Plot of errors e versus time. The errors all quickly converge to zero for this path.

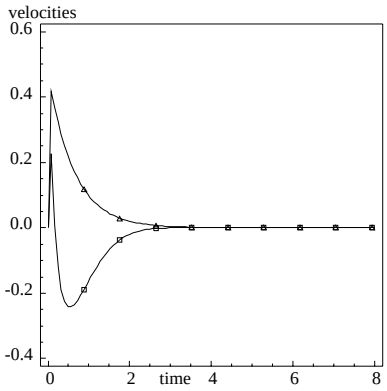

Figure 5.5: Graph of the error inputs w versus time. Note how all inputs are bounded and smooth.

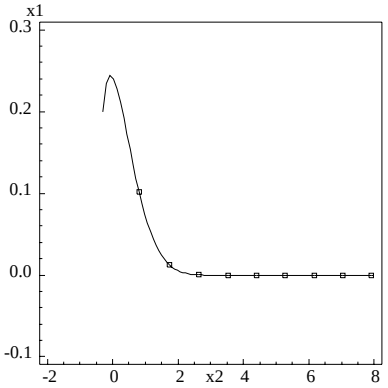

Figure 5.6: This x_1, x_2 phase plot shows the actual trajectory, projected onto the (x_1, x_2) plane. The desired trajectory is a straight line along the x_2 axis.

5.3.2 Trajectory Stabilization for Hilare

Again, one would hope the system's straightforward structure allows the control laws to be computed in closed form. The first step is to find the matrices $A(t)$, contained in $\mathbb{R}^{5\times5}$, and $B(t)$ which is contained in $\mathbb{R}^{5\times2}$:

$$\begin{aligned}
A(t) &= \begin{bmatrix} \frac{\partial f}{\partial x}(x^0, v^0) & \frac{\partial f}{\partial v}(x^0, v^0) \\ 0 & 0 \end{bmatrix} \\
\frac{\partial f}{\partial x}(x^0, v^0) &= \begin{bmatrix} 0 & 0 & -\sin(x_3^0)v_1^0 \\ 0 & 0 & \cos(x_3^0)v_1^0 \\ 0 & 0 & 0 \end{bmatrix} \\
\frac{\partial f}{\partial v}(x^0, v^0) &= \begin{bmatrix} \cos(x_3^0) & 0 \\ \sin(x_3^0) & 0 \\ 0 & 1 \end{bmatrix}
\end{aligned}$$

Now the state transition matrix associated with this particular $A(t)$ may be found. Using the fact that $\Phi(t_0, t_0) = I$ and that $\Phi(t, t_0)$ satisfies the differential equation $\dot{\Phi}(t, t_0) = A(t)\Phi(t, t_0)$, it may be shown that

$$\begin{aligned}
\Phi(t, t_0) &= \begin{bmatrix} \Phi_{11}(t, t_0) & \Phi_{12}(t, t_0) \\ 0 & I \end{bmatrix} \\
\Phi_{11}(t, t_0) &= \begin{bmatrix} 1 & 0 & f_s(t, t_0) \\ 0 & 1 & f_c(t, t_0) \\ 0 & 0 & 1 \end{bmatrix}
\end{aligned}$$

where

$$\begin{aligned}
f_s(t, t_0) &= \int_{t_0}^{t} -\sin\left(x_3^0(\tau)\right) u_1^0(\tau) d\tau \\
f_c(t, t_0) &= \int_{t_0}^{t} \cos\left(x_3^0(\tau)\right) u_1^0(\tau) d\tau \ .
\end{aligned}$$

The expression of $\Phi_{12}(t, t_0)$ is complicated. Now that we have the state transition matrix, we can solve for the derivative of $H_c(t_0, t)$ as follows,

$$\dot{H}_c(t, t_0) = e^{4\alpha(t_0 - t)} \Phi(t_0, t) B(t) B(t)^T \Phi(t_0, t)$$

However, for the nominal trajectories x^0 that we have chosen to simulate, the integrals f_s, f_c do not have a closed form. Thus we cannot directly compute the control

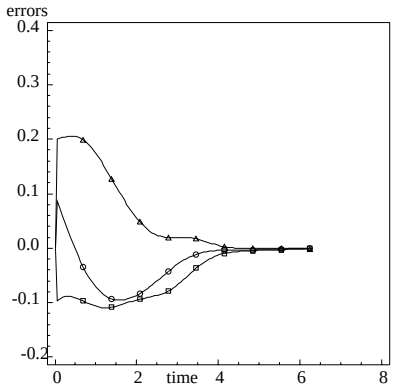

Figure 5.7: Plot of the errors in the trajectory versus time.

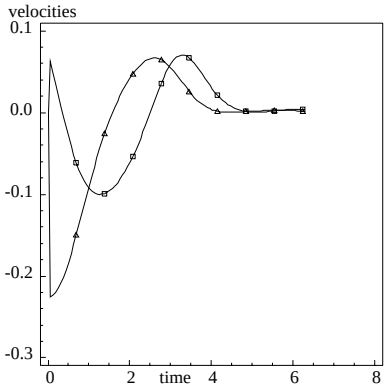

Figure 5.8: Plot of the errors in the velocities versus time.

law, and so we must compute the matrix P_c and the control law numerically. In doing so the following identity is useful:

$$\dot{\Phi}(t, t+\delta) \quad = \quad A(t)\Phi(t, t+\delta) - \Phi(t, t+\delta)A^T(t+\delta)$$

The first nominal trajectory for this system (Hilare) is generated by the velocity $v_1 = \sin(t), v_2 = \cos(t)$. We set $\alpha = 0.1, \delta = 1.0$. After one cycle these velocities steers the system in the direction given by the Lie bracket of the two input vector fields, or $[f_1, f_2]$. The initial condition was chosen to be (-0.1, 0.2, 0.1), and the simulation was run for 2π seconds. See Figures 5.7 - 5.9 for results.

The second nominal trajectory to which we have applied our stabilization procedure is a circular path. This choice was inspired by the work of Reeds and Shepp [36],

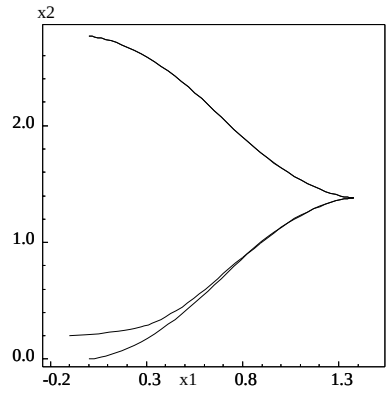

Figure 5.9: This phase plot shows the nominal and actual trajectories projected onto the (x_1, x_2) plane (the orientation of the robot is not shown). The desired trajectory starts at (0,0) whereas the actual trajectory has an initial offset of (-0.1,0.2). Note how quickly and smoothly the system converges to the desired trajectory.

who showed that time-optimal paths for Hilare-like robots with actuator limits consist of straight-line segments and arcs of circles.

The nominal velocity for this trajectory is $v^0 = (1, 1)$. We set $\alpha = 0.1, \delta = 1.0$ as before. We again choose an initial condition error of (-0.1, 0.2, 0.1), and run the simulation for 2π seconds. See Figures 5.10 - 5.12 for the results.

Although we have used the same values of α, δ and initial error as in the previous example, the convergence seems less rapid, indicating that the convergence rate depends on the chosen trajectory. However, the convergence rate is also a function of α, which we are

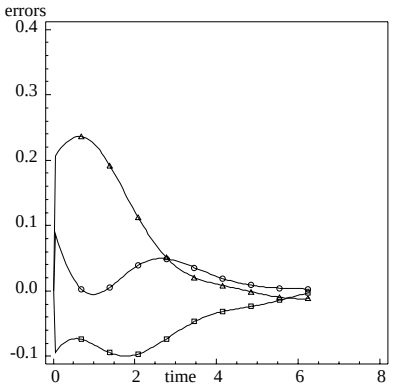

Figure 5.10: Plot of the errors in the trajectory versus time.

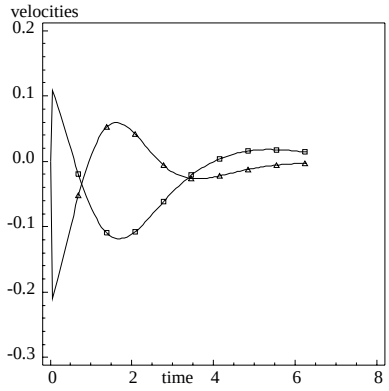

Figure 5.11: Plot of the errors in velocity versus time.

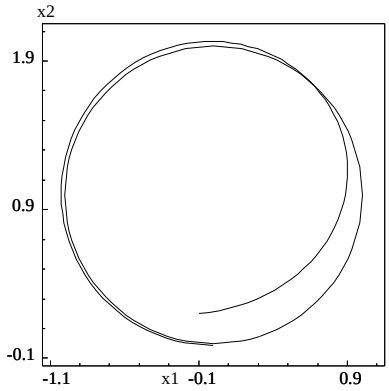

Figure 5.12: This phase plot shows the nominal and actual trajectories, projected onto the (x_1, x_2) plane (the orientation of the robot is not shown). The desired trajectory is the perfect circle. Note how quickly and smoothly the system converges to the desired trajectory.

free to choose. If we needed faster convergence, we could simply choose a larger α.

5.3.3 Trajectory Stabilization for a Front Wheel Drive Car

Now consider the front wheel drive car, since it is a more sophisticated example with four states and a two level chain when in power form.

The matrix $A(t)$ is

$$A(t) = \begin{bmatrix} \frac{\partial f}{\partial x}(x^0, v^0) & \frac{\partial f}{\partial v}(x^0, v^0) \\ 0 & 0 \end{bmatrix} \tag{5.17}$$

$$\frac{\partial f}{\partial x}(x^0, v^0) = \begin{bmatrix} 0 & 0 & -\cos(x_4^0)\sin(x_3^0)v_1^0 & -\cos(x_3^0)\sin(x_4^0)v_1^0 \\ 0 & 0 & -\sin(x_3)\sin(x_4^0)v_1^0 & \cos(x_3^0)\sin(x_4^0)v_1^0 \\ 0 & 0 & 0 & 0 \\ 0 & 0 & \frac{1}{L}\cos(x_3^0)v_1^0 & 0 \end{bmatrix}$$

$$\frac{\partial f}{\partial v}(x^0, v^0) = \begin{bmatrix} \cos(x_3^0)\cos(x_4^0) & 0 \\ \cos(x_3^0)\sin(x_4^0) & 0 \\ 0 & 1 \\ \frac{1}{L}\sin(x_3^0) & 0 \end{bmatrix}.$$

Inspired by [31], we chose the nominal input $v^0 = (\sin(t), \cos(2t))$, roughly corresponding to a parallel- parking maneuver (see Figure 14). Again, we chose $\alpha = 0.1, \delta = 1.0$. After one period ($T = 2\pi$), this input steers the system in the direction given by the second-level nested Lie bracket of the two input vector fields (*i.e.* One write the system as $\dot{x} = f_1(x)v_1 + f_2(x)v_2$, thus the nested Lie bracket would be $[f_1, [f_1, f_2]]$). Because the equations for this example are not simple, we have not tried to find H_c in closed form; all of the computations were done by the simulation program. The initial condition was chosen to be (0.1, -0.1, 0.05, 0.2), and the simulation was run for 2π seconds. Figures 5.13 - 5.15 show the results. Note the rapid convergence to zero in the error terms.

5.4 Conclusion

The control law and simulation results presented in this chapter suggest that for nonholonomic systems, stabilizing to a trajectory is perhaps a better problem to consider than stabilizing to a point. It can be noted that for drift-free systems, *all* points are equilibrium points (in the sense that with zero input, the system will remain at any configuration).

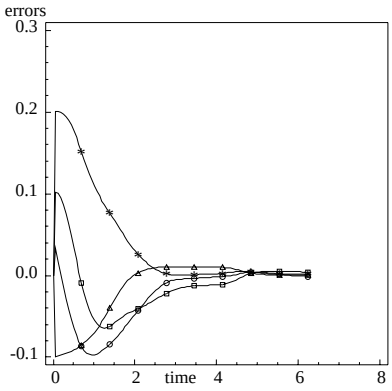

Figure 5.13: Plot of errors in the trajectory versus time.

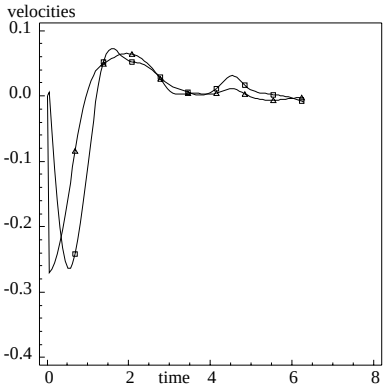

Figure 5.14: Plot of the errors in velocities versus time. Note they are bounded, smooth, and go to zero.

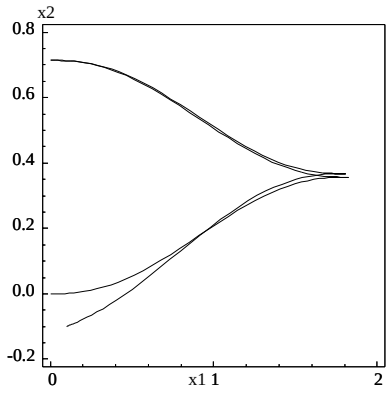

Figure 5.15: This phase plot shows the desired and the actual trajectories projected onto the (x_1, x_2) plane (the orientation of the car and the steering wheel angle are not shown). The desired trajectory is the one which starts at (0,0). Note how quickly and smoothly the control law stabilizes the system to this trajectory.

However, if one adopts this point of view, one must also face the problem of finding feasible trajectories; a rich problem which has not been solved for all systems. Excellent work has been done [24, 31, 36, 39] in this area, and methods for finding trajectories exist for a wide range of nonholonomic systems.

The control law presented in this chapter is robust to three types of error: initial condition errors, perturbations introduced along the trajectory, and noise in the sensor data. We have only shown the convergence results when there is an error in the initial condition, but it can be seen that the effects of the other two types of errors also are reduced using this law.

Chapter 6

Path Planning

-

This chapter is devoted to solving the path planning problem for the specific example systems of chapter 3. We wish to find a trajectory $x(t)$ or $g(t)$ which satisfies the constraints ω_i. If we view the problem in this manner, path planning is inherently a kinematic problem. We assume direct control over the velocities, using (2.3) to model the system. In order to find the $u(t)$ which generates the desired trajectory and velocities, we differentiate the desired velocity. The results of this chapter are based largely on the results presented in the author's work with collaborators in [43, 45, 46].

6.1 Steering Power Form Systems

Given that most of the mechanical systems considered can be locally transformed into power form, it is tempting to write a path planner for this general class. This is, of course, ignoring the fact that for most systems this transformation to power form is a local property. Path planning by definition involves large distances; hence, very likely, will require changes in these local charts.

However, when the coordinate chart changes can be avoided, many planners may be applied. We present one in this section derived from the stabilizing law of chapter 4. As in the point stabilization section, the principal nature of the equations inspires a two step

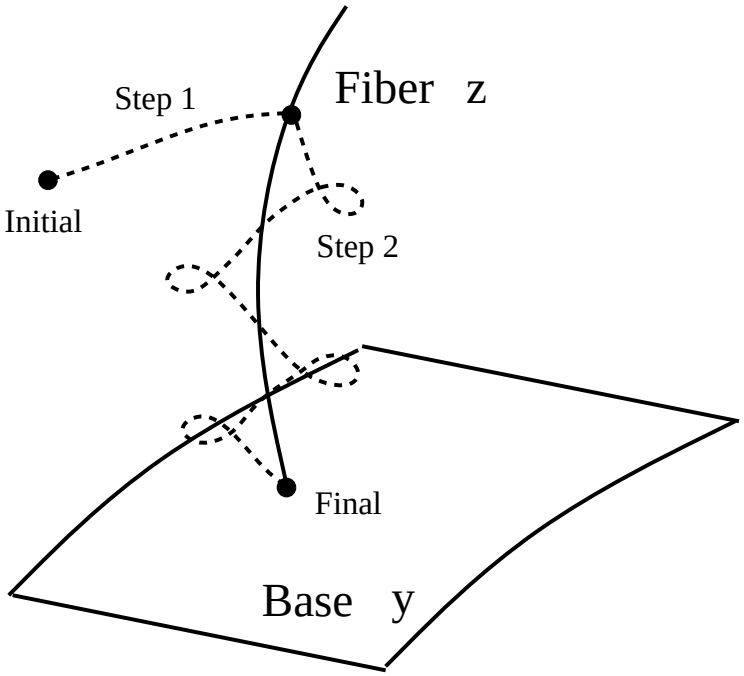

Figure 6.1: This figure illustrates a general sub-optimal path planner for power form systems. The first step corrects for the error on the base coordinates. The second step corrects for the error on the fiber.

planning process. We write the kinematic system as

$$\begin{aligned} \dot{y}_j &= v_j \quad 0 \leq j \leq (p) \\ \dot{z}^k_{j0} &= \frac{1}{k!} (y_0)^k \dot{y}_j \quad 1 \leq k \leq \ell_j,\ 1 \leq j \leq p \end{aligned} \tag{6.1}$$

where v, the velocity of y, is considered the input. Note that these equations are almost identical to (4.2), except that v controls $\dot{y}$, not $\ddot{y}$.

Given some goal configuration, for example, $(y, z) = 0$ and some initial configuration $y(0), z(0)$, we may set $v = -y(0)$. At the end of one second we have that $y(1) = 0$ and $z(1)$ is some nonzero vector. All we must do then is construct some procedure for correcting this last error without perturbing the y.

First we make some definitions in order to be specific. Define the vector $z \in \mathbb{R}^m$ as $z = (z_1^T, z_2^T, \ldots z_p^T)^T$ where $z_j = (z_j^1, z_j^2, \ldots, z_j^{\ell_j})^T$. We define the matrices β_j as the lower triangular matrices derived in chapter four, with $(\beta_j)_{kh} = \beta^k_{jh}$. Recall that $\beta^k_{jk} > 0$, thus each β_j is invertible. Define the matrix β to be the block triangular $m \times m$ matrix with diagonal blocks β_j, which is invertible since each diagonal sub-block is.

Algorithm (Steering for Power Form Systems):

Base Correction, $(0, \frac{T}{3})$**.**

Apply: velocity $v = -\frac{3}{T}\left(y(0) - (1, 0, \ldots, 0)^T\right)$ for $\frac{T}{3}$ seconds.

Fiber Correction, $(\frac{T}{3}, \frac{2T}{3})$**.**

Define: $c \in \mathbb{R}^m = (c_1, c_2, \ldots, c_p)^T = -\frac{3}{T}\beta^{-1} z(\frac{T}{3})$ with $c_j = (c_j^1, \ldots c_j^{\ell_j})$.

Apply: velocities $v_0 = \frac{6\pi}{T}\sin(\frac{6\pi}{T}t)$,

$v_j = \sum_{k=1}^{\ell_j} c_j^k \cos(k\frac{6\pi}{T}t)$.

Final Base Correction, $(\frac{2T}{3}, T)$**.**

Apply velocity: $v = -\frac{3}{T}y(\frac{2T}{3})$ for $\frac{T}{3}$ seconds.

Verification: To verify that this planner works, we need to calculate the net movement of the system under the controls u. Certainly in step one, the error in y is corrected, leaving $y = (1, 0, 0, \ldots)^T$. What requires checking are the controls for step two. The velocity of z is given by

$$\dot{z}_j^k = \frac{1}{k!}\cos^k(\frac{4\pi}{T}t)\left(\sum_{k=1}^{\ell_j} c_j^k \cos(k\frac{4\pi}{T}t)\right) \tag{6.2}$$

which is, of course, very similar in form to the control law of chapter 4. If we integrate the $\dot{z}$ equation of a time $\frac{T}{3}$, all of the periodic terms will be set to zero. The only terms of note are then the steady state terms. We conclude

$$z(\frac{2T}{3}) = \frac{3}{T}\beta c + z(\frac{T}{3}) \tag{6.3}$$

and with our choice of constant vector c, we have $z(T) = 0$.

The previous discussion uses a simple general strategy for planning trajectories. The strategy corrects first the error in the base and next in the fiber. The correction in the fiber is simplified when the equations are principal. The required motion in the base is dependent only on the desired change in z and not on z itself.

6.2 Applications

We now examine some of the applications in detail. First we consider the car, and apply the power form planner to it. Planning for the planar acrobot, even though it is not in power form, is very similar though singular configurations must be avoided. Similar geometric arguments will motivate a path planner for the symmetric satellite.

6.2.1 The Car

We build a planner based on the general procedure outlined in the previous section. We will assume that the car will remain in the valid region of the coordinate transformation. To apply the planner, first we compute the effect of the velocities

$$\begin{aligned} v_0 &= \frac{4\pi}{T}\sin(\frac{4\pi}{T}t) \\ v_1 &= c_1\cos(\frac{4\pi}{T}t) + c_2\cos(2\frac{4\pi}{T}t)\ . \end{aligned} \tag{6.4}$$

The derivative of the fiber coordinates is

$$\begin{aligned} \dot{z}_1 &= \cos(\frac{4\pi}{T}t)\left(c_1\cos(\frac{4\pi}{T}t) + c_2\cos(2\frac{4\pi}{T}t)\right) \\ \dot{z}_2 &= \frac{1}{2}\cos^2(\frac{4\pi}{T}t)\left(c_1\cos(\frac{4\pi}{T}t) + c_2\cos(2\frac{4\pi}{T}t)\right)\ . \end{aligned} \tag{6.5}$$

Now expand the previous expression.

$$\begin{aligned} \dot{z}_1 &= \frac{1}{2}\left(c_1 + c_2\cos(\frac{4\pi}{T}t) + c_1\cos(2\frac{4\pi}{T}t) + c_2\cos(3\frac{4\pi}{T}t)\right) \\ \dot{z}_2 &= \frac{1}{2}\left(c_1\cos(\frac{4\pi}{T}t) + c_2\cos(2\frac{4\pi}{T}t)\right) + \\ &\quad \frac{1}{4}\left(c_2 + c_1 cos(\frac{4\pi}{T}t) + c_1 cos(3\frac{4\pi}{T}t) + c_2 cos(4\frac{4\pi}{T}t)\right) \end{aligned} \tag{6.6}$$

In conclusion we have that at the end of step two, the z coordinates are given by the formula

$$\begin{aligned} z_1(\frac{2T}{3}) &= \frac{T}{6}c_1 + z_1(\frac{T}{3}) \\ z_2(\frac{2T}{3}) &= \frac{T}{12}c_2 + z_2(\frac{T}{3}) \end{aligned} \tag{6.7}$$

The planner then corrects the remaining error in y_0 without affecting the fiber, in step three. The choice of gains c is clear.

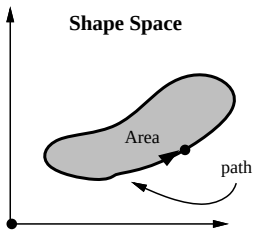

Figure 6.2: The application of Green's theorem to the planar acrobot.

6.2.2 The Planar Acrobot

For the planar acrobot, we develop a planner similar in spirit to the power form steering algorithm, except this time we improve the method by insuring that regions were planar acrobot cannot be transformed into a power form system are avoided. Not all of our example systems are globally diffeomorphic to the power form system. For example, consider the fire truck in the jack knife configuration. Away from this configuration, the coordinate change holds.

In keeping with the spirit of the power form steering algorithm, we first correct error in the base variable, then consider how motions in the base changes the fiber coordinate. Although the system is not in power form, it is principal. We will use this fact in what follows.

Given some motion in the base y, we reconstruct the change in the fiber z, by applying Green's theorem. The time integral of the derivative of z may be converted into a line integral in the base space. We start with the case where the path in the shape space is a simple closed curve. We assume without loss of generality that the trajectory is one second long.

$$\begin{aligned} z(1) - z(0) &= \int_0^1 (b_1(y_1, y_2)\dot{y}_1 + b_2(y_1, y_2)\dot{y}_2)\, dt \\ &= \int_{line} (b_1(y_1, y_2)dy_1 + b_2(y_1, y_2)dy_2) \\ &= \int_{area} \left(\frac{\partial b_2}{\partial y_1}(y_1, y_2) - \frac{\partial b_1}{\partial y_2}(y_1, y_2) \right) dA \end{aligned}$$

The integrand been calculated above as $\xi(\cdot)$. Thus we may write the following.

$$z(1) - z(0) = -\int_{area} \xi(y) dA \tag{6.8}$$

The shift in z is sometimes referred to as the *geometric phase*. In general, the

procedure for finding the geometric phase can be broken down into three increasingly complicated cases

Case 1 *The path is a simple closed curve.* The positive orientation case has been discussed above. If the curve is negatively oriented change the sign of (6.8).

Case 2 *The path is a self-intersecting closed curve.* Divide the curve into simple closed pieces and apply case 1 to each piece. Add the results together.

Case 3 *The path is an open curve.* Join the end points with a straight segment and compute the line integral over this segment. The resulting figure is a possibly self intersecting closed curve. Apply case 1 or 2 and then subtract value of the line integral.

Given this analysis, one path planning algorithm becomes evident. The fact that $\xi(\cdot) = 0$ only on a one-dimensional subset of the y space implies that there exists an open subset of the shape space where $\xi(\cdot)$ is strictly positive or negative. Any simple closed curve contained in this region will result in a non-zero geometric phase if it is followed as a path. The sign of the correction in z changes if the direction traveled in this path is reversed.

We will simply pick circles for our loops in the y space. Given any initial configuration (y, z), and a final one, the final one may be reached using this procedure:

Step 1 (Initial Base Error Correction): Using constant inputs v_1, v_2, drive the system to the desired y ignoring the drift in the z term. Measure the amount of phase shift in z required to bring the system to the exact desired location.

Step 2 (Singularity Avoidance): Let k be the amplitude of the driving sinusoids for which one loop will give the desired phase shift of z. Figure (6.3) shows the graph of this relation for a particular set of parameter values. If the needed phase shift is larger than the maximum value shown in figure (6.3), then two or more loops may be required. Again using constant inputs, drive the system to $(-\pi/2 + k, \pi/2)$. The offset is to ensure the path is centered at $y = (-\pi/2, \pi/2)$.

Step 3 (Fiber Correction): Drive the system with $v_1 = k\sin(t), v_2 = k\cos(t)$ for enough cycles to obtain the desired phase shift.

Step 4 (Final Base Adjustment): By following the same path used in step two, return the system to the desired y. Because this return route lies on top of the route generated

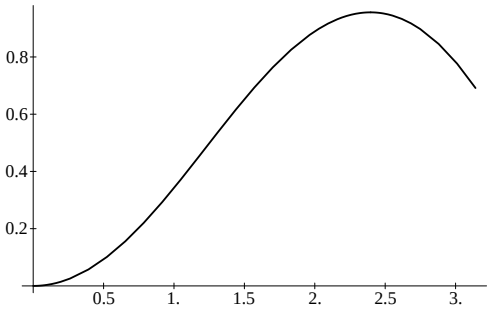

Figure 6.3: This graph shows the net phase shift in z as a function of radius k for circular motions in shape space about the point $(-\frac{\pi}{2}, \frac{\pi}{2})$.

in step 2 together they enclose no area. Consequently, the phase shift of the total path generated in steps 2 through 4 is equal to the phase shift obtained in step 3 only.

Even if there are limits on the joint angles, there still will exist an open subset of the shape space in which the system is free to move. Thus there will exist a feasible closed path enclosing an area of shape space where $\xi(\cdot)$ has only one sign. With this loop and other similar ones inside of it one may design an analogous path planner for this restricted system.

6.2.3 The Satellite

The last path planner we consider solves the steering problem for the symmetric satellite. The angular velocity about the first two principal axes are considered as inputs. Recall that the control system may be viewed as

$$\dot{g} \quad = \quad g\left(\hat{e}_1 v_1 + \hat{e}_2 v_2\right) \ . \tag{6.9}$$

This may require an input transformation and a change of coordinates if $\omega_3 \neq 0$.

We again will construct a path planner similar in spirit to the power form steering algorithm. A good choice for the base space of a symmetric satellite is the sphere. As noted in chapter three, coordinates for the sphere are bound to have some singularities. We will, for the time being, avoid these coordinates.

First we check if this base space is free of velocity constraints. Indeed, one may

examine the allowed velocities as projected down into $\mathbb{R}^3$.

$$\begin{aligned}\frac{d}{dt}ge_3 &= g\left((e_1v_1 + e_2v_2)\times\right)e_3 \\ &= g(e_1 \times e_3)v_1 + g(e_2 \times e_3)v_2\end{aligned}$$

Note that this velocity is perpendicular to ge_3 for all c_1, v_2. Thus, it is contained in the tangent plane of the sphere at the point ge_3. Finally, note also that these two input velocities are not collinear; thus, they span the tangent plane to the sphere at the point ge_3.

Now we wish to examine how the orientation of the satellite changes if the path in shape space is a closed loop. As noted before, the change in orientation is called the *geometric phase.*

Call the starting and ending orientations of the satellite g_0 and g_1 respectively. By assumption $g_1e_3 = g_0e_3$ so we may conclude that $g_0^Tg_1e_3 = e_3$, implying that $g_0^Tg_1$ is a rotation about e_3. We wish to compute the angle of this rotation.

The matrix $g(t)$ will represent the orientation of the satellite at time t. Attach at $g(t)e_3$ on S^2 embedded $\mathbb{R}^3$ an orthonormal frame with one axis collinear with e_3. This frame tracks the true orientation of the satellite. Notice that by construction the inputs may not rotate this frame only about the axis collinear with e_3. This implies that the frame is parallel transported along this path. Assume that the path is constructed out of finitely many smooth segments parameterized by arc length. Label each one of these segments C_i and the region they enclose R. By the Gauss-Bonnet Theorem [8],

$$2\pi\chi(R) = \sum_{i=1}^{3}\int_{C_i} k_g(s)ds + \int_R K\,d\sigma + \sum_{i=1}^{3}\theta_i$$

where $\chi(R)$ is the Euler-Poincaré characteristic of the region, K being the curvature at each point, k_g being the geodesic curvature of curve C_i, and θ_i being the exterior angle at each discontinuity in the path.

In the case of the sphere, $\chi(R)$ is equal to 1, so we may disregard the term on the left hand side since it is a multiple of 2π. In addition, the curvature of the sphere is constant and equal to 1 therefore the surface integral is equal to the area enclosed by the path. Finally the two summations give the net phase shift in the parallel transported frame and hence the angle of rotation about e_3 of the original system.

This result may be generalized to more complicated paths in exactly the same manner as with the planar acrobot. As in the case of the planar skater, an algorithm for steering becomes apparent from the analysis.

6.3 Optimization

The original motivation for using the path planners in the previous sections was to find paths more efficient, in some sense, than those produced by the regulating feedback laws. Further improvement requires a quantitative measure of how a good a path solving the end point conditions is. Our choice of cost will be the square of the required velocities integrated over the trajectory. The goal is to find a trajectory $g(t)$ or $x(t)$ which minimizes this cost.

$$\text{cost} \quad = \quad \int \sum_{j=0}^{p} v_j^2 dt \tag{6.10}$$

This is very similar to the integral of the Lagrangian for mechanical systems, if we label $L(x,v) = \sum_{j=0}^{p} v_j^2$. The formulation is the same in the Lie group context.

We will apply the calculus of variations to help solve this problem. There are substantial differences between solving this optimal control problem and standard mechanics. In particular, the Lagrangian is usually not regular. This has to do with constraints on the allowable variations: those directions which are disallowed have undefined cost.

From this point on, we will use the Lie group formulation because we will be planning large motions. The control system considered is

$$\dot{g} \quad = \quad g\left(\hat{e}_c(g,v)\right) \ . \tag{6.11}$$

with the cost of any given trajectory $(g(t), v(t))$ being

$$J(g(t), v(t)) \quad = \quad \int L(g,v)dt \tag{6.12}$$

where $L(g,v)$ is called the Lagrangian for the optimal control problem.

6.3.1 The Maximum Principle

Associated with the control system and a particular Lagrangian is a controlled Hamiltonian. Typically the cost is thought of as an extra state, g_0, with co-state p_0. The derivative of g_0 is the Lagrangian, $L(g,v)$.

$$H(g,\hat{p},v) \quad = \quad p_0 L(g,v) + \hat{p}\left(e_c(g,v)\right) \tag{6.13}$$

Notice as there is no dependence on g_0, p_0 is a constant of the motion. It is equivalent to consider all non-zero values of p_0, so this is typically set to -1. Trajectories generated with

$p_0 = -1$ are called normal extremals. However, if $p_0 = 0$ then the nature of the trajectories changes dramatically. These extremals are called abnormal, and they will not be considered as viable trajectories in the path planning algorithms.

We now state the maximum principle as it applies to Lie groups. A coordinate free version similar the this one can be found in [21]. For details on a proof, see [16, 17, 50].

Proposition 16 (The Maximum Principle)

Given: *a trajectory $(g(t), v(t))$ of system (6.11), optimal with respect to (6.12) on $[0, T]$, relative to boundary conditions $g(0), g(T)$,*

Then: *$g(t)$ is a projection of a curve of $H_{v(t)}$, given by (6.13), with $p_0 \in \{0, 1\}$ and $H_{v(t)} \geq H_u$ for any u, for almost all $t \in [0, T]$.*

By $H_{v(t)}$ we mean H evaluated on $v(t)$. The Maximum principle provides a recipe for finding candidate solutions to the optimal control problem. Solutions to (6.13) are called extremals, and satisfy necessary but not sufficient conditions.

In order to compute the extremals, we need to know how to compute Hamilton's equations in the Lie group setting. Given an optimal Hamiltonian $H(g, \hat{p})$, recall that $\frac{\partial H}{\partial \hat{p}}(g, \hat{p}) = \hat{e}_c(g, v)$, which corresponds to the derivative of g. As for the derivative of $\hat{p}$, we may solve for this in coordinates using the natural symplectic two-form on $T(\mathcal{G} \times \mathfrak{g}^*)$ [1].

$$\omega_{(g,\hat{p})}((\hat{e}_a, \hat{p}_a), (\hat{e}_b, \hat{p}_b)) = \hat{p}_a(\hat{e}_b) - \hat{p}_b(\hat{e}_a) - \hat{p}([\hat{e}_a, \hat{e}_b]) \tag{6.14}$$

The derivatives of the coordinate functions $P_i(g, \hat{p}) = \hat{p}(\hat{e}_i)$ can then be computed by examining the Poisson bracket between the function and H. The Poisson bracket is, in this case, the symplectic form operating on the partials of the functions on $G \times \mathfrak{g}^*$. Recall that for a function $f : \mathcal{G} \times \mathfrak{g}^* \to \mathbb{R}$, $\frac{\partial f}{\partial g} \in \mathfrak{g}^*$ and $\frac{\partial f}{\partial \hat{p}} \in \mathfrak{g}$.

$$\begin{aligned} \dot{P}_i &= \{P_i, H\} \\ &= \omega_{(g,\hat{p})}\left(\left(\frac{\partial P_i}{\partial \hat{p}}, \frac{\partial P_i}{\partial g}\right), \left(\frac{\partial H}{\partial \hat{p}}, \frac{\partial H}{\partial g}\right)\right) \\ &= \frac{\partial P_i}{\partial g}\left(\frac{\partial H}{\partial \hat{p}}\right) - \frac{\partial H}{\partial g}\left(\frac{\partial P_i}{\partial \hat{p}}\right) - \hat{p}([\frac{\partial P_i}{\partial \hat{p}}, \frac{\partial H}{\partial \hat{p}}]) \end{aligned} \tag{6.15}$$

We refer to [17, 50] for the proof. However, we will offer a plausibility argument in the form of a much weaker theorem. It only considers normal extremals; further, it only considers systems where the optimal $v(t)$ satisfies $\frac{\partial H}{\partial v}(g, \hat{p}, v(t)) = 0$. All of our examples meet these criteria.

Proposition 17 (Normal Extremals)

Given: *a solution to (6.13) with* $p_0(t) = -1$, *with maximizing* $v(t)$ *satisfying* $\frac{\partial H}{\partial v}(g, \hat{p}, v(t)) = 0$,

Then: *the solution* $g(t), v(t)$ *extremizes the functional* g_0 *with respect to variations leaving the boundary conditions fixed.*

Proof: We consider a Lagrangian formulation of the optimal control problem, using Lagrange multipliers to enforce the control system constraint. The reader may be rightly worried about the lack of regularity. Regularity guarantees that we have well defined Euler-Lagrange equations, as well as equivalence between Hamilton's and Lagrange's formulations. It is a sufficient but not necessary condition, as will be illustrated in this case.

To enforce the constraint, we expand the space to include a Lagrange multiplier, $\lambda(t) \in \mathfrak{g}^*$. The new Lagrangian is then:

$$\begin{aligned} \text{cost} &= \int_{t=0}^{T} L(g, \hat{e}, v) - \lambda \left(\hat{e}(t) - \hat{e}_c(g, v)\right) dt \\ &= \int_{t=0}^{T} \tilde{L}(g, \lambda, \hat{e}, v) dt \end{aligned} \tag{6.16}$$

Notice that as the argument of $\lambda(t)$ is zero for all trajectories that satisfy the constraint, this cost is equivalent to (6.12) as long as $g(t)$ is a valid trajectory. Of course, to be a proper variational argument with side conditions, we should have a λ_0 and a g_0 as defined earlier. As with p_0, λ_0 would be a constant of the motion. In this treatment, however, we will not consider the abnormal case thus we implicitly set $\lambda_0 = 1$. Now consider the three parts of the Euler-Lagrange equations.

$$\frac{d}{dt}\left(\frac{\partial \tilde{L}}{\partial \hat{e}}\right)(\cdot) \quad = \dot{\lambda}(t)(\cdot) \quad = \lambda\left([\hat{e}_c(g, v), \cdot] + \frac{\partial \tilde{L}}{\partial g}(\cdot)\right)$$

This equation tells us how $\lambda(t)$ evolves as a function of time. Since $\tilde{L}$ is independent of the time derivative of λ, we the following relation.

$$\begin{aligned} 0 &= \frac{\partial \tilde{L}}{\partial \lambda} \\ &= \hat{e}(t) - \hat{e}_c(g, v) \end{aligned}$$

Thus we have that trajectories extremizing (6.16) satisfy our side condition, $\hat{e}(t) = \hat{e}_c(g, v)$. The last specifies conditions for the inputs. Note that $\tilde{L}$ is independent of $\dot{v}$. Thus we know

something about $\frac{\partial \tilde{L}}{\partial v}$.

$$\begin{aligned} 0 &= \frac{\partial \tilde{L}}{\partial v} \\ &= \frac{\partial L}{\partial v} - \frac{\partial}{\partial v}\left(\lambda\left(e_c(g,v)\right)\right) \end{aligned}$$

In all of our examples, the equation $\frac{\partial \tilde{L}}{\partial v} = 0$ may be solved uniquely for v for fixed λ and g.

Now we show that a solution of (6.13) solves these equations. First, set $\hat{p} = \frac{\partial \tilde{L}}{\partial \hat{e}} = \lambda$. Define the following Hamiltonian:

$$\begin{aligned} H(g,\hat{p},v) &= \hat{p}\left(\hat{e}_c(g,v)\right) - \tilde{L}(g,v), \\ &= \hat{p}(\hat{e}(g,v)) - L(g,v) \end{aligned}$$

Note that this is simply the controlled Hamiltonian with $p_0 = -1$. Let us examine the formula obtained by maximizing this Hamiltonian at a fixed point in T^*G. By assumption, this unique v sets $\frac{\partial H}{\partial v} = 0$.

$$\begin{aligned} \frac{\partial H}{\partial v} &= 0 \\ &= \frac{\partial}{\partial v}\left(\lambda\left(e_c(g,v)\right)\right) - \partial_3 L \\ &= -\frac{\partial \tilde{L}}{\partial v} \end{aligned}$$

Consequently, at every point $g, \hat{p}$ we have the same controls. Using the canonical two-form on T^*G we may verify, in a similar manner, that the evolution of λ agrees with the evolution of $\hat{p}$, finishing the proof.

In general when computing the dynamics of g and $\hat{p}$, the formula for the optimal input v in terms of $g, \hat{p}$ is substituted in *after* the computation of the v dependent dynamics. The formula for the inputs may be inserted before the dynamics computation. We find this more convenient and do so.

6.3.2 Extremal Characteristics

We have a very special class of systems and cost functional. For all systems without drift, the two norm of inputs is shown to be a constant of the motion. For left invariant systems without drift, there exists a right (material) symmetry for the system and at least $n+2$ conserved quantities. We examine these structures in the following.

Proposition 18 (Norm Preservation [37])

Given: a drift-free control system $\mathcal{G}$, whose evolution is a normal extremal described by (6.13),

Then: then two norm of the control inputs v is a constant of the motion.

Remark (Monotonically Related Optimization): This proposition implies that it is equivalent to minimize the integral of any monotonically increasing functions of the norm. Examples include the square of the two norm, $\|v\|^2$.

Proof: We first will show that $\|v\|^2$ is a constant of the motion. That the norm is preserved follows. We assume the control system is linear in the inputs v,

$$\hat{e}_c(g,v) \quad = \quad \sum_{j=1}^{p} \hat{e}_c^j(g) v_j \ .$$

Define the control momenta to be

$$P_j(g,\hat{p}) \quad = \quad \hat{p}(e_c^j(g)) \ . \tag{6.17}$$

Note that for left invariant system, P_j will be independent of g. The controlled Hamiltonian for normal extremals is given by

$$H(g,\hat{p},v) \quad = \quad \sum_{j=1}^{p} \left(P_j v_j - \frac{1}{2} v_j^2 \right) \tag{6.18}$$

which may be maximized by setting the controls $v_j = P_j$. The Hamiltonian under these controls simplifies to

$$H(g,\hat{p}) \quad = \quad \frac{1}{2} \sum_{j=1}^{p} P_j^2 \ . \tag{6.19}$$

Note that 6.19 is $\mathcal{G}$ invariant for left invariant control systems. Now we compute the time derivative of $\|v\|^2$.

$$\dot{P}_i \quad = \quad \sum_{i=1}^{p} P_j \{P_i, P_j\} \tag{6.20}$$

Using this and noting that $\{P_i, P_j\} = -\{P_j, P_j\}$, we find

$$\dot{v} \quad = \quad S(g,\hat{p}) v \tag{6.21}$$

where $S(g,\hat{p})$ is a skew symmetric matrix, completing our proof.

Now we consider the consequences of having a left invariant control system in addition to the drift free property. The symmetric satellite and Hilare are left invariant.

Proposition 19 (Reduction)

Given: a left-invariant control system on $\mathcal{G}$, whose evolution described by (6.19),

Then: the evolution of the co-state $\hat{p}$ depends only on its initial conditions and not g.

That is, the evolution of the $\hat{p}$'s does not depend on g. This is known in the mechanics literature as reduction. We can evolve the co-state $\hat{p}$ separately and later compute the phase (change in the state of g) if we wish. The real draw back of this approach is that the only thing we really care about *is* exactly the geometric phase. For the proof, we pick a basis for $\mathfrak{g}$ so that the first p elements correspond to the vector fields of the control system.

Proof:

$$\begin{aligned}
\dot{P}_i &= \{P_i, H\} \\
&= \sum_{j=1}^{p} P_j \{P_i, P_j\} \\
&= \sum_{j=1}^{p} P_j \hat{p}([\hat{e}_i, \hat{e}_j])
\end{aligned}$$

The next proposition concerns itself with the conserved quantities generated when symmetries are present.

Proposition 20 (Noether's Theorem Applied)

Given: a left-invariant control system on $\mathcal{G}$, whose evolution described by (6.19),

Then: there exists $n+1$ constants of the motion, given by H and $\beta_i = \hat{p}(g^{-1}\hat{e}_i g)$.

Proof: Certainly $\dot{H} = \{H, H\} = 0$. For the others, simply differentiate the formula.

$$\begin{aligned}
\dot{\beta}_i &= \dot{\hat{p}}(g^{-1}\hat{e}_i g) + \hat{p}(\dot{g}^{-1}\hat{e}_i g + g^{-1}\hat{e}_i \dot{g}) \\
&= -\hat{p}([g^{-1}\hat{e}_i g, \hat{e}]) + +\hat{p}(-\hat{e}g^{-1}\hat{e}_i g + g^{-1}\hat{e}_i g\hat{e}) \\
&= -\hat{p}([g^{-1}\hat{e}_i g, \hat{e}]) + \hat{p}([g^{-1}\hat{e}_i g, \hat{e}]) \\
&= 0
\end{aligned}$$

These constants arise naturally as the left Lagrangian is $\mathcal{G}$ invariant. The constants are the left costates mapped to the right. The left co-states change, represented by the functions P_i dependent on $\mathcal{G}$ and the constants. For the rigid body, the left (body) frame Lagrangian is independent of g. An application of Noether's theorem finds the right-constants, the total angular momentum. The left translation of these are exactly the body

angular momenta, which may be solved using the g and the total angular momenta constants.

6.3.3 Applications

In this section we consider several of the examples and discuss solution techniques, exploiting what ever structure may exist. In general, since one cannot solve the optimal control problem explicitly, a numerical strategy is required. Numerical optimization concerns itself with minimizing functions of n variables subject to equality and inequality constraints [26, 35].

Our problem involves finding inputs $u(\cdot)$ which belongs to a function space. By using Pontryagin's maximum principle, we need consider only an n dimensional subset of this space. These n degrees of freedom are parameterized by the initial co-state values.

How we decide to characterize the path planning problem determines which techniques we use. We could have even ignored the results of Pontryagin and attempted to form approximate problems, restricting the inputs to lie in some r dimensional function space and solving a series of sub-problems of increasing dimension r. Such methods are referred to as semi-infinite [35].

We, however, have a great deal of structure. We can find the optimal inputs v as a function of $g, \hat{p}$ and numerically compute the resulting phase, $g(T, P)$. This may be compared in the most natural way to g_f, by setting

$$g_e(T, P) = g(T, P) g_f^{-1}.$$

To convert this error term to a vector in $\mathbb{R}^n$, it is natural to take the logarithm of $g_e(T, P)$. That is to say, we find η_e such that $\mathrm{Exp}(\eta_e) = g_e(T, P)$. If $\eta_e = 0$, then $g(T, P) = g_f$. At this point we have formed an n dimensional root finding problem. Even with the relatively simple systems we consider here, this is difficult to solve.

Consider, for example, the positive scalar function $f(T, P) = \eta_e^T \eta_e$. Many shooting methods can be applied with such a function, depending on the amount of information and computational time one is willing to expend. The simplest approach uses the simplex method [14]. This method requires no derivative or gradient information and is the easiest to program, though convergence is slow and not guaranteed.

For the computational price of a gradient calculation, steepest descent methods offer more speed and reliability. It can be shown to converge linearly [26, 35] in certain

convex situations. If one is willing to compute the Hessian, quadratic convergence is locally given by Newton-Raphson [35] methods. Conjugate-gradient methods offer a compromise between the two by estimating the Hessian using the past history of the algorithm. Local convergence rate is faster than gradient decent, slower than Newton-Raphson.

Since we have a root finding problem, we use Newton-Raphson methods. The inherent instability [35] in the technique is handled by using an Armijo step size rule [35]. The methods converge quickly, provided we start with good seeds.

The Symmetric Satellite

As before, we write the kinematics of the symmetric satellite as follows.

$$\dot{g} = g\hat{e}_1 v_1 + g\hat{e}_2 v_2 \tag{6.22}$$

where the matrices $\hat{e}_i$, $i \in \{1, 2, 3\}$, form a basis set for the tangent space of $SO(3)$ at the identity in this particular representation, and hence form a basic for the Lie algebra $so(3)$. The norm of the inputs is conserved, and in addition, the system is left invariant. The optimal inputs are

$$\begin{aligned} v_1 &= c_1 \cos(c_2 t + c_3) \\ v_2 &= c_1 \sin(c_2 t + c_3) \end{aligned} \tag{6.23}$$

which are a family of sinusoids.

Hilare

We now embed the configuration of Hilare into the 3-dimensional matrix Lie group $SE(2)$. The configuration will be represented by a 3×3 matrix, g, below:

$$g = \begin{bmatrix} R & x \\ 0 & 1 \end{bmatrix}$$

with $R \in SO(2)$, a 2×2 rotation matrix, and with $x \in \mathbb{R}^2$.

The dynamics will be given as:

$$\dot{g} = g \begin{bmatrix} 0 & -v_2 & v_1 \\ v_2 & 0 & 0 \\ 0 & 0 & 0 \end{bmatrix}$$

with v the scalar inputs corresponding to driving and turning velocity. This can be written more compactly as

$$\dot{g} = g\hat{e}_1 v_1 + g\hat{e}_3 v_2 \tag{6.24}$$

where the $\hat{e}_i$, $i \in \{1,2,3\}$ form a basis set for the tangent space of $SE(2)$ at the identity in this particular representation, and hence form a basis for the Lie algebra $se(2)$. They are given by

$$\hat{e}_1 = \begin{bmatrix} 0 & 0 & 1 \\ 0 & 0 & 0 \\ 0 & 0 & 0 \end{bmatrix} , \quad \hat{e}_2 = \begin{bmatrix} 0 & 0 & 0 \\ 0 & 0 & 1 \\ 0 & 0 & 0 \end{bmatrix} , \quad \hat{e}_3 = \begin{bmatrix} 0 & -1 & 0 \\ 1 & 0 & 0 \\ 0 & 0 & 0 \end{bmatrix} . \tag{6.25}$$

The maximizing inputs are given by $v_1 = P_1, v_2 = P_2$. Their norm is conserved. The optimal inputs solve the following equation,

$$\begin{aligned} v_1 &= c_1 \cos(\theta) \\ v_2 &= c_1 \sin(\theta) \\ \ddot{\theta} &= \frac{c_1^2}{2} \sin(2\theta) \end{aligned} \tag{6.26}$$

where $c_2 = \theta(0)$ and $c_3 = \dot{theta}(0)$. These equations are those of a pendulum.

The Planar Acrobot

There are only two velocity inputs to the system, and their norm is a constant of the motion. We can then write the optimal inputs as

$$\begin{aligned} v_1 &= c_1 \cos(\theta + c_2) \\ v_2 &= c_1 \sin(\theta + c_2) \\ \dot{\theta} &= c_3 \xi(y) \ , \end{aligned} \tag{6.27}$$

where $\xi(y)$ is as defined in (3.29). These formulae are easily verified by differentiation. Recall that $v_1 = P_1, v_2 = P_2$. We have,

$$\begin{aligned} \dot{v}_1 &= -P_2\{P_1, P_2\} \\ \dot{v}_1 &= P_1\{P_2, P_1\} \end{aligned} \tag{6.28}$$

We set $\dot{\theta} = \{P_1, P_2\}$, which is related to the bracket of f_c^1, f_c^1 as before, which picks out c_3 and $\xi(y)$.

6.4 Conclusion

We have considered a small number of path planners for control systems with nonholonomic constraints. The literature contains many such planners [31, 46, 22, 41, 24, 33]. Optimal planning, while desirable, poses numerical difficulties. Consequently, as is often the case in engineering, the best approach is determined by the application and not the engineer. For example, the savings offered by optimal paths may not justify the computational expense of finding them. However, the approach of computing off-line a large set of trajectories and selecting among them at run time is viable as information storage is inexpensive.

Chapter 7

Conclusion

We have presented a strategy for controlling a class of mechanical systems with nonholonomic velocity constraints. There were two control objectives. First, we wished to reach the neighborhood of a goal configuration in an efficient manner, even with disturbances. We also wished to remain in this neighborhood again despite disturbances. Several new methods were presented which achieve these objectives.

The work of the dissertation included the following results along with examples of their application.

- In chapter 2, we presented a set of coordinates and a feedback law which when applied to the example mechanisms transformed them into control canonical form.
- Sets of coordinates and feedback laws under which the example mechanisms appeared control reduced were detailed in chapter 3, along with
- a special set of coordinates and a feedback law for the satellite mounted with thrusters.
- Chapter 4 focused on a feedback law which renders the configuration of multiple-input power form dynamic systems stable.
- A feedback law stabilizing the attitude of the asymmetric satellite was also presented in chapter 4.
- A tracking control law which insured that the desired trajectories were followed was detailed in chapter 5.

- A suboptimal path planner for nonholonomic mechanisms was presented in chapter 6, along with
- an optimal path planner for nonholonomic mechanisms.

Many questions remain unanswered. In addition, there is much room for improvement in each of the results presented. Some directions for future research include the following.

- The feedback laws assumed unlimited control authority, and consequently the kinematic properties of the example systems dominated the analysis. It would be interesting to study the example systems in regimes where dynamic properties dominated the analysis.
- The satellite is representative of a large class of underactuated systems. Generalizing the laws developed for the asymmetric satellite seems a promising avenue of future research. In addition, it would be good to understand the connections between the results in the dissertation and the energy-momentum methods found in the literature.
- Point stabilizing control laws would be more robust with respect to disturbances if they had faster convergence rates.
- By restricting the optimal path planning problem to a small but relevant subclass of problems, the numerical effort required to plan trajectories may be reduced. For example, consider the problem of planning trajectories for airplanes near airports. The airplane may be modeled as a left invariant control system on the Lie group $SE(3)$. The optimal planning problem in such a case has a great deal of structure, which, when exploited, reduces computational effort.

Bibliography

[1] R. Abraham and J. Marsden. *Foundations of Mechanics.* Benjamin/Cummings Publishing Company, 1978.

[2] V. I. Arnold. *Mathematical Methods of Classical Mechanics.* Springer-Verlag, New York, New York, second edition, 1989.

[3] A. Block, P. S. Krishnaprasad, J. Marsden, and R. Murray. Nonholonomic mechanical systems with symmetry. Ohio State University, 1994.

[4] R. W. Brockett. Control theory and singular Riemannian geometry. In P. J. Hilton and G. S. Young, editors, *New Directions in Applied Mathematics*, pages 11–27. Springer-Verlag, New York, 1981.

[5] R. W. Brockett. Asymptotic stability and feedback stabilization. In R.W. Brockett, R.S. Millman, and H.J. Sussman, editors, *Differential Geometric Control Theory*, pages 181–191. Birkhauser, 1983.

[6] L. Bushnell, D. Tilbury, and S. S. Sastry. Steering three-input chained form nonholonomic systems using sinusoids: The firetruck example. In *European Control Conference*, pages 1432–1437, 1993. Also as Electronics Research Laboratory Memo M93/43.

[7] C. I. Byrnes and A. Isidori. On the attitude stabilization of a rigid spacecraft. *Automatica*, 27, No. 1:87–95, 1991.

[8] Manfredo P. Do Carmo. *Differential Geometry of Curves and Surfaces.* Prentice-Hall, Inc., Englewood Cliffs, New Jersey, 2nd edition, 1984.

[9] J. Carr. *Applications of Center Manifold Theory.* Springer-Verlag, New York, 1981.

[10] V. H. L. Cheng. A direct way to stabilize continuous-time and discrete-time linear time-varying systems. *IEEE Transactions on Automatic Control*, AC-24, No. 4:641–643, 1979.

[11] W-L. Chow. Über systeme von linearen partiellen differentialgleichungen erster ordnung. *Math. Annalen*, 117:998–1005, 1940-41.

[12] J-M. Coron. Global asymptotic stabilization for controllable systems without drift. *Mathematics of Control, Signals, and Systems*, 5(3):295–312, 1992.

[13] Peter E. Crouch. Spacecraft attitude stabilization: Applications of geometric control theory to rigid body models. *IEEE Transactions on Automatic Control*, AC-29, No. 4:321–331, April 1984.

[14] J. Dennis and D. Woods. Optimization on microcomputers: The nelder-mead simplex algorithm. In Arthur Wouk, editor, *New Computing Environments: Microcomputers in Large-Scale Computing*. SIAM, 1992.

[15] D. C. Deno. *Control theoretic investigations of the Visual Smooth Pursuit System*. PhD thesis, University of California at Berkeley, 1991.

[16] L.S. Pontryagin et al. *The Mathematical Theory of Optimal Processes*. J. Wiley and Sons, 1962.

[17] R.V. Gramkrelidze. *Principles of Optimal Control*. Plenum Press, New York, 1978.

[18] J. Guckenheimer and P. Holmes. *Nonlinear Oscillations, Dynamical Systems, and Bifurcations of Vector Fields*. Springer-Verlag, New York, 1983.

[19] A. Isidori. *Nonlinear Control Systems*. Springer-Verlag, second edition, 1989.

[20] R. Montgomery J. E. Marsden and T. Ratiu. Reduction, symmetry and phases in mechanics. *Memoirs of the American Mathematical Society*, 88(436), 1990.

[21] V. Jurdjevic. Optimal control problems on Lie groups: Crossroads between geometry and mechanics. In B. Jakubczyk and W. Respondek, editors, *Geometry of Feedback and Optimal Control*. Marcel-Decker, 1992.

[22] G. Lafferriere and H. J. Sussmann. Motion planning for controllable systems without drift. In *Proceedings of the IEEE International Conference on Robotics and Automation*, pages 1148–1153, 1991.

[23] J-P. Laumond. Controllability of a multibody mobile robot. In *Proceedings of the IEEE International Conference on Control and Applications*, pages 1033–1038, Pisa, Italy, 1991.

[24] J-P. Laumond and T. Siméon. Motion planning for a two degrees of freedom mobile robot with towing. In *Proceedings of the IEEE International Conference on Control and Applications*, 1989.

[25] Johann Benedict Listing. *Vorstudien zur topologie.* 1847. In *Gottingen Studien*, chapter 10.

[26] D. Luenberger. *Linear and Nonlinear Programming.* Addison-Wesley Publishing Company, Reading, Massachusetts, 1984.

[27] J. Marsden and T. Ratiu. *Mechanics and Symmetry.* Spinger-Verlag, 1994. Texts in Applied Math, Vol. 17.

[28] Jerrold E. Marsden and Jürgen Scheurle. The reduced Euler-Lagrange equations. *Fields Institute Communications 1*, pages 139–64, 1993.

[29] George Meyer. Design and global analysis of spacecraft attitude control systems. Technical Report R-361, NASA, March 1971.

[30] R. Montgomery. Isoholonomic problems and some applications. *Communications in Mathematical Physics*, 128:565 –592, 1990.

[31] R. M. Murray and S. S. Sastry. Nonholonomic motion planning: Steering using sinusoids. *IEEE Transactions on Automatic Control*, 38(5):700–716, May 1993.

[32] R. M. Murray, G. Walsh, and S. S. Sastry. Stabilization and tracking for nonholonomic systems using time-varying state feedback. In *Proceedings of the IFAC Nonlinear Control Systems Design Symposium*, pages 182–191, Bordeaux, France, 1992.

[33] Y. Nakamura and R. Mukherjee. Nonholonomic path planning of space robots via bi-directional approach. In *Proceedings of the IEEE International Conference on Robotics and Automation*, pages 1764–1769, 1989.

[34] P. J. Olver. *Applications of Lie Groups to Differential Equations.* Springer-Verlag, New York, New York, 1986.

[35] E. Polak. *Fundamentals of Optimization.* PrePrint, Univeristy of California at Berkeley, 1993.

[36] J. A. Reeds and L. A. Shepp. Optimal paths for a car that goes both forwards and backwards. *Pacific Journal of Mathematics*, 145(2), 1990.

[37] S. S. Sastry and R. Montgomery. The structure of optimal controls for a steering problem. In *Proceedings of the IFAC Nonlinear Control Systems Design Symposium*, pages 385–390, Bordeaux, France, 1992.

[38] Michael Spivak. *Differential Geometry*, volume 1. Publish or Perish, Inc., Houston, Texas, 2nd edition, 1970.

[39] H. J. Sussmann and W. Lui. Limits of highly oscillatory controls and the approximation of general paths by admissable trajectories. In *Proceedings of the IEEE Conference on Decision and Control*, 1991.

[40] A. Teel, R. Murray, and G. Walsh. Nonholonomic control systems: From steering to stabilization with sinusoids. In *Proceedings of the IEEE Conference on Decision and Control*, pages 1603–1609, 1992. Also as Electronics Research Laboratory Memo M92/28.

[41] D. Tilbury, J-P. Laumond, R. Murray, S. Sastry, and G. Walsh. Steering car-like robots with trailers using sinusoids. In *Proceedings of the IEEE International Conference on Robotics and Automation*, pages 1993–1998, Nice, France, 1992.

[42] G. Walsh and L. Bushnell. Stabilization of multiple input chained form control systems. *Systems and Control Letters*, 1994. To appear. Also in the 1993 IEEE *Proceedings of the Conference on Decision and Control.*

[43] G. Walsh, R. Montgomery, and S. S. Sastry. Optimal path planning on matrix lie groups. In *Proceedings of the IEEE Conference on Decision and Control*, 1994. Submitted.

[44] G. Walsh, R. Montgomery, and S. S. Sastry. Orientation control of the dynamic satellite. In *Proceedings of the American Control Conference*, pages 138–142, 1994.

[45] G. Walsh, A. Sarti, and S. S. Sastry. Algorithms for steering on the group of rotations. In *Proceedings of the American Control Conference*, pages 1312–1316, 1993. Also as Electronics Research Laboratory Memo M93/44.

[46] G. Walsh and S. Sastry. On reorienting rigid linked bodies using internal motions. *IEEE Transactions on Robotics and Automation*, 1994. Accepted and being scheduled. Appears also in the 1991 IEEE *Conference on Decision and Control.*

[47] G. Walsh, D. Tilbury, S. Sastry, R. Murray, and J.P. Laumond. Stabilization of trajectories for systems with nonholonomic constraints. *IEEE Transactions on Automatic Control*, 39(1):216–222, January 1994. Also in the 1992 IEEE *Proceedings of the International Conference on Robotics and Automation.*

[48] F. W. Warner. *Foundations of Differentialble Manifolds and Lie Groups.* Springer-Verlag, 1983.

[49] J. Wen and K. Kreutz-Delgado. The attitude control problem. *IEEE Transactions on Automatic Control*, 36, No. 10:1148–1161, October 1991.

[50] L.C. Young. *Optimal Control Theory.* Chelsea Publishing Company, New York, N.Y., 1980.